EAI/Springer Innovations in Communication and Computing

Pandian Vasant · Igor Litvinchev
José Antonio Marmolejo-Saucedo
Editors

Innovative Computing Trends and Applications

EAI
RESEARCH MEETS INNOVATION

Springer

EAI/Springer Innovations in Communication and Computing

Series editor
Imrich Chlamtac, CreateNet, Trento, Italy

Editor's Note

The impact of information technologies is creating a new world yet not fully understood. The extent and speed of economic, life style and social changes already perceived in everyday life is hard to estimate without understanding the technological driving forces behind it. This series presents contributed volumes featuring the latest research and development in the various information engineering technologies that play a key role in this process.

The range of topics, focusing primarily on communications and computing engineering include, but are not limited to, wireless networks; mobile communication; design and learning; gaming; interaction; e-health and pervasive healthcare; energy management; smart grids; internet of things; cognitive radio networks; computation; cloud computing; ubiquitous connectivity, and in mode general smart living, smart cities, Internet of Things and more. The series publishes a combination of expanded papers selected from hosted and sponsored European Alliance for Innovation (EAI) conferences that present cutting edge, global research as well as provide new perspectives on traditional related engineering fields. This content, complemented with open calls for contribution of book titles and individual chapters, together maintain Springer's and EAI's high standards of academic excellence. The audience for the books consists of researchers, industry professionals, advanced level students as well as practitioners in related fields of activity include information and communication specialists, security experts, economists, urban planners, doctors, and in general representatives in all those walks of life affected ad contributing to the information revolution.

About EAI

EAI is a grassroots member organization initiated through cooperation between businesses, public, private and government organizations to address the global challenges of Europe's future competitiveness and link the European Research community with its counterparts around the globe. EAI reaches out to hundreds of thousands of individual subscribers on all continents and collaborates with an institutional member base including Fortune 500 companies, government organizations, and educational institutions, provide a free research and innovation platform.

Through its open free membership model EAI promotes a new research and innovation culture based on collaboration, connectivity and recognition of excellence by community.

More information about this series at http://www.springer.com/series/15427

Pandian Vasant • Igor Litvinchev
José Antonio Marmolejo-Saucedo
Editors

Innovative Computing Trends and Applications

Springer

EAI
RESEARCH MEETS INNOVATION

Editors
Pandian Vasant
Faculty of Science and Information Technology
Universiti Teknologi Petronas
Seri Iskanda, Malaysia

Igor Litvinchev
Universidad Autónoma de Nuevo León
San Nicolás de los Garza
Nuevo León, Mexico

José Antonio Marmolejo-Saucedo
Facultad de Ingeniería
Universidad Panamericana
Ciudad de México, Mexico

ISSN 2522-8595 ISSN 2522-8609 (electronic)
EAI/Springer Innovations in Communication and Computing
ISBN 978-3-030-03897-7 ISBN 978-3-030-03898-4 (eBook)
https://doi.org/10.1007/978-3-030-03898-4

Library of Congress Control Number: 2018965928

This Springer imprint is published by the registered company Springer Nature Switzerland AG
The registered company address is: Gewerbestrasse 11, 6330 Cham, Switzerland

Preface

The 2nd EAI International Conference on Computer Science and Engineering (COMPSE) 2018, held on March 2–3, 2018, at the Furama Silom Hotel, Bangkok, Thailand, convened several specialists in the field of engineering. The COMPSE has been established as an excellence EAI conference for researchers and practitioners to disseminate, exchange, and discuss all recent creations and innovations related to new technologies in computer science and engineering. The technical program of the COMPSE 2018 was formed with 3 keynote speeches and technical paper presentation sessions with two special sessions and posters/demos and workshop. The COMPSE 2018 provided golden opportunities for the participants and delegates to refresh their knowledge and experiences and explore innovations in the field of data technology. This conference offered great research collaboration, cooperation, and networking opportunities, providing the participants with the opportunity to discuss and interact with leading researchers and colleagues across the planet. The great success and achievement of the conference was based on the dedicated efforts and hard work of conference organizing committee members, EAI authority, and reviewers. The COMPSE 2018 is indebted to many volunteers who contributed to planning and organizing both the technical program and supporting social arrangements. In particular, the Technical Program Committee, led by our TPC Chair, Prof. Jose Antonio Marmolejo Saucedo, who completed a peer review process of technical papers and made a high-quality technical program. Recognition should also go to our Steering Committee Organizer Prof. Imrich Chlamtac, Steering Committee Member Prof. Igor Litvinchev, Workshop Organizer Prof. Valeriy Kharchenko, and Conference Manager Lenka Bilska, who worked hard to arrange important details of the conference programs and social activities. It has been a great honor and delight for me to contribute as the General Chair of COMPSE 2018. I hope that all delegates and participants have found this conference stimulating, fulfilling, and enjoyable.

Finally, I would like to sincerely thank Nuevo Leon State University (Mexico), Panamerican University (Mexico), Universiti Teknologi PETRONAS (Malaysia), Federal State Budgetary Scientific Institution “Federal Scientific Agroengineering Center VIM” (Russia), and Furama Silom Hotel (Bangkok) for their wonderful support.

Tronoh, Malaysia Pandian Vasant
San Nicolás de los Garza, Mexico Igor Litvinchev
Mexico, Mexico José Antonio Marmolejo-Saucedo

Contents

Chapter 1
A Multi-objective Simulation-Based Optimization Approach Applied to Material Handling System

Chris S. K. Leung and Henry Y. K. Lau

1.1 Introduction

Simulation modelling is indeed a powerful industrial engineering technique for studying the functioning, performance and operation of complex systems. As such, it becomes a useful tool for decision makers in various industries. Unlike a mathematical model, simulation can handle a variety of complex factors that are commonly found in real world. More importantly, the accuracy of the performance measures of the complex systems obtained from simulation models is normally higher than that of analytical methods because analytical methods in general involve making unrealistic assumptions for the systems or problems under investigation [1].

In real world, many problems no matter whether they are in the domain of engineering, finance, business or science can be formulated into different forms of optimization problems. These problems are characterized by the requirement of finding the best possible solution(s) that fulfils certain criteria. Most of the real-world optimization problems normally involve multiple objectives rather than one single objective, in which some objectives conflict with others. However, using simulation modelling alone cannot provide us optimal solutions to these optimization problems. Therefore, an optimization algorithm is needed to guide the search process to the optimal solutions. The study reported in this paper demonstrates how a complex real-life multi-objective optimization problem in distribution industry where material handling system (MHS) is involved can be solved by a simulation-based optimization approach that comprises a simulation tool together with a hybrid AIS-based algorithm.

C. S. K. Leung (✉) · H. Y. K. Lau
Department of Industrial and Manufacturing Systems Engineering, The University of Hong Kong, Hong Kong, China
e-mail: hyklau@hku.hk

P. Vasant et al. (eds.), *Innovative Computing Trends and Applications*, EAI/Springer Innovations in Communication and Computing,
https://doi.org/10.1007/978-3-030-03898-4_1

1.2 Literature Review

Optimization of MHS via Simulation

In the literature, there are a number of studies that dedicatedly contribute to the optimization of MHS via simulation. For example, Elahi et al. [2] studied the General Motors paint shop conveyor system by developing a simulation model. The model works firmly with a decision optimizer incorporating integer linear programming model and dynamic programming model at critical points such as the beginning and end of buffer conveyors in the system in order to regroup batches of different colour cars. Leung and Lau [3] proposed a simulation-based optimization framework that combines the processes of optimization and simulation for solving typical linear optimization problems related to logistics and production operation. The framework integrates an AIS-based algorithm with a simulation tool for the evaluation of optimal system parameters and to reveal the performance of systems. Subulan and Cakmakci [4] made use of ARENA simulation program and Taguchi experimental design method to build a solution model for effectively designing material handling–transfer systems and optimizing the performance of automation technologies in automobile industry. Chang et al. [5] proposed a framework that integrates simulation optimization and data envelopment analysis techniques to find out the optimal vehicle fleet size for a multi-objective problem in automated material handling systems. Lin and Huang [6] extended the optimal computing budget allocation by adding genetic algorithm together with the help of a simulation model for optimizing the vehicle allocation for the automated material handling system in semiconductor industry.

Multi-objective Optimization Problems

Finding the solutions to the multi-objective optimization problems has long been a challenge to researchers because both the Pareto optimality and the diversity of the generated solutions must be simultaneously addressed. Unlike solutions in single objective optimization problems, which can easily be compared according to the value of the objective function, solutions in multi-objective problems cannot directly be compared with each other unless employing classical techniques, such as weighted objective aggregation methods and constraint approaches. Nevertheless, many real-world problems involving complex and nonlinear properties do not readily fit into these classical approaches [7]. Therefore, modern evolutionary algorithms such as genetic algorithm (GA), evolutionary strategy (ES), artificial immune systems (AIS), etc. incorporating the concept of Pareto optimality are proposed and become popular. These methods have been proved to be effective for solving multi-objective optimization problems by finding the approximated Pareto front, for example, NSGA-II [8], SPEA2 [9], micro-GA [10], omni-aiNet [11], NNIA [12], omni-AIOS [13], etc.

1.3 Multi-objective Simulation-Based Optimization Algorithm

This optimization approach adopted in this paper is a modified version of Leung and Lau's work [3], which incorporates a multi-objective optimization algorithm instead of a single objective algorithm. The multi-objective algorithm is named Suppression-Controlled Multi-objective Immune Algorithm (SCMIA) proposed by Leung and Lau [14]. The fundamental of the algorithm was inspired from mechanisms of biological immune system and biological evolution. It was developed by hybridizing the clonal selection principle and immune network theory with the idea from GA. The algorithm makes use of the Pareto dominance for fitness assignment and some common AIS-based algorithm's features for guiding the search process, such as clonal selection and expansion, affinity maturation, antibody concentration, meta-dynamics and immune memory. The interesting feature of this algorithm is the introduction of an innovative suppression operator, which is used to help eliminate similar antibodies, hence significantly minimizing the number of unnecessary searches and increasing the population diversity. The similarity among antibodies is determined in terms of both the objective space and the decision variable space to ensure that only similar antibodies are eliminated in the suppression operation. Moreover, a modified crossover operator originated from the biological evolution was also developed to help further enhance the diversity of the clone population and the convergence of the algorithm because some good genes from the elite parents can be passed to the offspring for facilitating the search of optimal solutions; otherwise it may take a longer time to converge towards the Pareto front [15] especially in simulation-based optimization context.

The algorithm comprises five immune operators, cloning operator, hypermutation operator, suppression operator, selection and receptor editing operator and memory updating operator, and one genetic operator, crossover operator. Each of them takes responsibility for different tasks for the purpose of finding uniformly distributed Pareto front. The cloning operator generates a number of copies to explore the solution space where better individuals are given more chances for being cloned. The hypermutation operator works on the clones to bring variation to the clone population, hoping for producing better offspring and increasing population diversity. The crossover operator is used to enhance the diversity of the clone population and the convergence of the algorithm. The suppression operator works on the whole population including the mutated clones and parent cells to eliminate similar individuals in order to avoid a particular search space being overexploited. The selection and receptor editing operator works like a director to guide the search towards the promising regions of a given fitness landscape by selecting the best antibodies to form the next generation and allowing the genes of the less fit to be randomly restructured for changing their specificity through the receptor editing process. The memory updating operator works as an elitist mechanism for helping preserve the best solutions that represent the Pareto front found over the search process. Both the selection and receptor editing operator and memory updating operator can help avoid the problem of losing good solutions during the optimization process due to random effects. The algorithm is conducted by applying these heuristic and stochastic operators on the antibody population for balancing both the local and global search capabilities. For the details of this hybrid AIS-based algorithm, one can refer to [14].

1.4 Simulation-Based Optimization Study

In this study, two experiments based on the complex real-life multi-objective optimization problem were conducted to evaluate the performance and capability of the optimization approach. All these experiments were conducted using a computer with Xeon E5-2620 2 GHz CPU with 2 GB RAM, and the optimization algorithm was implemented with Excel VBA, whereas the simulation models were developed by using the FlexSim simulation tool [16].

Performance Metrics

In this study, two performance metrics, namely, error ratio (ER) [17] and spacing (S) [18], were adopted to examine the quality of solution set in terms of the optimality and diversity. However, ER was modified by using reference Pareto front PF_{ref} instead of true Pareto front PF_{true} for computing ER. This was because the PF_{true} could hardly be found in simulation-based optimization, and hence we used the reference Pareto front, that is, the best approximation of the true Pareto front "PF_{ref}", for measuring the optimality of each solution set instead. The PF_{ref} was found by using all of the algorithms used in this research. To achieve this, a Pareto front for each algorithm was firstly generated by running 100 iterations over 20 trials, and then, all the fronts obtained by all the trials of all the compared algorithms were merged together to form a reference Pareto front.

Experimental Setup

The distribution operation of the material handling system (MHS) implemented at the distribution centre (DC) of SF Express (Hong Kong) Limited was studied through the simulation-based optimization approach. Its service network covers almost all areas of Hong Kong, which is mainly served by the DC located in Tin Shui Wai (TSW) in northern New Territories (Fig. 1.1). Its service stores are located in 30 areas of Hong Kong [19].

In this study, we focus on the physical goods flow at the DC, where the items are imported from China and then distributed to all parts of Hong Kong. At the DC, the items received at inbound docks are directly transferred to outbound docks and then

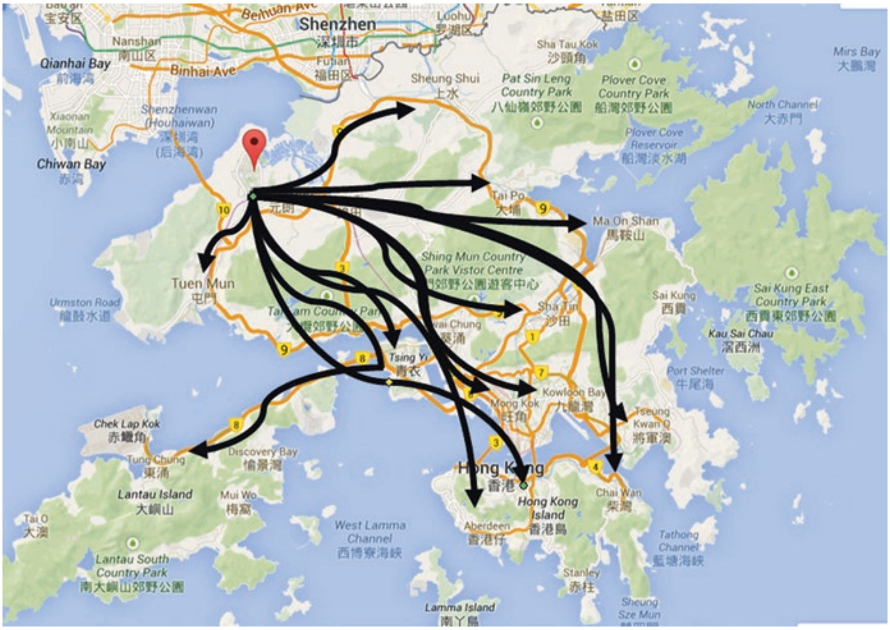

Fig. 1.1 The distribution flow of SF Express's imported goods in Hong Kong

shipped to the final destinations with little material handling in between, such as deconsolidation and sortation. This approach is called cross-docking. To implement cross-docking effectively and efficiently, timely distribution of freight and better synchronization of all inbound and outbound shipments are required by making use of information systems and advanced automated MHS, such as automated conveyor system, warehouse management system, real-time material identification and tracking system (e.g. barcode).

Current Physical Layout and Labour Deployment of the MHS The MHS is a circular shaped automated conveyor system, which comprises a number of interconnected conveyor units. The layout of the MHS is depicted in Fig. 1.2. Each conveyor unit has a programmable logic controller to control the movement (such as speed, direction, etc.) of the items being put on it and to communicate with the central computer. The conveyor system has 4 entrances connecting to 4 inbound docks and 16 exits connecting 30 outbound docks (each outbound dock serves trucks for distributing parcels to one destination).

At each conveyor entrance, seven workers are deployed to unwrap the incoming bulky consolidated parcels uploaded from the big inbound truck (16 tonnes) for facilitating the subsequent sortation process. To enable the distribution process to go well and items to be accurately sorted according to customer requirements, four workers are assigned to each conveyor exit serving two destinations (except two

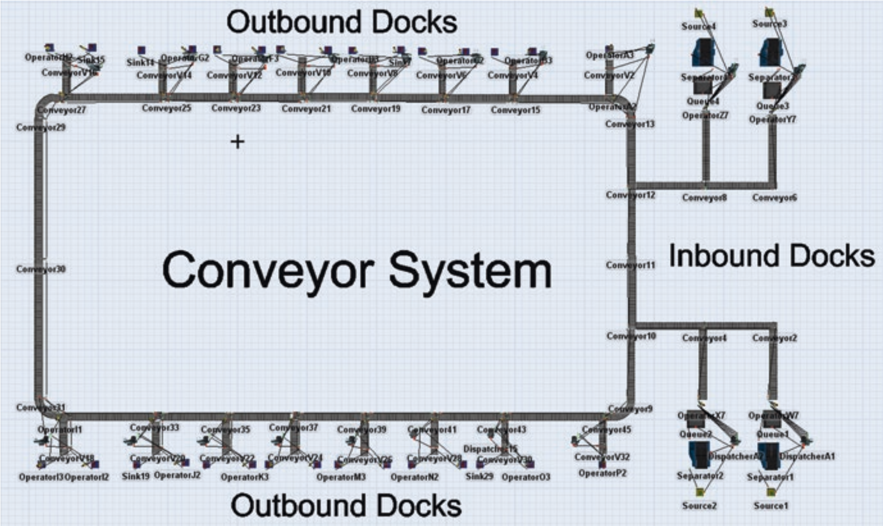

Fig. 1.2 The simulation model of the MHS implemented with FlexSim

exits close to the entrances serving one destination, which require two workers) and equipped a barcode reader for confirming the destination of each small parcel and helping to load the parcel to the small outbound truck (5.5 tons).

Simulation Model The simulation model with specific system configuration and behaviour is implemented with FlexSim (Fig. 1.2). Details of model components and initial model settings (Table 1.1) are as follows:

- Entities are 400 bulky consolidated parcels and 4000 small parcels deconsolidated from the bulky parcels, which are processed through the system causing changes in the system state over time.
- Activities are the deconsolidation of bulky consolidated parcels unloaded from each incoming truck (represented by a source in the simulation model) and the picking of small parcels from the circular conveyor to each outgoing truck (represented by a sink in the simulation model) according to their destinations.
- Item attribute is the product type associated with its destination (one product type corresponds to one specific destination).

Parameter Setting Based on the results of the sensitivity analysis, the parameters of SCMIA were set as follows: SCMIA, initial population size, $N = 30$; size of active population, $N_A = 12$; size of the memory population, $N_m = 30$; maximum number of clones for each cell, $max\_clone = 6$; exponential distribution coefficient, $\rho = 0.05$; and number of simulation replications per fitness evaluation, $replication = 10$. To allow a fair comparison among the algorithms compared, the parameters of the benchmarking algorithms were set with similar values and the values suggested by the authors.

Table 1.1 Initial model settings

Item	Value
Conveyor speed	2.5 m/s (limit: 1–2.5 m/s)
Conveyor spacing	1 parcel
Number of workers deployed for each conveyor entrance	7 workers (limit: 1–9 workers)
Number of workers deployed for each conveyor exit (serving 1 destination)	2 workers (limit: 1–4 workers)
Number of workers deployed for each conveyor exit (serving 2 destinations)	4 workers (limit: 1–6 workers)
Handling capacity of worker	1 parcel
Arrival pattern for each source	Uniform distribution with a min. of 5 s and a max. of 10 s
Processing time of deconsolidation process	Normal distribution with a mean of 30 s and a standard deviation of 2 s
Demand for each destination	Uniform distribution with a min. of 220 units and a max. of 280 units

The above model parameters are set based on the real system settings and observation

Antibody Definition An antibody ab that has the direct impact on the system's performance in terms of cycle time (CT) and workers' utilization (WU) is defined as follows: x_1 is taken to be the conveyor speed, x_2 is the number of workers deployed for each conveyor entrance, x_3 is the number of workers deployed for each conveyor exit (serving two destinations), and x_4 is the number of workers deployed for each conveyor exit (serving one destination). Since the objective of the study is to optimize the performance of the MHS by minimizing the system cycle time and maximizing the workers' utilization, the optimization problem can be given by:

$$\underset{\mathrm{ab}\,\in\,\Omega}{\mathrm{Optimize}}\,\vec{f}\left(\mathrm{ab}\right)=E\left[\mathrm{CT},\mathrm{WU},\omega\right] \tag{1.1}$$

Subject to:

$$1 \le x_1 \le 2.5 \tag{1.2}$$

$$1 \le x_2 \le 9 \tag{1.3}$$

$$1 \le x_3 \le 6 \tag{1.4}$$

$$1 \le x_4 \le 4 \tag{1.5}$$

where a set of objective functions $\vec{f}\left(\mathrm{ab}\right)$ to be optimized in objective space are the expected values of the random output variables [CT, WU, ω] that are obtained from running the simulation model, ω is a sample path (i.e. the sequence of random numbers used in a simulation run), and Eqs. (1.2), (1.3), (1.4), and (1.5) define a set of physical constraints.

Experimental Results and Analysis

We conducted two experiments to evaluate the performance of the optimization approach based on the above-mentioned case study, that is, (1) to compare the results of integrating simulation and optimization with the results without using any optimization algorithm and (2) to benchmark SCMIA against two immune-inspired algorithms, MISA [20] and NNIA [12], and two other evolutionary algorithms, NSGA-II [8] and SPEA2 [9], under the same approach. All algorithms were run for 30 generations over 20 trials to obtain the average performance of each algorithm on the same condition.

Simulation Without Optimization vs. Simulation with Optimization The results shown in Table 1.2 are the optimized results obtained by making use of all optimization algorithms studied in this research.

The table shows that the cycle time of the whole distribution system at the DC reduces by about 12–16% and the workers' utilization increases by 40–51% when optimization algorithms are deployed in the simulation process. This proves that the use of the optimizers can enhance the performance in the system's cycle time and the workers' utilization. However, the higher the utilization achieved, the longer the cycle time spent, and vice versa. When comparing SCMIA with other benchmark algorithms, SCMIA is able to produce comparable results in both of the cycle time and the workers' utilization.

Table 1.2 Performance comparison between simulation without optimization and simulation with optimization (the best results are bolded)

	Cycle time (the improvement in % compared with the one without optimization)	Workers' utilization (the improvement in % compared with the one without optimization)
Simulation without optimization	6788.64 s	45.04%
Simulation-based optimization with SCMIA	5775.45 s (14.92%)	65.60% (45.65%)
Simulation-based optimization with MISA	5792.67 s (14.67%)	64.43% (43.05%)
Simulation-based optimization with NNIA	**5685.49 s (16.25%)**	62.83% (39.50%)
Simulation-based optimization with NSGA-II	5687.71 s (16.22%)	63.09% (40.08%)
Simulation-based optimization with SPEA2	5950.84 s (12.34%)	**67.06% (51.11%)**

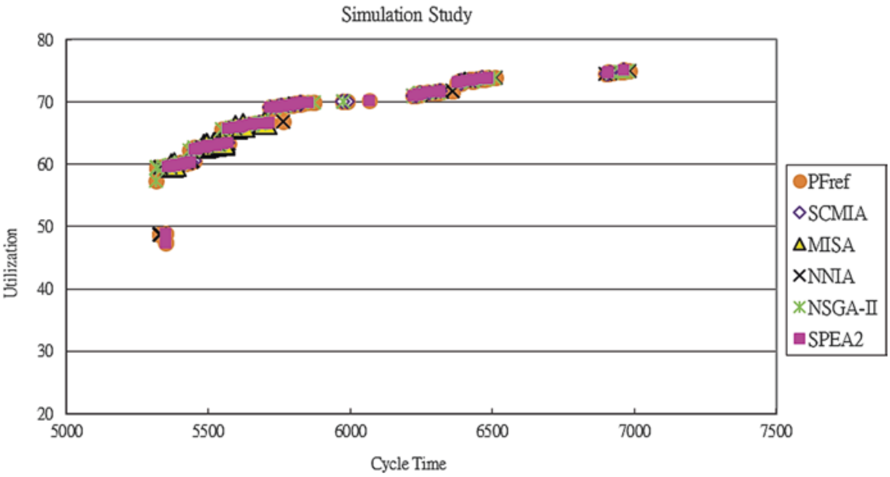

Fig. 1.3 Graphical comparison of the known Pareto fronts generated by the five algorithms

Performance Comparison Between SCMIA and Other Benchmark Algorithms The performance of the algorithms studied was compared by using the graphical representation together with the performance metrics mentioned in section "Performance Metrics". The comparison between the known Pareto fronts shown in Fig. 1.3 suggests that the overall Pareto front patterns generated by the five algorithms are largely similar in which the cycle time ranges from around 5300 s to 7000 s and the workers' utilization ranges from around 50% to 75%. From the figure, it is shown that the higher the utilization achieved, the longer the cycle time spent, and vice versa. This implies that increasing the utilization does not mean that the efficiency of the system can be increased. Therefore, although the optimal solution with 75% utilization while spending almost 7000 s and another case achieving less than 50% utilization while spending only around 5300 s both fall within the reference Pareto front PF_{ref}, the latter case is preferred in practice because the cycle time is much shorter, and hence the efficiency and productivity of the system are much higher. The utilization becoming lower in the latter case is mainly due to the increased values in the decision variables, namely, conveyor speed and number of worker. This implies that in order to further enhance both objectives at the same time for the DC, the company may need to do something other than just changing the system parameters, such as redesigning the layout of the conveyor system.

The performance regarding the optimality and the diversity of SCMIA in this multi-objective optimization problem was then examined. In this experiment, we compared the results of the mean and standard deviation of the 2 metrics over 20 trials obtained by SCMIA with that of the other benchmark algorithms. From the results shown in Table 1.3, we found that SCMIA generally is able to provide the best results in terms of the diversity and the optimality because it generates the low-

Table 1.3 Spacing and error ratio values generated by the five algorithms (the best results are bolded)

	SCMIA	MISA	NNIA	NSGA-II	SPEA2
	Mean (standard deviation)				
Error ratio (ER)	**0.71 (0.12)**	0.83 (0.17)	0.79 (0.18)	0.77 (0.15)	0.74 (0.06)
Spacing (S)	**38.83 (11.82)**	60.79 (53.90)	49.44 (28.22)	51.45 (17.47)	39.00 (35.58)

est values in the metrics of ER (0.71) and S (38.83) and the latter metric is significantly lower than most of the other algorithms. This implies that the generated front is very close to the PF_{ref}. In terms of the stability, SCMIA is also the best one among these five algorithms in error ratio and spacing because it has much lower standard deviations (0.12) and (11.82), respectively, than other algorithms except SPEA2, implying that SCMIA is able to provide a relatively consistent result for each trial.

Discussion Based on the results of the case study, SCMIA generally performs better than other benchmark algorithms especially in the diversity aspect. This is largely attributed to the operators employed in the algorithm. For example, the selection operator incorporates the crowding distance as a measure to select nondominated antibodies for undergoing the subsequent evolutionary processes so that the antibodies in less crowded regions will have a higher priority to be selected. The cloning operator and hypermutation operator are based on the same measure to generate a number of copies for exploring the solution space and bringing variation to the clone population, respectively, where less crowded individuals are given more chances for cloning and hypermutation in order to hopefully produce better offspring and increase population diversity. The crossover operator helps further enhance the diversity of the clone population and the convergence of the algorithm because some good genes from the active parent can be passed to the offspring. The suppression operator helps reduce antibody redundancy by eliminating similar individuals, hence significantly minimizing the number of unnecessary searches and increasing the population diversity. The memory updating operator takes account of the antibody similarity in terms of both the objective space and the decision variable space to formulate the memory population. As a result, SCMIA is able to generate a well-distributed set of solutions, while it is a good approximation to the reference Pareto front.

The results overall demonstrate the ability of the simulation-based optimization approach to serve as a decision support tool for helping management to effectively and efficiently find near-optimal system operating conditions and parameters such as the number of workers, the speed of various kinds of machines or any other decision variables of interest to fulfil different objectives including cycle time, machine utilization, etc. As a result, significant savings in money, energy, etc. are achieved through the cost-effective and efficient deployment of material handling systems and well-coordinated processing activities based on the optimized results generated from the approach.

1.5 Conclusion

This study applies a multi-objective simulation-based optimization approach incorporating a hybrid AIS-based optimization algorithm SCMIA for evaluating the optimality of the distribution system with respect to the two criteria – system cycle time and workers' utilization through simulation modelling.

Based on the findings of the current undertaking, it is worthwhile to extend the approach to tackle other complex problems involving many objectives to be considered in an efficient and effective manner in the future. Future research could also extend this approach to solve real-world complex business problems with real-world dynamics such as time-varying demand and supply and to solve other large-scale problems with a large number of parameters, operators and equipment involved in order to establish the practical value of the approach in the simulation-based optimization context.

References

1. Rosen, S.L.: Automated Simulation Optimization of Systems with Multiple Performance Measures Through Preference Modeling. Pennsylvania State University, Pennsylvania (2003)
2. Elahi, M.M.L., Záruba, G.V., Rosenberger, J., Rajpurohit, K.: Modeling and Simulation of a General Motors Conveyor System Using a Custom Decision Optimizer. University of Texas at Arlington, Arlington (2009)
3. Leung, C.S.K., Lau, H.Y.K.: An optimization framework for modeling and simulation of dynamic systems based on AIS. In: International Federation of Automatic Control World Congress, Italy, p. 11608 (2011)
4. Subulan, K., Cakmakci, M.: A feasibility study using simulation-based optimization and Taguchi experimental design method for material handling—transfer system in the automobile industry. Int. J. Adv. Manuf. Technol. **59**, 433–443 (2012)
5. Chang, K.-H., Chang, A.-L., Kuo, C.-Y.: A simulation-based framework for multi-objective vehicle fleet sizing of automated material handling systems: an empirical study. J. Simul. **8**, 271–280 (2014)
6. Lin, J.T., Huang, C.-J.: Simulation-based evolution algorithm for automated material handling system in a semiconductor fabrication plant. In: Proceedings of 2013 4th International Asia Conference on Industrial Engineering and Management Innovation (IEMI2013), Berlin, Heidelberg, pp. 1035–1046 (2014)
7. Nam, D., Park, C.: Multiobjective simulated annealing: a comparative study to evolutionary algorithms. Int. J. Fuzzy Syst. **2**, 87–97 (2000)
8. Deb, K., Agrawal, S., Pratap, A., Meyarivan, T.: A fast elitist non-dominated sorting genetic algorithm for multi-objective optimisation: NSGA-II. In: 6th International Conference on Parallel Problem Solving from Nature, pp. 849–858 (2000)
9. Zitzler, E., Laumanns, M., Thiele, L.: SPEA2: Improving the Strength Pareto Evolutionary Algorithm, Computer Engineering and Communication Networks Lab (TIK). Swiss Federal Institute of Technology (ETH), Zurich (2001)
10. Coello Coello, C.A., Pulido, G.T.: A micro-genetic algorithm for multiobjective optimization. In: Zitzler, E., Thiele, L., Deb, K., Coello Coello, C., Corne, D. (eds.) Evolutionary Multi-Criterion Optimization, vol. 1993, pp. 126–140. Springer, Heidelberg (2001)

11. Coelho, G., Von Zuben, F.: omni-aiNet: an immune-inspired approach for omni optimization, pp. 294–308 (2006)
12. Gong, M., Jiao, L., Du, H., Bo, L.: Multiobjective immune algorithm with nondominated neighbor-based selection. Evol. Comput. **16**, 225–255 (2008)
13. Zhang, Z.: Artificial immune optimization system solving constrained omni-optimization. Evol. Intell. **4**, 203–218 (2011)
14. Leung, C.S.K., Lau, H.Y.K.: A hybrid multi-objective immune algorithm for numerical optimization. In: 8th International Joint Conference on Computational Intelligence, Porto, Portugal, pp. 105–114 (2016)
15. Coello Coello, C., Lamont, G.B., Veldhuizen, D.A.V.: Evolutionary Algorithms for Solving Multi-Objective Problems, vol. 5, 2nd edn. Springer, New York (2007)
16. Flexsim Software Products Inc: (1 July 2016). www.flexsim.com
17. Van Veldhuizen, D.A.: Multiobjective Evolutionary Algorithms: Classifications, Analyses, and New Innovations. Air Force Institute of Technology/Wright-Patterson Air Force Base, Ohio (1999)
18. Schott, J.: Fault Tolerant Design Using Single and Multicriteria Genetic Algorithm Optimization. Massachusetts Institute of Technology, Cambridge (1995)
19. S.F. Express (Hong Kong) Limited: (16 Apr 2016). http://www.sf-express.com/hk/tc/
20. Coello Coello, C.A., Cortés, N.C.: Solving multiobjective optimization problems using an artificial immune system. Genet. Program. Evol. Mach. **6**, 163–190 (2005)

Chapter 2
Dataspace Management for Large Data Sets

Marko Niinimaki and Peter Thanisch

2.1 Introduction

Ever since researchers started talking about "Big Data," they have mentioned troubles related to it, alongside of its benefits [1]. These troubles often arise from the sheer volume of data but can also involve difficulties of processing, integrating, and analyzing the data. Indeed, an insightful definition of "Big Data" states that a data set can be called Big Data if it is formidable to perform capture, curation, analysis, and visualization on it using the current technologies [2].

However, these troubles sound familiar to computer scientists who have been exposed to statistical databases. Despite progress in data integration [3], use of an integrated business intelligence platform often requires a nontrivial process of identifying data sources, deciphering the meaning of their data, harmonizing the data, and then loading it into a system that can be used to analyze it. This process is known as ETL (Extract-Load-Transform) [4], and in business intelligence the resulting data often ends up in data warehouse servers and, when needed by an analyst, in online analytical processing (OLAP) cubes [5].

But in many organizations, ETL skills are in short supply, and incorporating a new ETL process into a production environment is a lengthy and arduous process. So what happens to the data sources that we find potentially interesting, yet we are unable to include in our current ETL processes? In the mid-2000s, the concept of dataspaces was introduced to describe a situation where there is "some identifiable scope and control across the data and underlying systems, and hence one can

M. Niinimaki (✉)
Department of Business and Technology, Webster University Thailand, Bangkok, Thailand
e-mail: niinimakim@webster.ac.th

P. Thanisch
School of Information Sciences, University of Tampere, Tampere, Finland
e-mail: peter.thanisch@sis.uta.fi

P. Vasant et al. (eds.), *Innovative Computing Trends and Applications*,
EAI/Springer Innovations in Communication and Computing,
https://doi.org/10.1007/978-3-030-03898-4_2

identify a space of data, which, if managed in a principled way, will offer significant benefits to the organization" [6]. Moreover, a dataspace support platform (DSSP) provides services for managing such collections of data. Specifically, a DSSP should provide services helping to identify sources in a dataspace and interrelate them, offering basic query mechanisms over them, including the ability to introspect about their contents [3].

In this paper, we present a DSSP specifically designed for data integration using Microsoft Excel data models [7]. The design of the DSSP is workflow-oriented: the user uploads the data sets in the DSSP and describes the semantics of the data by filling a form provided by the DSSP. This metadata can be utilized when the data is imported into the user's data model. We specifically address the problem known as *summarizability* [8, 9], by including in the DSSP metadata information needed to determine summarizability in OLAP. Moreover, we describe a process for utilizing the metadata when designing Excel data models using the DAX (Data Analysis Expression) language [10] and Excel's graphical data model designer.

Our aim is to build and support a dataspace where the data is used within an organization (like a university). This approach corresponds to Halevy et al.'s use case of a dataspace for scientific data management [3]. In other related research, Dittrich [11] presents iMeMex, a comprehensive personal data search and management system that unfortunately is no more functional. Mirza et al. discuss the practicality of a dataspace system from a user's point of view, mentioning specifically the challenge of combining online and local data sources [12]. Moilanen et al. [13] demonstrate a harmonization platform for XML, but their system is not very suitable for large data sets. Niinimaki and Niemi [14] demonstrate an ETL process with RDF/XML data, but do not discuss how the RDF ontologies and instances are built and populated. Contrary to these approaches, we emphasize a dataspace as a repository of large data sets, the design of data models, and verify the data model using the dataspace. The design of our platform supports the workflow described above.

In our use case, we use real data with magnitude of tens of millions of observations, demonstrate real analysis cases using the data model, and evaluate the performance of our system.

The rest of the paper is organized as follows. In Sect. 2.2, we describe the data that we plan to analyze. This serves as a generalizable basis for Sect. 2.3 that describes the design of our DSSP, and in Sect. 2.4 we study the system's performance. Finally, Sect. 2.5 contains a summary, research questions for future work, and conclusions.

2.2 Data and Summarizability

Our sample analysis concerns trade of electronic goods among various countries, and the data for the analysis comes from many sources. The most important data sets in the analysis are import-export data from UN COMTRADE (international

Export-of-commodities-2000s: Year, exporting country (reporter), importing country (partner), type of commodity (prod), value of trade in USD. Field prodgroupcode is derived from prod.
Prodgroup: HS 2-digit product group, product group's English name.
Cia_factbook_country_gdp: Country (ISO3 code), GDP per capita purchasing parity adjusted in 2004 USD.
Countrycodes: ISO3 codes and English names for countries and autonomous areas.

Fig. 2.1 Data set descriptions

trade statistics database),[1] HS (Harmonized System) trade group descriptions from the same source, and per-country GDP per capita figures from *CIA World Factbook.*[2] Moreover, we have written a program that translates country names used in *CIA World Factbook* and Wikipedia in ISO3 county codes and a program to download tables from Wikipedia in the CSV (comma-separated values) format.

All the data sets deal explicitly with countries on a yearly basis; thus a potential integration of the data is not especially hard. Yet, we need to ensure that roles like exporter and importer are sufficiently well expressed. The main data sets, as extracted, are shown in Fig. 2.1. The export-of-commodities set covers years 2000–2015 and has about 94 million lines. As a demonstration of data analysis after data integration, we have selected the following scenario: A company interested in producing electronics goods is seeking to expand outside high-income countries. An analyst is tasked to find out which low- and middle-income countries had largest increases in electronics exports in recent years (2000–2015).

In a multidimensional data model, there is a set of numeric measures that are the objects of analysis. Each of the numeric measures depends on a set of dimensions, which provide the context for the measure [5]. An implementation of this model is called a dimensional database or a cube. Figure 2.2 shows the data and relations prepared for a cube. Dimensions in a cube can be hierarchical, as product—product group. The entire hierarchy is called a dimension and product, and product groups are called its levels.

Within Excel, columns of data tables can be connected with a relation if they are compatible. Here we use simple technical criteria for compatibility of two columns: at least one of the columns must have unique values and both columns must share some values. The connected columns in Fig. 2.2 in export-of-commodities-2000s are reporter and partner to countrycode's ISO3 code and to cia_factbook's country, productgroupcode to prodgroup's prodgroupcode.

Summarizability can be informally defined as "correctness of aggregate data with respect to individual observations." In practice, this means that when a user queries a cube, the query should be inspected in such a way that the query's result cannot violate the conditions of summarizability. Niemi et al. [9] formulate the conditions as follows: (1) the aggregation operation (usually sum, mean, or count) is

[1] http://comtrade.un.org.

[2] https://www.cia.gov/library/publications/the-world-factbook/.

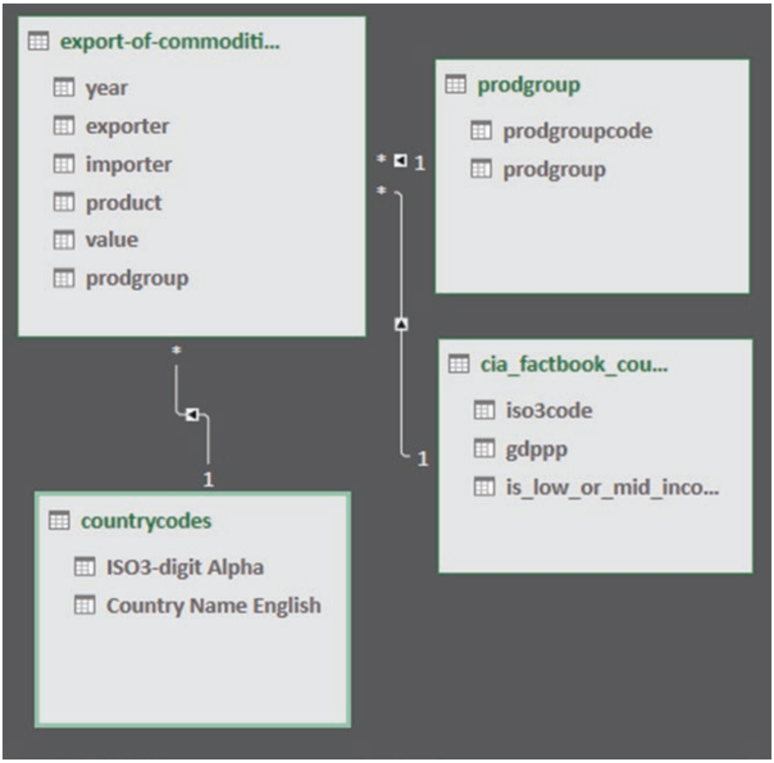

Fig. 2.2 Relations in the model

appropriate for the measure, and (2) the measure is appropriate for the aggregation levels in the cube's dimensions. We are specifically interested in:

- The statistical scales of measure variables (see [15]), nominal, ordinal, interval, and ratio scales, since they affect which aggregation operation can be applied to the data.
- The "eventness" type of measure variable. These we classify [9] as (1) tally measures that are intrinsic information about a specific event like quantity sold in sales data, (2) reckoning measures like inventory levels, and (3) snapshot measures that are indirect measurement based on data at hand like currency exchange rates.

With our dataspace system, we help the analyst detect problems with summarizability by collecting characteristics of data like the statistical scales and eventness of measures. Our ultimate goal is to construct a system that automatically detects summarizability problems in pivot tables created by data analysts.[3] The design of

[3] Niemi et al. [9] present an algorithm that discovers the correctness of additivity in OLAP queries expressed in an MDX-like query language. However, in addition to the statistical scale and "eventness," the algorithm uses "measure depends on dimension" information: for instance, a currency measure depends on country dimension. This kind of information is harder to provide in a dataspace application.

system at hand is less ambitious: the dataspace system lets us identify potential dimensions and measures and dimensions that are compatible. The compatibility of data within Excel is then checked by a macro that gets the information from the dataspace system. Details of the design of the dataspace system and its integration with Excel are given in the next section.

2.3 System Design

The goal of the design is to provide a catalogue of data sets, combined with their metadata. The users will upload data sets of their interest into the catalogue. After each upload the catalogue software lets the user specify a description of the data set. The data set is expected to have recognizable fields that represent potential measures or (levels of) dimensions. For each measure the user will record its statistical scale, “eventness,” and unit of measurement. For each dimension, the user will record a description and a set of fields in other data sets such that the dimension is compatible with them. The compatibility of fields is stored in the XML format to a file (compatibility.xml) accessible by the HTTP protocol. An interface for entering the metadata (and field compatibility data) after a file upload is shown in Fig. 2.3.

The uploaded data sets with their metadata are presented using a web interface shown in Fig. 2.4.

The dataspace management application is a Python program that utilizes the Flask web programming framework [16].

In our case study, a company is interested in expanding their business as described in the introduction: among low- and medium-income countries, which ones have grown their exports in electronics most during 2000–2015. The following data sets are thus selected using the interface shown in Fig. 2.4: export-of-commodities-2000s, prodgroup, cia_factbook_countries_by_gdppp, and countrynames_iso3. Assisted by the user interface (Fig. 2.4) or by using the DAX language, the data analyst imports the data in Microsoft Excel’s data model [17] and creates the relations within the data, as was shown in Fig. 2.2.

We can now verify some basic aspects of the data models using our verifier macro. We assume that the user has imported the data sets from the dataspace system as Excel tables, either as tables within Excel sheets or in the data model. The

Fig. 2.3 Metadata editor

Set name	Lines	Description	Fields
countrynames-iso3.csv	287	Country names with ISO3 counterparts	Country Name English:English name ISO3-digit Alpha:ISO3 code
cia_factbook_countries_by_gdppp.csv	231	Countries by GDP purch parity adjusted in 2004 USD	gdppp:GDP purch parity adjusted in 2004 USD -measure:USD -scale:ratio iso3code:ISO 3 letter code of the country
export-of-commodities-2000s.csv	94904739	Export of commodities COMTRADE 2000-1015	partner:importer prodcode:product code reporter:exporter value:value of trade -eventness:tally -measure:USD -scale:ratio year:year of trade

Fig. 2.4 Some uploaded data sets with metadata

Fig. 2.5 Excel macro compatibility warning

relations within the data can be expressed either using DAX-"related" expressions or using a graphical tool.[4] The verifier macro has two data sources:

- Compatibility of dimension fields as recorded in the compatibility.xml file (see above)
- The relations of tables accessible by the Excel VBA API as "primary table name/ primary column name" and "foreign table name/foreign column name"

By comparing the data set and column names in each of the sources, the macro prints if the fields are compatible.[5] If the macro discovers incompatibilities, it displays a message as in Fig. 2.5.

In our analysis case, a few adjustments to the data need to be done before the findings can be presented. First, a dummy field "is_low_or_mid_income" is introduced to the cia_factbook_countries_by_gdppp data, since it will be used as a

[4] In its simple form, DAX-related expressions state that a value in table$_1$/column$_a$ has a counterpart in table$_2$/column$_b$ like a country's ISO3 code has a country name counterpart. The graphical tool lets the users connect tables by their columns. For instance, trade data's exporter is given as an ISO3 code that we connect with country data's ISO3 column.

[5] In more detail: the macro iterates over data sources d and each data source's each field df. The names of the data sources and the fields are assumed to be the same as in the dataspace system. If a data source field d_if_j is connected to another d_kf_l, the macro tries to find the following entry in the compatible. xml file: <compatible><file>d_i</file><field>f_j</field><file>d_k</file><field>f_l</field></compatible>.

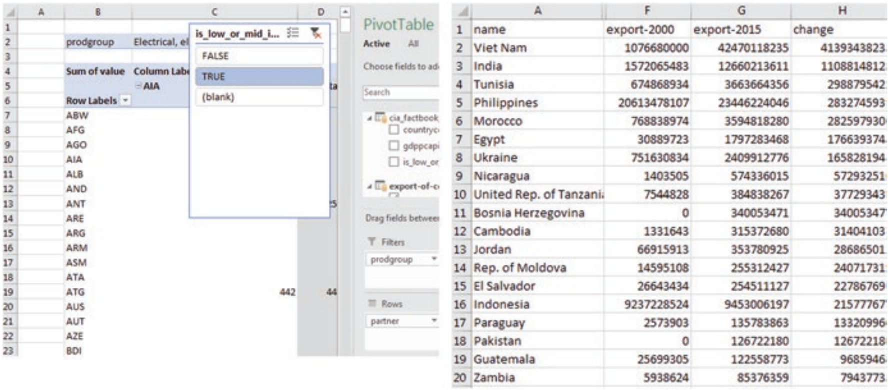

	A	F	G	H
1	name	export-2000	export-2015	change
2	Viet Nam	1076680000	42470118235	4139343823
3	India	1572065483	12660213611	1108814812
4	Tunisia	674868934	3663664356	298879542
5	Philippines	20613478107	23446224046	283274593
6	Morocco	768838974	3594818280	282597930
7	Egypt	30889723	1797283468	176639374
8	Ukraine	751630834	2409912776	165828194
9	Nicaragua	1403505	574336015	57293251
10	United Rep. of Tanzani	7544828	384838267	37729343
11	Bosnia Herzegovina	0	340053471	34005347
12	Cambodia	1331643	315372680	31404103
13	Jordan	66915913	353780925	28686501
14	Rep. of Moldova	14595108	255312427	24071731
15	El Salvador	26643434	254511127	22786769
16	Indonesia	9237228524	9453006197	21577767
17	Paraguay	2573903	135783863	13320996
18	Pakistan	0	126722180	12672218
19	Guatemala	25699305	122558773	9685946
20	Zambia	5938624	85376359	7943773

Fig. 2.6 Pivot table (left) and analysis based on the data model (right)

filter in the pivot table. Second, a product group code is added in the export-of-commodities-2000s data. The product group is simply the 2 first digits of the trade product HS code, 85 for electrical, electronic equipment, whereas the "prod" field in the export-of-commodities-2000s data is 6-digit, for instance, 850,890 for "parts, hand tools with self-contained electric motor."[6] Figure 2.6 shows the design of the pivot table such that we apply filters "exporter only low- and middle-income countries" and "product group only electrical, electronic equipment." Moreover, the figure demonstrates the result of the analysis.

2.4 Performance Measurements

In this section we discuss the time consumed in loading the data and the overhead imposed by the dataspace management system. The tests were performed on a computer with Intel Core i5 dual-core 2.4 GHz CPU, 4 GB RAM, and a normal 500 GB 7200 rpm disk. The operating system was 64-bit Windows 7 Enterprise with Microsoft Excel 2016 MSO 64-bit.

Performance of the Dataspace Application

We have tested the dataspace application with multiple random generated files in addition to real files discussed in Sect. 2.3. To eliminate network delays, the tests were performed on the same computer where the application was running. The upload speed is ca 5 MB/s and the download speed ca 38 MB/s. The size of the largest file, export-of-commodities-2000s, was 2.3 GB. Its upload time was 7 min 37 s and download time 1 min 3 s.

[6] https://comtrade.un.org/db/mr/rfCommoditiesList.aspx.

Data Loading Performance

Since the export of commodities 2000–2015 data set is very large, it had a dominant role when loading data into Excel's data model. We have used both this data set and artificially constructed sets to determine the performance. Overall, with our hardware configuration, Excel reads data from CVS files into its data model at ca. 1 million lines per minute, and the performance remains linear. Loading the export-of-commodities-2000s data set took 8 min 30 s, and generating the pivot table of Fig. 2.5 from the data took about 1 min.

2.5 Summary, Conclusions, and Future Work

In this paper we have presented a web-based dataspace management system for large data sets. Our principal aim is to help data analysts discover problems with data integration. This is done by storing the data sets together with their metadata. The metadata includes scale, "eventness," and unit for measures and a list of compatible fields for dimensions.

The web software was build using the Python Flask framework, available for Microsoft Windows and other operating systems. The software is freely available at https://sourceforge.net/projects/simple-dataspace-management.

Our future research will have three focus areas: summarizability, platform, and cloud integration.

We aim at providing full integrated support to detecting summarizability when the analyst creates an OLAP cube based on the data model. For this purpose we shall improve the "verifier" Excel macro so that it will be able to inspect all DAX language formulas from a pivot table. Since aggregation can be done using the DAX language, the macro will be able to compare the DAX aggregation formula with the metadata from the data management system and find out if the aggregation is correct in terms of summarizability.

The second focus is the dataspace platform itself. We shall expand the dataspace software to make it more user-friendly and capable of storing/inspecting data in various formats. Moreover, we are working on a feature that allows the user to test designs for OLAP cubes using the platform. Figure 2.7 demonstrates the feature: the user has selected the data sets and their fields, and the software analyzes if the combination will produce a good joined data set.

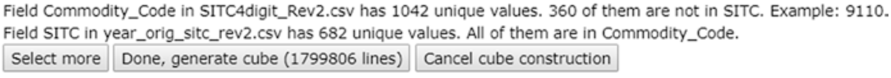

Fig. 2.7 Tools for analysis joining data

The third focus is obvious: when dealing with Big Data, cloud systems are its natural habitat (see [18]). We have started regrafting the dataspace manager as a Google Cloud [19] application, and the results have been promising.

Acknowledgments The authors wish to thank COMTRADE for the access to their export data and Dr. Leslie Klieb for comments.

References

1. McFedries, P.: The coming of data deluge. IEEE Spectrum. **48**, 19 (2011)
2. Chen, P., Zhang, C.-Y.: Data-intensive applications, challenges, techniques and technologies: a survey on big data. Inf. Sci. **275**, 314–347 (2014)
3. Halevy, A., Franklin, M., Maier, D.: Principles of dataspace systems. In: Proceedings of the Twenty-Fifth ACM SIGMOD-SIGACT-SIGART Symposium on Principles of Database Systems, 2006
4. Rahm, E., Do, H.H.: Data cleaning: problems and current approaches. IEEE Data Eng. Bull. **23**, 3–13 (2000)
5. Chaudhuri, S., Dayal, U., Vivek, N.: An overview of business intelligence technology. Comm. ACM. **54**(8), 88–98 (2011)
6. Franklin, M., Halevy, A., Maier, D.: From databases to dataspaces: a new abstraction for information management. ACM Sigmod Rec. **34**(4), 27–33 (2005)
7. Winston, W.: Microsoft Excel Data Analysis and Business Modeling, 5th edn, p. 864. Microsoft Press, Redmond (2016)
8. Lenz, H.-J., Shoshani, A.: Summarizability in OLAP and statistical data bases. In: Proceedings of the Ninth International Conference on Scientific and Statistical Database Management, 1997
9. Niemi, T., Niinimäki, M., Thanisch, P., Nummenmaa, J.: Detecting summarizability in OLAP. Data Knowl. Eng. **89**, 1–20 (2014)
10. Harinath, S., Pihlgren, R., Guang-Yeu Lee, D., Sirmon, J., Bruckner, R.R.: Professional Microsoft SQL Server 2012 Analysis Services with MDX and DAX. Wiley, Hoboken (2012)
11. Dittrich, J.-P.: iMeMex: a platform for personal dataspace management. In: Proceedings of Workshops of International ACM SIGIR Conference on Research and Development in Information Retrieval, 2006
12. Mirza, H.T., Chen, L., Chen, G.: Practicability of dataspace systems. Int. J. Digital Content Technol. Appl. **4**, 3 (2010)
13. Moilanen, K., Niemi, T., Näppilä, T., Kuru, M.: A visual XML dataspace approach for satisfying ad hoc information needs. J. Assoc. Inf. Sci. Technol. **66**(11), 2304–2320 (2015)
14. Niinimaki, M., Niemi, T.: An ETL process for OLAP using RDF/OWL ontologies. J. Data Semantics. **XIII**, 97–119 (2009)
15. Stevens, S.: On the theory of scales of measurement. Science. **103**(2684), 677–680 (1947)
16. Grinberg, M.: Flask Web Development: Developing Web Applications with Python. O'Reilly Media, Sebastopol (2014)
17. Winston, W.: Microsoft Excel Data Analysis and Business Modeling. Microsoft Press, Redmond (2016)
18. Hashem, I.A.T., Yaqoob, I., Anuar, N.B., Mokhtar, S., Gani, A., Khan, S.: The rise of "big data" on cloud computing: review and open research issues. Inf. Syst. **47**, 98–115 (2015)
19. Cusumano, M.: Cloud computing and SaaS as new computing platforms. Commun. ACM. **53**(4), 27–29 (2010)

Chapter 3
Influence of the Direction of Air Movement in the Microwave-Convection Drier on the Energy Intensity of the Process

Alexey Vasilyev, Dmitry Budnikov, Alexey A. Vasilyev, Nelli Rudenko, and Natalya Gracheva

3.1 Introduction

The use of electrotechnologies in grain drying allows to reduce energy consumption of the process and to increase the productivity of equipment. In FSAC VIM, studies are carried out on microwave-convective grain drying [1–3], and as a result of these studies, a system of algebraic equations and transfer functions describing heat and moisture exchange in the grain layer is obtained [4, 5].

With the use of this system of algebraic equations and transfer functions, a computer model of heat and moisture exchange in the grain layer has been developed, and the model considers the influence of a microwave field and a drying agent on the grain. To develop the model, Simulink was used [6].

3.2 Principles of the Computer Model Design

Usage of the staircase calculation method [7] has allowed to develop a drying model for a dense layer of grain based on the computer model of an elementary layer [8].

A. Vasilyev (✉) · D. Budnikov · A. A. Vasilyev
Federal State Budgetary Scientific Institution "Federal Scientific Agroengineering Center VIM" (FSAC VIM), Moscow, Russia

N. Rudenko
Federal State Budgetary Scientific Institution "Federal Scientific Agroengineering Center VIM" (FSAC VIM), Moscow, Russia

Azov-Black Sea Engineering Institute FGBOU VO Donskoy GAU, Zernograd, Russia

N. Gracheva
Azov-Black Sea Engineering Institute FGBOU VO Donskoy GAU, Zernograd, Russia

P. Vasant et al. (eds.), *Innovative Computing Trends and Applications*,
EAI/Springer Innovations in Communication and Computing,
https://doi.org/10.1007/978-3-030-03898-4_3

Table 3.1 Experimental data on the influence of grain moisture content and the distance to the magnetron on the energy absorbed by a unit of grain volume

Grain moisture content, W (%)	Distance to the magnetron along the axis, L (cm)	Energy per volume absorbed by grain at the control point, Qv (kJ/m^3)
21.3	3	3180.3
17.8	6	1646.2
16.9	9	913.9
15.9	3	3090.4
15	6	1632.5
13.9	9	911.4
12	3	3235.4

When constructing a computer model for microwave-convective drying of a grain layer, the results of investigations on the distribution of the microwave field in the microwave core were taken into account. Since the energy absorbed by a unit of grain varies depending on the moisture content of the grain and the distance to the magnetron, a two-factor experiment was conducted to determine this relation [9]. The results of the experiment are partially shown in Table 3.1.

Using the experimental data obtained, regression analysis was performed and the following regression model was obtained:

$$Qv = 5778 - 14{,}92\mathrm{W} - 846{,}2\mathrm{L} + 0{,}2332\mathrm{W}^2 - 3{,}727\mathrm{W}\cdot\mathrm{L} + 42{,}74\mathrm{L}^2. \quad (3.1)$$

The regression analysis was performed using MATLAB. Coefficients of the model are significant by the Student's criterion. The adequacy of the model was tested by the Fisher criterion. Indicators evaluating accuracy of the model are the following: SSE, 1.409×10^6; R-squared, 0.9731; adjusted R-squared, 0.9698; and RMSE, 185.4, which shows a good level of reliability of the model.

The regression Eq. (3.1) is used in the computer model, which allows to simulate the change in the energy density of the microwave field in the grain layer during the process of drying.

The thickness of the grain layer, which undergoes microwave-convective processing, was taken equal to 15 cm. Such thickness is comparable to the depth of penetration of the microwave field into the wheat grain layer of the normal moisture content (14%). It was assumed that the grain layer can be divided into sections of 5 cm thick, within which the microwave field is evenly distributed. Simulink model of the 15-cm-thick grain layer, divided into three layers of 5 cm, is shown in Fig. 3.1.

In the model, the grain layer is represented by three blocks "Grain layer," in each of which the microwave field has a different intensity, by analogy with the real grain layer. The drying agent successively passes through all the layers. Input parameters of the drying agent are set with the help of the blocks Tvh and Fvh.

With the help of the Relay block, switching on and switching off of the magnetrons are controlled. The magnetrons are switched off when the temperature of the grain reaches 55 °C at the point of maximum power of the microwave field. The

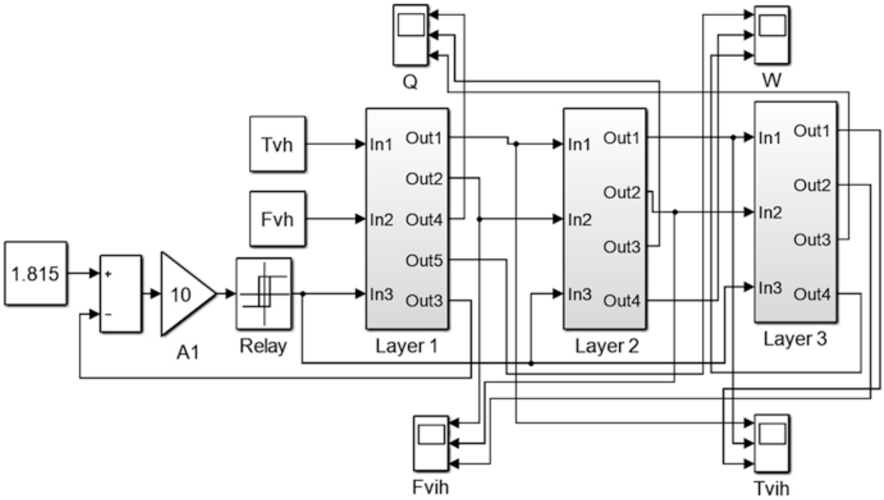

Fig. 3.1 Computer model of heat and moisture exchange in the grain layer under microwave-convective processing

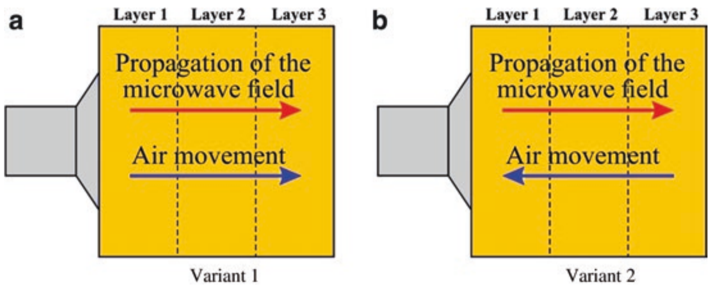

Fig. 3.2 Layout of the grain layers and distribution of the microwave field and drying agent in them. (**a**) Variant 1. (**b**) Variant 2

oscillograms display graphs of grain temperature change in each layer (block Q), grain moisture in the layers (block W), relative humidity of air going out of each grain layer (Fvih), and temperature of the drying agent going out of each grain layer (Tvih) [10].

When developing the design of microwave-convective zones, the direction of movement of the drying agent, its temperature, and uniformity of distribution in the grain layer are of great importance. Proceeding from this, modeling of the microwave-convective grain drying process was carried out. Figure 3.2 shows the schematic diagram of positions of the grain layers, propagation of the microwave field, and movement of the drying agent.

In the first variant of movement of the drying agent, it first passes through the grain Layer 1. Since this layer is closest to the source of the microwave field, it must have higher temperature than Layers 2 and 3. Therefore, when air passes successively through Layer 1 → Layer 2 → Layer 3, it must be heated from the grain in Layer 1. Then, air temperature might both decrease or be maintained at a constant level—it all depends on the specific modes of grain drying.

In the second variant of air distribution, it moves from Layer 3, in which the microwave field has the smallest power. Therefore, the change in the grain temperature and humidity of the drying agent depends on the initial parameters of the air supplied to Layer 3.

3.3 Results of Modeling

Figure 3.3 presents the results of modeling the change in grain temperature in the layers. The simulation was carried out with the following initial parameters: $W_0 = 22\%$, $F_0 = 65\%$, $T_0 = 20$ °C, and $V = 0.5\frac{m}{s}$.

With the relative air humidity of 65%, the equilibrium moisture content of the grain is 14%. This value of the relative air humidity is taken in order to estimate how drying of grain in the layers distant from the magnetron will change. It can be seen from the graphs that the air distribution scheme significantly affects the change of the grain temperature in the microwave-convective zone. With the first variant of air distribution, there is a significant difference in heating of the grain along the layers in the beginning of the drying process. Then, the difference in heating of the grain decreases and stays within 3 °C until the grain dries out. The maximum temperature does not exceed 55 °C. This allows to say that the microwave-convective drying process is sufficiently controlled in order to ensure the preservation of the technological qualities of the grain.

With the second variant of air distribution, the difference in heating of the grain zones is even higher than with the first variant. Moreover, the difference in heating of the grain between Layer 1 and Layers 2 and 3 changes insignificantly during the drying process. Layer 3 is less affected by the microwave field, so grain temperature there does not increase significantly. Besides, it is constantly affected by the drying agent having the temperature of 20 °C. Therefore, temperature of Layer 3 does not exceed 35 °C.

Herewith, air heated by the grain in Layer 3 enters Layer 2. Density of the microwave field in Layer 2 is also higher than in Layer 3. Therefore, temperature of the grain in the layer already reaches 37–39 °C. In Layer 1 of the grain, the maximum power of the microwave field is emitted, so the magnetron is switched off when the grain temperature reaches 55 °C. And air in Layer 1 is already heated from Layer 2, so the fluctuations in the temperature of grain heating in Layer 1 are minimal.

The increase in temperature of the air, when it passes through the grain layer, affects its moisture-absorbing capacity. This can significantly affect the speed of grain drying in the layers. To discover the dependency, modeling of moisture content dynamics was carried out. The simulation results are shown in Fig. 3.4.

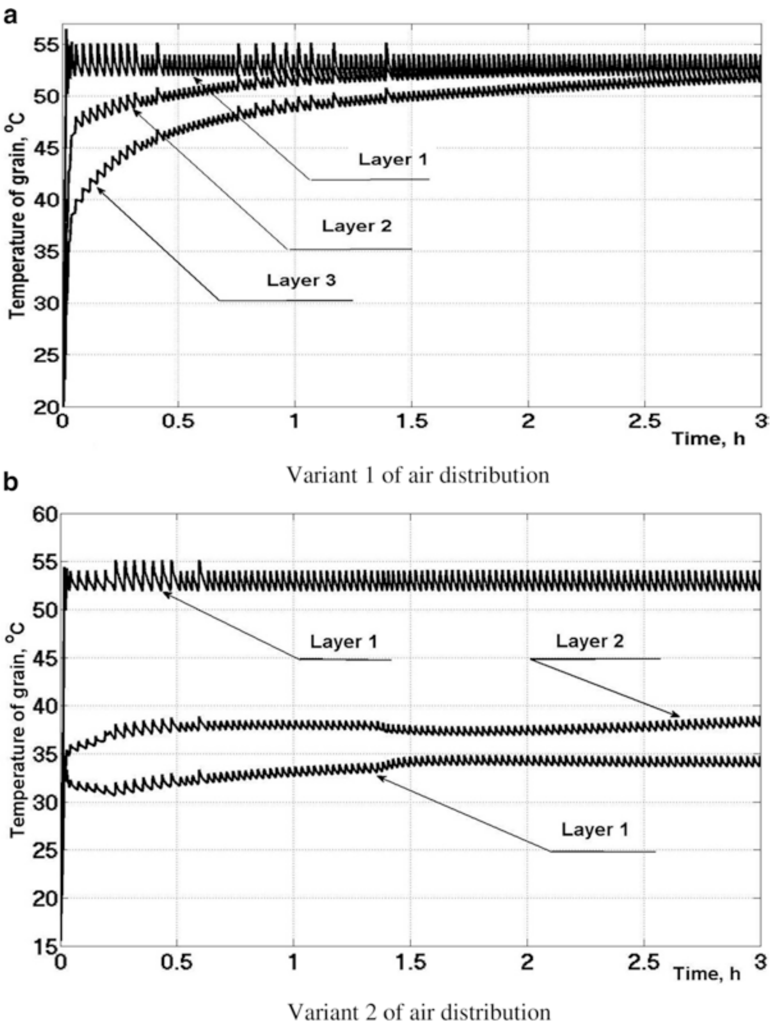

Fig. 3.3 Change in the temperature of grain layers during the process of microwave-convective processing. (**a**) Variant 1 of air distribution. (**b**) Variant 2 of air distribution

Results of the simulation show that the change of the air distribution scheme in the grain layer significantly affects the change of moisture content across the grain layers. With the first variant of air distribution, uniform decrease in humidity across all layers is observed. The drying speed is significantly different in the grain layers, and the maximum power density of the microwave field, absorbed by specific grain layer, does not ensure the maximum drying speed at all. The first layer does not dry up to the normal moisture content of 14% even during 4 hours, while the second layer reaches that moisture content in 1.5 h and the third in 1.3 h. Herewith, the average moisture content of all layers reaches 14% in 1.7 h. Unevenness of moisture content in the layers is 3%.

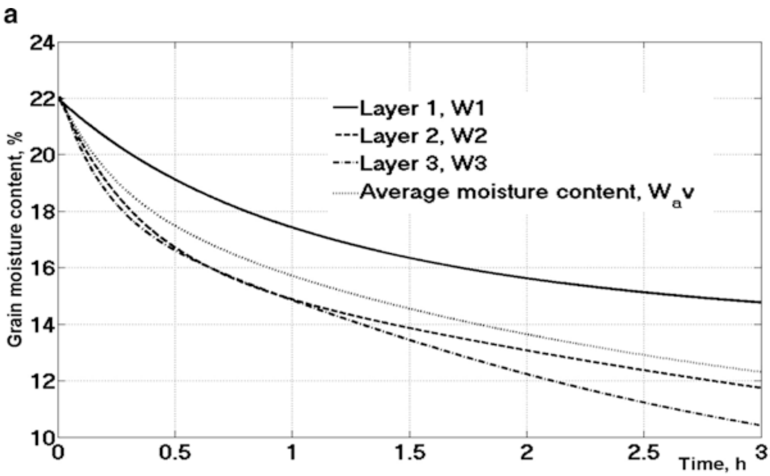

Variant 1 of air distribution

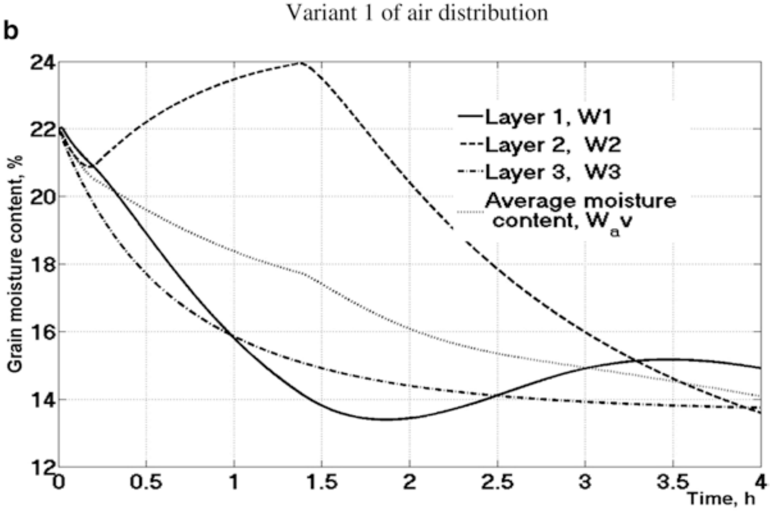

Variant 2 of air distribution

Fig. 3.4 Graphs of drying for the layers. (**a**) Variant 1 of air distribution. (**b**) Variant 2 of air distribution

With the second variant of air distribution, Layer 1 dries to the moisture content of 14% in 1.4 h. For the other 0.3 h, it continues to dry and then starts to moisten. Layer 3 dries to the normal moisture content in 2.5 h. In Layer 2, the first stage is the moistening of the grain and then drying to the normal moisture content in 4 h. Such scheme of air distribution provides rather largely uneven drying of the grain over for different layers and increases durations of the process. Thus, the average moisture content of the grain in the layer will reach 14% in only 4 h, which is more than twice as much as in the first variant of air distribution.

3.4 Conclusions

Developed computer model of heat and moisture exchange in a grain layer under microwave-convective impact makes it possible to study the drying process with changing parameters of the drying agent and the grain layer and also with a change in the direction of air movement.

Simulation results show that the rate of grain drying varies for different parts of grain layer. What is more, for maximum speed of drying, it is not necessary to provide the maximum power density of the microwave field.

The best variant of drying in terms of speed and energy intensity of the process is the air distribution scheme in which air moves sequentially from the grain layers with higher power density of the microwave field to the layers of grain that are less heated by the field.

References

1. Vasilyev, A.N., Budnikov, D.A., Gracheva, N.N., Severinov, O.V.: Improvement of the Technology of Drying Grain in a Dense Layer with the Use of Electrotechnologies, Automated Control Systems and Modeling of the Process. FSBSI FSAC VIM, Moscow (2016)
2. Vasilev, A.N., Ospanov, A.B., Budnikov, D.A., Karmanov, D.K., Shalginbayev, D.B., Vasilev, A.A.: Controlling reactions of biological objects of agricultural production with the use of electrotechnology. Int. J. Pharm. Technol. **8**(4), 26855–26869 (2016)
3. Vasilev, A.N., Budnikov, D.A., Vasilev, A.A., Rotachev, Y.Y., Gusev, V.G.: Modular setup for grain processing. Agric. Mach. Technol. **5**, 27–30 (2014)
4. Vasilev, A.N., Vasilev, A.A., Budnikov, D.A.: Mathematical description of heat exchange in grain under microwave field impact. Multitopic online scientific journal of the Kuban State Agrarian University. Krasnodar: KubGAU, **101**(07) (2014). http://ej.kubagro.ru/2014/07/pdf/118.pdf
5. Vasilev, A.N., Budnikov, D.A., Vasilev, A.A.: Modelling of the processes of heating and cooling of a caryopsis under the impact of a microwave field. Agrar. Sci. **1**, 27–29 (2015)
6. Dyakonov, V.P.: SIMULINK 5/6/7. Tutorial. DMK-Press Publ, Moscow (2008)
7. Vasilev, A.N., Severinov, O.V.: Model of drying in a dense layer with the use of elementary grain layers. Innovations Agric. **4**(14), 71–77 (2015). http://ej.viesh.ru/wp-content/uploads/2016/02/insel14.pdf
8. Vasilev, A.N., Severinov, O.V., Makarova, Y.M.: Development of computer model of heat and moisture exchange in a dense grain layer. Rep. NSEI. **4**(59), 63–71 (2016). http://elibrary.ru/item.asp?id=26083913
9. Budnikov, D.A.: Research on distribution of microwave field potential in a grain layer. Eng. Rep. Don **3** (2015). http://www.ivdon.ru/ru/magazine/archive/n3y2015/3234
10. Vasilev, A.N., Budnikov, D.A., Vasilev, A.A.: Computer model of heat and moisture exchange in a grain layer under microwave-convective impact. Eng. Rep. Don. **3** (2017). http://www.ivdon.ru/ru/magazine/archive/N3y2017/4310

Chapter 4
Energy-Saving Device for Microclimate Maintenance with Utilization of Low-Grade Heat

Dmitry Tikhomirov, Alexey N. Vasilyev, Dmitry Budnikov, and Alexey A. Vasilyev

4.1 Introduction

The most energy-intensive process in the heat supply systems of livestock farms is to support a microclimate. More than 60% of the thermal energy of the total heating cost of the whole object are spent for this purpose. Issues of not only saving the heat (energy) but also purification and disinfection of air inside the room and removed from it become important [1].

An important research topic is thermal technological processes with the use of electrical energy in the supplying of microclimate in livestock facilities. A new highly effective method [2] of decentralized heat supply in creating a microclimate in livestock buildings based on the principles of heat recovery, ozonization, and deep air recirculation has been developed on the basis of studies and experiences [3, 4].

4.2 Methods and Results of Research

The structural diagram of the ventilation-heating unit implementing the described method (Fig. 4.1) includes plastic film heat exchanger, built-in peak electric heating coil, fans of inlet and exhaust air, ozone generator, and recirculation channel with the mixing chamber. Significant recirculation of removed from the premises warm air possible with its deep cleaning and disinfection including the use of the ozonization method [5].

Developed methodical principles and methods of calculating ventilation and the heating system include heat power, hydromechanical, and electrical calculations.

D. Tikhomirov (✉) · A. N. Vasilyev · D. Budnikov · A. A. Vasilyev
Federal State Budgetary Scientific Institution, "Federal Scientific Agroengineering Center VIM" (FSAC VIM), Moscow, Russia

P. Vasant et al. (eds.), *Innovative Computing Trends and Applications*,
EAI/Springer Innovations in Communication and Computing,
https://doi.org/10.1007/978-3-030-03898-4_4

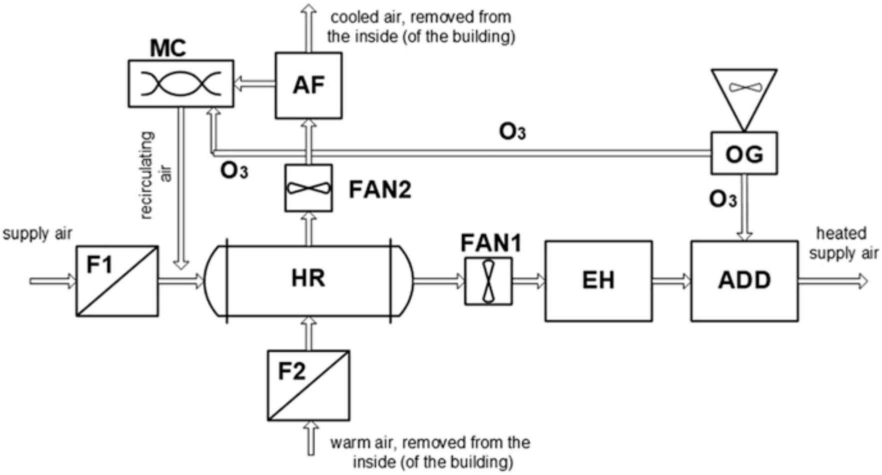

Fig. 4.1 Structural diagram of the ventilation-heating unit with heat recovery, ozonization, and air recirculation: *F1* and *F2* filters, *HR* heat exchanger, *FAN1* and *FAN2* intake and exhaust fans, *EH* electric heater, *ADD* air supply distributor, *OG* ozone generator, *MC* mixing chamber, *AF* adjustable air valve, O_3 ozone tube

The feature of thermal power calculation is the calculation of critical parameters—heat transfer coefficient when part team are condensed from flow of moist exhaust air and calculation of the possible snow coat thickness and its distribution along the length of the surface of the heat exchanger [6].

In general, the equation of heat balance for heat exchanger is (4.1):

$$Q = G_1 c_1 \left(t_{12} - t_{11} \right) = G_2 c_2 \left(t_{21} - t_{22} \right) \eta. \tag{4.1}$$

If the coolant changes its aggregate state (to condensate), then the calculation should be carried out according to the expression (4.2):

$$Q = G_1 c_1 \left(t_{12} - t_{11} \right) = G_2 \left(i_{21} - i_{22} \right) \eta. \tag{4.2}$$

The heat transfer coefficient for film heat exchanger:

$$k = \frac{1}{\frac{1}{\alpha_1} + \frac{\delta_{pf}}{\lambda_{pf}} + \frac{1}{\alpha_2} + R_p}, \tag{4.3}$$

where G_1, G_2 are coolant flow rates, kg/s; c_1, c_2 the average heat capacity of the coolant, J/kg °C; t_{11}, t_{12}, t_{21}, t_{22} the initial and final temperatures of supply (cold) and exhaust (warm) air, °C; i_{21}, i_{22} the enthalpy of the removed exhaust air before and after heat exchange, j/kg; η the coefficient taking into account the heat loss of the device into the environment; δ_{pf} the thickness of the polymer film, m; λ_{pf} the coefficient of thermal conductivity of the polymer film, W/m °C; R_p the thermal resistance of the layers of dirt on both sides of the polymer film, m^2 °C/W; α_1, α_2 the coefficients of heat transfer from the heat exchanger wall to the air supply and from the exhaust air to the wall of the heat exchanger, W/m^2°C.

The calculated value of the heat transfer coefficient is 21–24 kW/m^2°C.

The criterion equations, by which the heat transfer coefficient α for supply and exhaust air must be determined, are defined after evaluating the mode of air movement in the channels of the heat exchanger by the Reynolds criterion.

For dry air:

$$\mathrm{Nu} = 0.021\,\mathrm{Re}^{0.8}\,\mathrm{Pr}^{0.43}\left(\mathrm{Pr}/\,\mathrm{Pr}_{\mathrm{CT}}\right)^{0.25}. \tag{4.4}$$

For wet air:

$$\alpha_{\mathrm{w}} = \alpha_{\mathrm{d}} + \beta r \Delta p / \Delta t. \tag{4.5}$$

$$\mathrm{Nu}_m = \beta d_e / D_p;\ \mathrm{Pr}_m = \upsilon / D_c;\quad D_p = D_c / R_n T; \mathrm{Nu}_m = 0.023\,\mathrm{Re}^{0.8}\,\mathrm{Pr}_m^{0.4} \tag{4.6}$$

where Nu, Pr, Re are Nusselt, Prandtl, and Reynolds numbers [7]; β the coefficient of mass transfer in vapor condensation from wet air, related to the gradient of partial pressures, s/m; Δt the temperature difference between the wet air and the wall, °C; Δp the difference of partial pressures of steam in the core flow and the near wall, Pa; r the heat of vaporization, J/kg·K; D_P the diffusion coefficient [8]; α_c, α_d the coefficients of heat transfer for wet and dry air, W/m^2°C.

In the case of freezing of condensate on the surface of the heat transfer from the exhaust duct side, the average δ_{av} and maximum thickness $\delta_{\max}$ of the snow coat are determined by the expressions (4.7, 4.8):

$$\delta_{\max} = -\frac{\left(\alpha_w t_{22} + \alpha_1 t_{11}\right)\lambda_s}{\alpha_w \alpha_1 t_{22}}, \tag{4.7}$$

$$\delta_{\mathrm{av}} = -\frac{\left(\alpha_w t_{2\mathrm{av}} + \alpha_1 t_{1\mathrm{av}}\right)\lambda_s}{\alpha_w \alpha_1 t_{2\mathrm{av}}}, \tag{4.8}$$

where $t_{1\mathrm{av}}$, $t_{2\mathrm{av}}$ are the average temperatures of supply and exhaust air while passing through the heat exchanger, °C; $\lambda_s = 0.116$ the coefficient of thermal conductivity of snow coat, W/m°C.

The correctness of the mathematical description of heat and mass transfer processes in heat exchanger design and calculation of the surface area of heat transfer are confirmed by the results of tests of an experimental sample where the differences between parameters do not exceed 5%.

The hydromechanical calculation of heat exchanger has been made to determine fan power at the minimum possible flow resistance of the intake and exhaust tracts [5].

The design power of the additional heater of air supply, built-in electric air heater, is calculated for the cold period of year at a given ambient temperature t_o.

The heating element for inline electric heater is made from nichrome ribbon of rectangular cross section with small thickness. It is evenly spaced around the circumference. This design can significantly reduce the hydraulic resistance of moving air while providing high heat removal. Heat flow by convection from the built-in into the device the electric heater is determined by the formula:

$$P_c = \alpha_c F_h \left(t_h - t_a\right), \tag{4.9}$$

where F_h is the area of the heat transfer surface of the heater, m^2; t_h the surface temperature of heater, °C; t_a the temperature of air, °C.

The expression (4.10) has been obtained using the mathematical method of experiment planning that connects the convection coefficient α_c with air speed ω (m/s) through the heaters and the equivalent diameter d_e of the heating element, mm [5].

$$a_c = 106.5 + 10.6\omega - 10.4d_e,$$

$$4 \le \omega \le 12; 2 \le d_e \le 6. \tag{4.10}$$

The electric power and structural parameters of the electric air heater were determined with the help of the expression (4.10).

The method of ozonization is applied for the disinfection and cleaning of the return and air supply.

The validation of the parameters was performed, and the corona discharge ozonator for the described ventilation and heating system was calculated and selected. The technological scheme of the ventilation-heating unit is shown in Fig. 4.2, and its novelty is protected by the patent.

The algorithm of controlling the air supply by changing the ratio of flows of supply and exhaust air with the use of partial recirculation of internal air was developed to improve the effectiveness and efficiency of the device when significant negative ambient air temperatures occur ($t \le -12$ °C) and to prevent freezing of the heat transfer surfaces. The intelligent system of automatic mode control of the unit leads to a decrease in energy consumption for additional heating of the incoming air using the built-in electric heater.

A circuit diagram was developed for the implementation of the above operation modes.

The requirements were created and the experimental sample of the module the ventilation-heating unit with recycling, ozonization, and recirculation of air for livestock buildings air with output up to 1500 m^3/h was built according to the results of theoretical research and of calculations.

The laboratory stands, including temperature measurement devices (УКТ 38), humidity and air flow (TPM) [9], interface adaptors (AC2, AC4), physical quantity sensors [10], power supply (PS), and personal computer (PC), were developed (Fig. 4.3) to automate the collection and recording of experimental data.

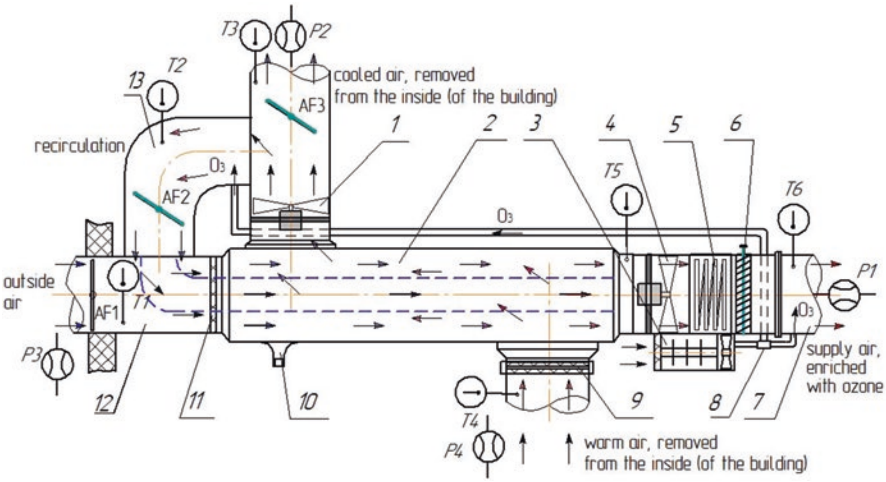

Fig. 4.2 Technological scheme of the ventilation-heating unit: *1*—exhaust fan, *2*—polymer heat exchanger, *3*—ozone generator, *4*—intake air fan, *5*—built-in electric heater, *6*—the air supply regulator, *7*—air supply dispenser, *8*—ozone feeding pipeline, *9* and *11*—filter, *10*—condensate trap, *12*—supply duct, *13*—return air duct with mixing chamber, *T1*…*T6*—thermometers, *P1*…*P4*—flow meters

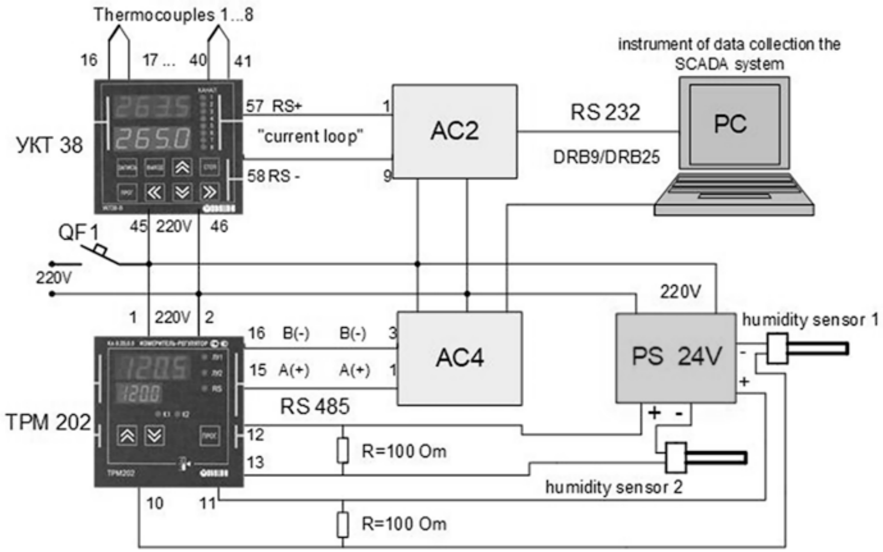

Fig. 4.3 A computerized system for collecting experimental data of ventilation and heating device

The dependence of the heat flux returned by the heat exchanger from the difference between temperatures of external and internal air was obtained on the basis of statistical processing of experimental data (Fig. 4.4).

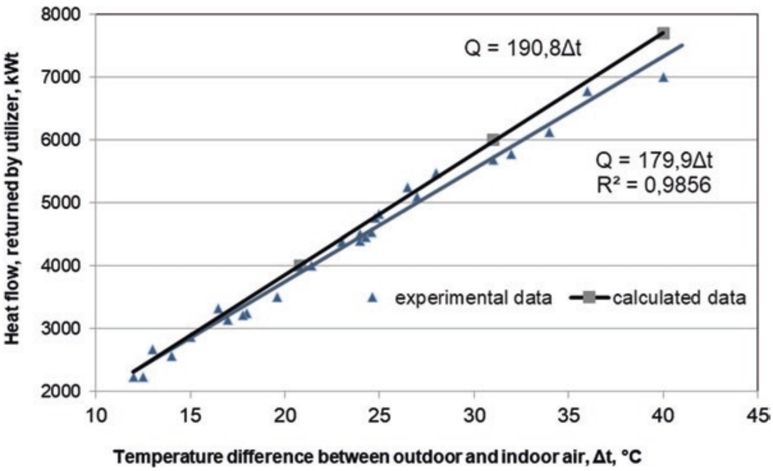

Fig. 4.4 Calculation of the constant value of the heat exchanger A_{hr}

$$Q_{hr} = A_{hr}\left(t_{21} - t_{11}\right) \tag{4.11}$$

where A_{hr} is the heat exchanger constant, W/°C, which characterizes its design features and determines the amount of heat return with an indoor and outdoor air temperature difference of 1 °C.

The heat exchanger recovers low-grade heat from the exhaust air.

The exergy efficiency of a device, without producing a work, can be calculated according to the equation [10]:

$$\eta_e = E_2 / E_1 = 1 - \left(D / E_1\right), \tag{4.12}$$

where E_2, E_1 are the exergy flows at the inlet and outlet of the heat exchanger, W; D the total loss of exergy in heat exchanger, W.

The values of thermal exergy for gas are determined by the expression:

$$E_i = G_i\left[c_{pi}\left(T_i - T_0\right) - T_0\left(c_{pi}\ln T_i / T_0 - R\ln P_i / P_0\right)\right], \tag{4.13}$$

where G_i is the mass flow rate, kg/s; c_{pi} the average specific heat of coolant, J/kgK; T_i, T_0 the temperatures of the coolant and the environment, K; P_i, P_0 the pressures of the coolant and the environment, Pa; R the gas constant of air, kJ/kgK.

For the given design of heat exchanger, exergy losses occur due to the finite temperature difference D_t and hydraulic resistance in channels of supply and exhaust air Dh and heat loss to the environment D_0.

$$D_t = T_0 Q\left(\frac{1}{T_{2av}} - \frac{1}{T_{1av}}\right), \tag{4.14}$$

where Q is the heat flow, W; T_{1av}, T_{2av} the average temperatures of coolant, K.

$$D_h = T_0 G_i R \ln \frac{P_i'}{P_i''}, \tag{4.15}$$

where P_i', P_i'' are the pressures of the coolant at the inlet and outlet from the apparatus, Pa.

The exergy losses from the hydraulic resistance can make the operation of the intake and exhaust fans of heat exchanger.

In general, the losses in the environment are determined by the formula (4.16):

$$D_0 = Q_{L1}\left(1 - \frac{T_0}{T_{1av}}\right) + Q_{L2}\left(1 - \frac{T_0}{T_{2av}}\right), \tag{4.16}$$

where Q_{L1}, Q_{L2} are the heat flows into the environment from the coolant, W.

Since the heat exchanger is arranged in the room, the losses in the surrounding environment can be ignored.

After substituting the calculated numerical values of parameters of the heat exchanger, the magnitude of the exergy efficiency is equal to $\eta_e = 0.48$.

A research on heat and power operational parameters of the device under various environmental conditions, including icing of heat exchange surfaces from the exhaust air, was made. The influence of the recirculation rate of the internal space air at the amount of heat return by the heat exchanger; the efficiency of the embedded electric heater capable of preheating the inlet air at the temperature of 20 °C (Fig. 4.5) has been found by practice.

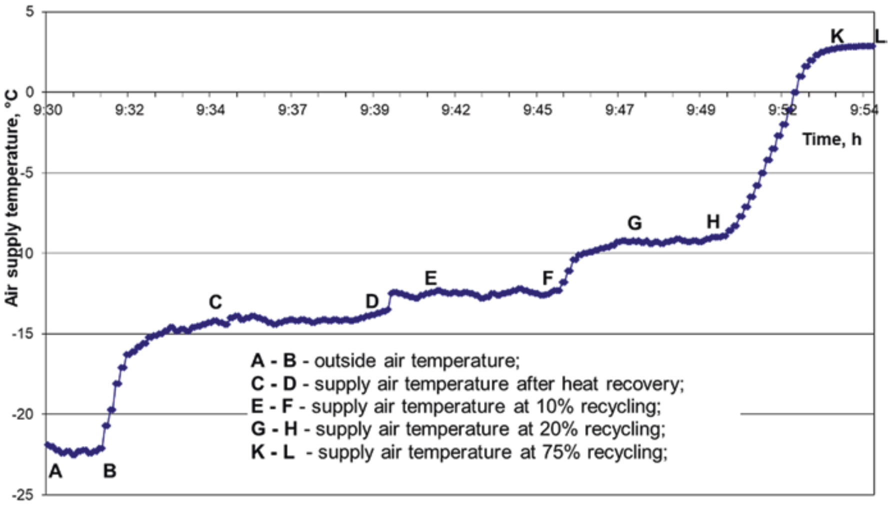

Fig. 4.5 Modes of ventilation-heating unit with the utilization and recirculation of internal air

The use of partial (30%) recirculation of internal air leads to a further increase in the return of warmth to 20%. In the heating the air supply in the heat exchanger mode and at 75% recirculation of the internal air the air intaking into the room has temperature about 3 °C (Fig. 4.5). In this case, energy costs are reduced up to 60%.

4.3 Conclusion

The methods of calculating new ventilation and heating system to create a necessary microclimate in livestock buildings confirmed by practical results, in which the design difference between the calculated and the experimental data does not exceed 5%.

New dependencies of the coefficient of heat transfer from the heating elements of the built-in electric air heater to air supply and the heat exchanger constant determining the amount of the return of warmth are discovered.

An exergy analysis of heat exchanger, evaluating the impact of each type of exergy losses in the heat exchanger on its efficiency ($\eta_e = 0.48$), is performed.

The installation has successfully passed the economic tests for supplying a predetermined atmosphere in the calf house (50 goals) of the dairy farm.

References

1. Sventitsky, I., Alkhazova, E., Mudrik, V., Obynochny, A.: Energy saving by improving efficiency of using energy resources in agriculture and housing. In: Scientific-Methodical Recommendations on the Definition of Energy Efficiency and Calculation of Power Equipment for Modernization of Power Supply in Agriculture and Housing, 64 p. GNU VIESH, Moscow (2011)
2. Markelova, E., Petrov, L., Ukhanova, V., Tikhomirov, A., Tikhomirov, D., Pershin, A.: Method and device to clean air environment in livestock and poultry areas. Patent No. 2473213 of the Russian Federation, IPC A01K1/03, GNU VIESH, No. 2011109389/13, Appl. 13 Mar 2011, Publ. 27 Jan 2013, Bull. No. 3–7 p
3. Panova, T.: Development and validation of the parameters of supply and exhaust heat exchanger to improve microclimatic conditions in livestock buildings: dissertation ... of candidate of technical sciences: 05.20.01. 187 p (2011)
4. Mishurov, N.: Energy-saving equipment for microclimate in livestock buildings. Mishurov, N., Kuzmina, Tn. Rosinformagrotech. 94 p (2004)
5. Tikhomirov, D.: Methodology of calculation heat and energy saving ventilation and heating installations for animal farms for alternative energy and ecology. **2**(Pt. 1), 125–131 (2013)
6. Tikhomirov, D.A.: Electrical and thermal calculation of air heater recuperative heat exchanger. Mechaniz. Electrific. Agric. **1**, 15–17 (2013)
7. Whitaker, S.: Forced convection heat transfer correlation for flow in pipes, past flat plates, single cylinders, single spheres and in flow in packed beds and tube budles. AICHE J. **18**, 361 (1972)
8. Doctorov, A.: Thermodynamics. A Course of Lectures, 82 p. Novosibirsk State University, Novosibirsk (2003)
9. Equipment for automation. The product catalog. Production Association OWEN, 448 p. OWEN (2014)
10. Official website of the company “Production Association OWEN” [electronic resource]: www.owen.ru

Chapter 5
Liberalization of the Mexican Electricity Sector: A Study of Technical Efficiency

Román Rodríguez-Aguilar and José Antonio Marmolejo-Saucedo

5.1 Introduction

The present study develops an estimation of DEA-CCR (data envelopment analysis developed by Charnes, Cooper, and Rhodes) for a set of thermoelectric units in Mexico. As part of the recent reform in the Mexican electricity sector, the electricity market has been liberalized, so that the single supplier before the reform must guarantee competitiveness in order to participate in the electricity market. One of the key decisions for the parastatal is to define their portfolio of generating units to compete in the best possible conditions in the electricity market. In this context it is necessary to take into account that it is not only important to determine the most efficient plants in a product input logic, but that it is necessary to consider those plants that are more efficient in operation and in terms of costs, which will allow offering energy at competitive prices with the lowest operating cost.

It has been documented that techniques traditionally used as is the case of the DEA-CCR present weaknesses in those cases in which the productive units contain atypical values, that is to say that there exist large efficient units or small efficient units which affect the efficiency levels estimated for all the set of units. In the case of thermoelectric plants in Mexico, in general, the behavior is homogeneous. An advantage to use DEA-CCR is the fact to provide radial efficiency measures, input or output oriented and convexity, strong free removal of inputs and outputs and constant returns to scale.

R. Rodríguez-Aguilar
Faculty of Engineering, Anahuac University, Mexico, Mexico
e-mail: roman.rodriguez@anahuac.mx

J. A. Marmolejo-Saucedo (✉)
Facultad de Ingeniería, Universidad Panamericana, Augusto Rodin 498, 03920, Ciudad de México, México
e-mail: jmarmolejo@up.edu.mx

P. Vasant et al. (eds.), *Innovative Computing Trends and Applications*,
EAI/Springer Innovations in Communication and Computing,
https://doi.org/10.1007/978-3-030-03898-4_5

The information for the electricity sector of the period 2009–2013 was used only for thermoelectric power plants, since they represent 19% of the electric power generation in Mexico. It is therefore of great importance to be clear that plants are more efficient in generation and in costs and that they would be able to compete in a liberalized market. It was considered a universe of 21 power plants, which are still in operation in Mexico. The results of the estimated model show that the thermal generation in Mexico is very costly due to the inefficiency of the plants; for this reason a set of plants that are in a range of acceptable minimum efficiency is observed, and, if not, a small set of central shows efficiency in generation and costs. Due to the above, the ranking generated classified those plants with a minimum efficiency level representing at least 50% of the thermoelectric generation in Mexico to guarantee the supply and in turn to make more efficient the participation of the public sector in the electric market.

The work is structured as follows. The first section describes the operation of the Mexican electricity sector until 2013, before the reform, and subsequently outlines the new framework of operation generated by the liberalization as well as the main instruments through which the market will operate. In the second section, the methodological framework is developed, analyzing the DEA-CCR methodology. The third section presents the results of the analysis performed. The final section presents the conclusions and recommendations.

5.2 Power Generation

The Mexican electricity sector even before the liberalization of the market operated with a parastatal company as sole supplier, the Federal Electricity Commission (CFE). In addition, other generators participated in the sector through self-generation schemes, independent producers, cogeneration, small producers, export centers, and continuous own uses (Table 5.1).

As can be seen in Table 5.1, CFE and independent power producers accounted for 86% of the national gross generation. The objective of the liberalization of the

Table 5.1 Gross generation by type of generator, 2014

Generator	GWh	%
Small producers	212	0.0
Own uses	1002	0.0
Exports	7050	2.0
Cogeneration	15,258	5.0
Self-generation	19,154	6.0
Independent power producers	87,589	29.0
CFE	172,541	57.0
Total gross generation	302,806	100

Source: Ministry of Energy

electricity sector is to accommodate private investment so that they can compete in the sector by generating lower energy prices, as well as the diversification of the energy matrix allowing the promotion of clean energy.

By 2014, the total net electricity generation in the Mexican electricity sector was 302, 806 GWh; the energy matrix is concentrated in technologies based on the use of fossil fuels, such as the combined cycle and generation by internal combustion (see Fig. 5.1).

Of the total CFE and PIE generation, 65.7% use primary fuel, fossil fuels, 13% use coal, 15% use hydro, and the rest is distributed between clean energy sources such as geothermal, nuclear, wind, and photovoltaic (Table 5.2).

The generation of electricity using fossil fuels in Mexico is a process with broad participation; in 2011 the plants that only used fossil fuels accounted for 72.6% of the total electricity and are expected to remain wide in participation to meet the

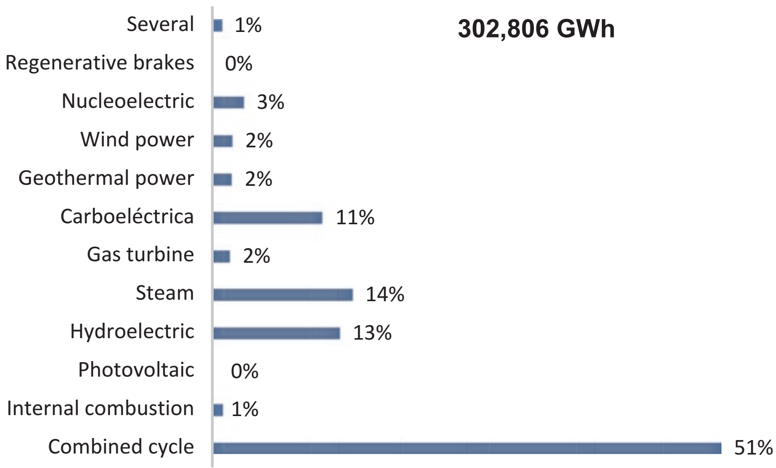

Fig. 5.1 Gross generation by type of technology, 2014. Source: Ministry of Energy

Table 5.2 Gross generation by primary fuel source, 2014

Primary source	GWh (CFE + IPP)	%
Gas	143,172	55.1
Fuel oil	26,199	10.1
Diesel	1429	0.5
Carbon	33,437	12.9
Hydroelectric	38,145	14.7
Nucleoelectric	9677	3.7
Geothermal power	6000	2.3
Wind	1897	0.7
Photovoltaic	12.7	0.0
Total	259,968	100

Source: Ministry of Energy

future electricity demand [1]. The use of fossil fuels for power generation has been severely questioned due to the production of carbon dioxide (CO_2) that contributes to the accumulation of greenhouse gases (GHGs) emitted into the atmosphere.

Therefore, there are two prospective scenarios of capacity expansion for the period 2013–2027. The first is the planned expansion of the public power generation companies with a share of 31.9% with the use of clean technologies in 2027—18.4% of hydro capacity, 4.1% wind power, 1.8% nuclear, and 2.4% remaining with geothermal, solar, and biogas capacity. In the alternative scenario, the expansion program is aligned to the goals set in local laws, seeking to increase its generation with nonfossil sources to 35% in 2027 [2].

This means that, although fossil fuel generation will be reduced, its use will be located in the worst case at 65% in 2027. Therefore, the total elimination of fossil fuels for power generation is nearly impossible, because it still represents one of the economic lower cost options in Mexico. The generation of electric energy based on fuel oil represents the most expensive form of electric power generation. However, it represents around 10% of the total generation in the country. As expected, the consumption of fuel oil has a similar behavior to generation, because of the context of a non-liberalized sector, which was the case of Mexico until 2016. Where the main objective of the parastatal company providing the electric service was to maintain the supply at all times and avoid load cuts at any cost, this is not compatible with a liberalized market [3].

One of the major problems of having a generator company focused on ensuring the cost is that it must necessarily maintain levels of fuel inventory large enough to guarantee generation and avoid load cuts. However, this decision involves assuming the cost of maintaining an inventory of these characteristics.

The behavior of the fuel oil consumption of power plants over time is directly related to the behavior of generation; i.e., power generation is a function of the consumption. Both behaviors follow the same trend, but do not match on the same points throughout the timeline; i.e., there is a difference between consumption and generation. In some years, the points almost coincide and graphical difference is very low, but in other years this differential increases and the points are away. It could be concluded that when the points of consumption and generation are far apart, we have a period of technical inefficiency.

In 2013 the production of generation per unit volume (m^3) increased, the lowest difference it can be seen. A total of 4.9 MWh/m^3 was generated in 2013, while in 2010 it was of 4.3 MWh/m^3. IDEA-CCRlly, the points must coincide throughout the timeline, i.e., 100% of technical efficiency.

Regarding the level of fuel oil inventory (useful existence), we can mention that it is a policy relating to reducing the risk of not meeting the demand of electricity. In terms of generation costs, the level cost represents the estimated cost for the entire life of the generating plant, which is why it is an efficient mechanism for evaluating generation projects, as well as a mechanism that allows optimizing the generation based on a diversified energy matrix. Figure 5.2 shows the level cost of the different technologies that make up the energy matrix for Mexico; as mentioned the generators with turbogas technology with diesel and gas and those of internal

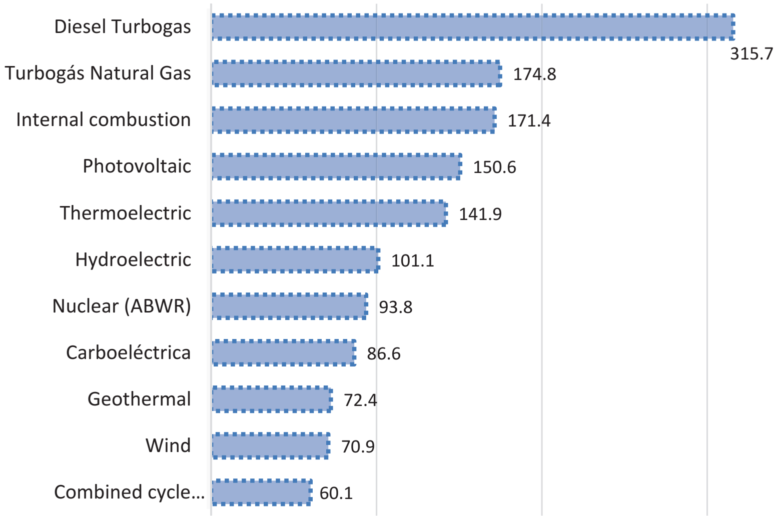

Fig. 5.2 Technology-level cost (dollars per net MW). Source: Ministry of Energy

combustion are the most expensive plants with a maximum of up to $ 315.7 per MW in the case of diesel.

5.3 The Wholesale Electricity Market

As a result of the energy reform implemented in Mexico, the wholesale electricity market (WEM) was created, a market based on variable costs. The purpose of the WEM is to efficiently cost and ensure the supply of electricity in the country. It is a newly created market whose operation began in February 2016. At present, there is a small group of private suppliers that have joined the WEM, but it is expected that as the market matures, market concentration will decrease, allowing the reduction of generation costs.

The WEM is a newly created market. Therefore, as a prudent measure to guarantee supply, a legacy contract was created through which generation contracts are assigned to a group of power plants belonging to CFE in such a way as to guarantee a minimum margin of supply according to the expected demand. It is expected that as more suppliers to the WEM enter, the market share of the parastatal company will decrease and only operate with a portfolio of plants that are efficient and economically competitive. Due to the above, it is of great relevance for CFE to know the level of efficiency of its plants to be able to form a portfolio of highly competitive plants and to be able to participate in equal conditions in the WEM.

The WEM is formed by a set of market instruments that facilitate the transition to a liberalized market; among the main instruments that contribute to the development of the WEM, we can mention (Fig. 5.3):

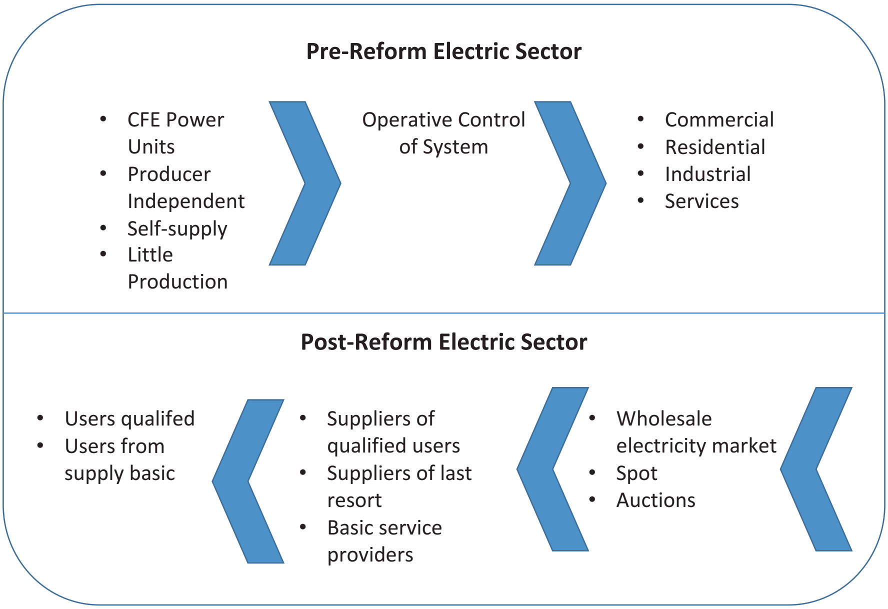

Fig. 5.3 Organization of electric sector pre- and post reform. Source: Ministry of Energy

- Power market: The power market seeks to guarantee the generation of energy in the long term, by generating incentives for the establishment of generation plants in areas where there is greater demand. Depending on the technology of the plant, the generators can offer power, just as the consumers of electric energy are obliged to acquire power in proportion to their consumption.
- Clean energy certificate market: The market for clean energy certificates (wind, solar, geothermal, oceanic, bioenergy, hydroelectric, nucleoelectric, and efficient cogeneration, among others) allows encouraging the generation of removable energy, through an economic incentive to make these technologies competitive in their participation in the WEM.
- Financial transmission rights market: The financial transmission rights (DFT) grant the owner the right to charge or the obligation to pay the difference of the marginal congestion components of the local marginal prices of the market of the day in advance, between a destination node and a source node. The DFT market seeks to offer coverage to market participants of price volatility generated by the congestion of transmission lines.
- The mechanism by which these markets will operate will be through auctions carried out by the market operator and the National Energy Control Center (NECC), which will determine the price and quantities to be marketed in each market, as well as the optimal allocations for the generation in the Mexican electricity sector.
- Medium- and long-term auctions: Auctions are a mechanism that gives transparency and certainty to the market. Auctions will be held in two planning horizons, in the medium and long term, allowing basic service providers and other respon-

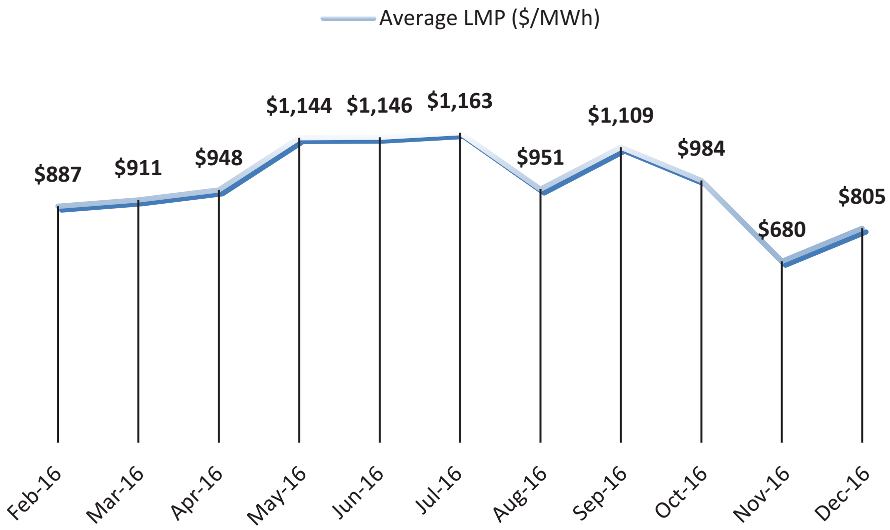

Fig. 5.4 Evolution of PLM in Mexico (Mexican pesos per MWh). Source: Ministry of Energy

sible entities to conclude coverage contracts with generators and marketers. In the case of long-term auctions, placement adjustment mechanisms will be considered, giving greater certainty on congestion costs and rewarding or penalizing the generator according to the location, which will generate incentives to locate the new plants where they are most needed.

The WEM started operations in February 2016; in the first year of operation, energy prices recorded in the market show some volatility. The local margin prices that reflect the cost of the energy in the delivery node also reflect the variable cost of energy generation, plus the cost per congestion and the cost of the losses. The main reasons for the high volatility of PMLs at the onset of WEM may be due to climatic aspects, fuel availability, congestion, as well as network failures. The evolution of the PML in what is carried out by the WEM is shown in Fig. 5.4.

5.4 Technical Efficiency

The efficiency analysis is based on microeconomic analysis, through maximizing a given production function using a set of inputs and technology. There are two approaches to the optimization of a production function either through the maximization of production or cost minimization given a certain level of production.

The efficiency analysis is based on the concepts of partial and total factor productivity in the case of partial productivity output per input used is determined and in total productivity index products and an inputs index are constructed to evaluate total factor productivity used. In [4] were proposed two conceptual visions of economic efficiency:

- Technical efficiency: The ability of a production unit to obtain the highest level of product, a given level of inputs and technology.
- Allocative efficiency: The ability of a production unit to use the inputs in optimal proportions, given a price level and technological level.

The usefulness of technical efficiency lies in generating information to improve management capacity of the production units, knowing the information of input use and generation of production to define optimal strategies for improvement. There are several methods of estimating technical efficiency: parametric, nonparametric, deterministic, and stochastic.

- Parametric: Assume a functional form of the production function.
- Nonparametric: Do not assume any functional form of the production function.
- Deterministic: Part of the approach that all distance between the border of production and production value observed for a productive unit corresponds to technical inefficiency.
- Stochastic: Production presents a stochastic component that attaches the technical inefficiency as a part of the error generated by the production unit is away from the production frontier, a component of error is random and one attributable to technical inefficiency.

Techniques for estimating technical efficiency according to the adopted approach can be classified among the primal and dual approaches; in the case of primal approach, technical efficiency is estimated based on maximizing production or minimizing function costs. In the case of dual approach, technical efficiency for both functions is estimated [16–18]. Models can also be categorized in terms of temporality, in models of cross section or panel data.

The nonparametric models generally used are estimates based on data envelopment analysis (DEA-CCR) methodologies constructed from mathematical programming. The great goodness of using DEA-CCR is that a specific functional form of the production function is not required, and the main disadvantage is that it is a deterministic model that can be affected by the number of inputs used and the presence of outliers [5].

5.5 Data Envelopment Analysis

Data envelopment analysis is a well-known technique for conducting technical efficiency studies; [6] developed the first approach in 1978; fundamentally, this method follows the basic concepts of [4]. Over the years, modifications and contributions have been made by many other authors, generating a much more stylized version of the technique.

Data envelopment analysis is a nonparametric method of measuring efficiency based on obtaining an efficiency frontier from the set of observations that are considered without the estimation of any production function. The objective is to optimize the efficiency measure of each unit analyzed to create an efficient frontier based on the Pareto criterion [6]. First, the frontier of empirical production is constructed and then the efficiency of each. In addition, it is not a parametric method, nor is it statistic, since it does not assume that the unobserved efficiency follows any kind of probabilistic distribution.

Among the advantages of using the DEA-CCR are as follows: (a) it applies to sectors that employ n-inputs in their process and generate n-outputs and (b) does not require prior knowledge of the production function. The disadvantages of using the DEA-CCR are as follows: (a) it requires homogeneity of the productive units; (b) it has influence on the results of atypical data; and (c) the difference between the efficient frontier and each productive unit is attributed to efficiency only.

In recent years, authors such as [7] showed that "most representative efficient points" can be found using a direct approach and may differ from those obtained by multistage DEA-CCR. Assuming the economic production activities, convexity, strong disposability, and CRS, we can develop the linear program as a type of piecewise linear frontier. Input-oriented CRS efficiency is defined as Eq. (5.1) by applying the piecewise linear frontier to the input requirement set [5].

The goal of the input-oriented DEA-CCR model is to maximize the virtual input, relative to a given virtual output, subject to the constraint that no DMU can operate beyond the production possibility set and the constraint to nonnegative weights. The input-oriented model of DEA-CCR is expressed in accord with Eq. (5.1).

$$\max_{v,u} h_0 = \frac{\sum_{r=1}^{s} u_r y_{r0}}{\sum_{i=1}^{m} v_i x_{i0}} \tag{5.1}$$

Subject to:

$$\frac{\sum_{r=1}^{s} u_r y_{rj}}{\sum_{i=1}^{m} v_i x_{ij}} \leq 1; j = 1, 2, \ldots, n$$

$$u_r, v_i \geq 0$$

Where:

- They are considered n units($j = 1, 2, \ldots, n$), each of which uses the same inputs (in different quantities) to obtain the same outputs (in different quantities).
- x_{ij} ($x_{ij} \geq 0$) represents the quantities of input i ($i = 1, 2, \ldots, m$) consumed by the j-th unit.
- x_{ij} represents the amount of input i consumed by the unit that is evaluated, unit 0.
- y_{rj} ($y_{rj} \geq 0$) represents the observed quantities of output r ($r = 1, 2, \ldots, s$) produced for the j-th unit.
- u_r ($r = 1, 2, \ldots, s$) and v_i ($i = 1, 2, \ldots, m$) represent the weights (or multipliers) of the outputs and inputs, respectively.

The dual problem can be expressed according to Eqs. (5.2) and (5.3).

$$\min \theta_{\theta} \tag{5.2}$$

$$\min_{\lambda, s^+, s^-} \sum -s^+ - s^- \tag{5.3}$$

Subject to:

$$\theta x_j - X\lambda - s^- = 0$$

$$Y\lambda + s^+ = y_j$$

$$\lambda \geq 0$$

λ, s^+, s^- are semi positive vectors in R^k; θ is a real variable.

The single-stage DEA-CCR model solves (1), and two-stage DEA-CCR model solves (2) followed by (3), consecutively. In this model is assumed constant returns to scale (CRS).

5.6 Efficiency of Thermal Power Units in Mexico

The study includes data for a group of 21 thermoelectric units, and annual average gross electricity generation, level of consumption, and useful existence of fuel oil are analyzed. A balanced panel data for 21 thermoelectric units was built for the period 2009–2013. The useful existence and consumption of fuel oil are expressed as an annual average in cubic meters and annual average gross generation of electrical energy in MWh.

The objective of measuring technical efficiency in the production of electrical energy is to assess whether levels of consumption and useful existence correspond with the level of production of each thermoelectric plant, assuming a technology given.

Data Envelopment Analysis

The results generated by the DEA-CCR show great variation among the estimated efficiency indices; the lowest efficiency power plant is Lerdo with a value of 0.29, and the most efficient plants are Tula Vapor, Rio Bravo, and Baja California Sur I, with values of unit efficiency.

It is worth mentioning one of the main criticisms of the nonparametric models estimated by DEA-CCR, since in this case a set of three units with very low values of efficiency is observed in contrast to three units with unit values. This is attributed to the values observed in the inputs and outputs for these plants, so the production boundary is influenced by atypical values.

On the other hand, one of the advantages of using DEA-CCR is that it allows working with sets of inputs and sets of outputs. The results show very low values of efficiency for most plants since only four plants had efficiency indexes above 0.8 (Fig. 5.5).

An additional analysis that is usually performed using DEA-CCR is to identify possible influence variables that represent the causes of variability of technical efficiency. In this case, power plants only have information about whether the total maintenance programmed during the year was carried out at each plant. In order to compare this variable with the estimated technical efficiency level, a dummy variable was constructed, which takes the value of 1 if all maintenance programmed during the year was performed and a value of 0 if at least one of them.

The estimated tobit regression considers as an independent variable the estimated technical efficiency and as an independent variable the dummy variable constructed with the information about maintenance. The results of the tobit regression show that the dummy variable considered is not statistically significant at 95% confidence (Table 5.3).

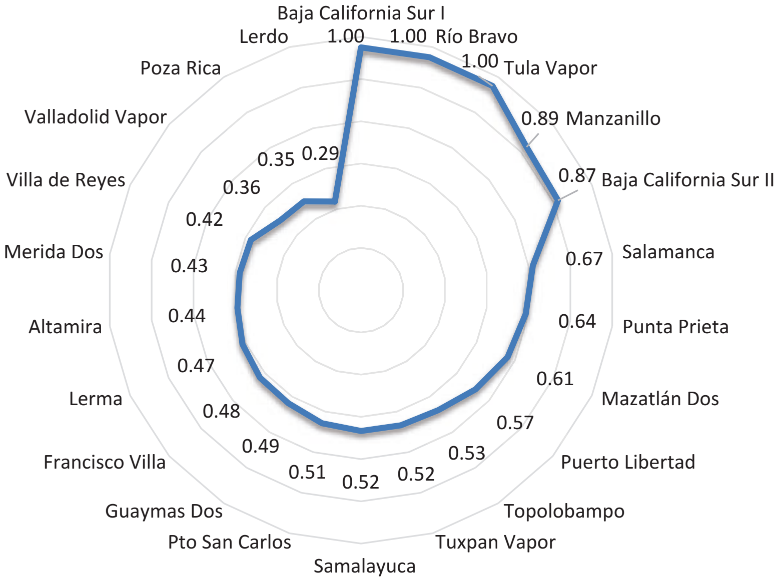

Fig. 5.5 Technical efficiency: DEA-CCR, 2013. Source: The authors

Table 5.3 Tobit regression analysis

Theta	Coef.	Std. err.	*t*	*P* > *t*	[95% Conf. interval]	
Maintenance	0.043081	0.1062439	0.41	0.689	−0.1778653	0.2640272
_cons	0.5871584	0.0712578	8.24	0.000	0.4389697	0.735347
/sigma	0.2453271	0.0416399			0.1587322	0.331922

Source: Data estimated in STATA

These results will be discussed later, because one of the main reasons attributed to the low technical efficiency is the lack of maintenance of the plants. But it should be reWEMbered that the results generated by the DEA-CCR show that there is a very low efficiency and probably the built boundary is influenced by atypical values of the inputs and outputs. This is because although the technology of the comparative plants is similar, the operation and administration of the same is heterogeneous.

Analysis of Inefficiency

There are several factors that affect the productivity of the systems, for example, technical efficiency, which can be incorporated in the stochastic frontier. The reason why technical efficiency showed a downward trend in all thermoelectric plants could be for the wear and tear of the generating units since in many cases the right kind of maintenance determined by the number of operation hours (inspection, minor, intermediate, and major) is not given, mainly due to limited budget or other politic factors (Table 5.4).

The diagnosis of the operation of an energy system is to discover and interpret the signs of malfunction of equipment that compose and quantify their effects in terms of additional consumption of resources, i.e., where, how, and how much the overall consumption of resources can be saved, holding constant the quantity and product specifications of the system.

For thermoelectric plants a malfunction of certain equipment such as boilers will have a major economic impact, even for small deviations in their performance with respect to what is expected by design. A good diagnosis of the operation must be preceded by a conceptual development that explains the origin of the increase.

5.7 Conclusions

Mexican electricity sector went through an important reform in recent years; the liberalization of the electricity market allowed the private participation in the generation of electric energy. However, the transition will not be an immediate process,

Table 5.4 Type of maintenance that should be given to a steam turbine

Maintenance type	Period (OH)
Inspection	4000
Lower	8000
Intermediate	16,000
Major	32,000

Source: Own estimations

and that is why CFE should guarantee its participation in the wholesale electricity market through the formation of a portfolio of efficient and competitive plants.

The study for a set of thermoelectric power plants allows providing technical evidence for decision-making. In this case, DEA-CCR was used to test the results. It is of utmost importance to consider the nature of the information available and the problem to be addressed in order to decide the appropriate methodology.

DEA-CCR was influenced by the presence of atypical values of the inputs and outputs, which determined that a set of power plants presented very low efficiency and a smaller set of unit efficiency. Additionally, the estimation of a tobit model allowed to evaluate the effect of the maintenance of the power plants in terms of efficiency, which apparently was not significant. In contrast, available information shows that if there is a relationship between maintenance costs and in the type of maintenance performed at each plant, this should be done with caution until more information is available.

In general, 80% of the thermoelectric units have technical inefficiency; one reason of this could be that technical inefficiency effects are significantly related to maintenance levels. The evaluation of technical efficiency is a useful indicator for monitoring the operation of thermoelectric units and their performance, in order to identify which units require particular attention to achieve maximum performance.

The results generated show an indication that all plants should be evaluated more thoroughly to decide if they should be part of the portfolio of plants with which CFE will participate in the wholesale electricity market.

References

1. Salazar, M.S.: Una estrategia para mejorar la administración de los inventarios de diesel en las centrales termoeléctricas: un estudio de caso. M.S. Thesis, Engineering Systems Department, National Autonomous University of Mexico, México, 100 p (2015)
2. Secretaría de Energía. Prospectiva del sector eléctrico 2013–2027, México (2013) [Online]. Available at: http://sener.gob.mx/res/PE_y_DT/pub/2013/Prospectiva_del_Sector_Electrico_2013-2027.pdf. Accessed 19 Dec 2014
3. González Santaló, J.M.: La generación eléctrica a partir de combustibles fósiles. Boletin IIE. Octubre-diciembre (2009) [Online]. Available at: http://www.iie.org.mx/boletin042009/divulga.pdf. Accessed 19 Dec 2014
4. Farrell, M.: The measurement of productive efficiency. J. R. Stat. Soc. **120**(3), 253–290 (1957)
5. Cooper, W.W., Seiford, L.M., Tone, K.: Data Envelopment Analysis: A Comprehensive Text with Models, Applications, References and DEA-Solver Software, 2nd edn. Springer, New York (2007)
6. Charnes, A., Cooper, W., Rhodes, E.: Measuring the efficiency of decision making units. Eur. J. Oper. Res. **2**, 429–444 (1978)
7. Cherchye, L., Van Puyenbroeck, T.: Product mixes as objects of choice in non-parametric efficiency measurement. EJOR. **132**(2), 287–295 (2001)

Chapter 6
Impacts of Sleeping Time During the Day on the Timing and Level of Basal Heart Rate: Analysis of ALLSTAR Big Data

Emi Yuda, Yutaka Yoshida, and Junichiro Hayano

6.1 Introduction

Heart rate (HR) is the most popular index of physical and mental stresses. It increases with allostasis [1] and decreases with relaxation. With recent widespread use of wearable sensors, vast heart rate data during daily activities are accumulated, and interests in their effective utilization are increasing [2, 3]. Because heart rate differs with age, sex, and individual fitness level [4, 5], individual reference points are required for its appropriate interpretation.

One of the most promising candidates for the reference point is basal heart rate (BHR), i.e., the minimum heart rate in the day. In a previous study, we investigated the effects of age and sex on BHR in 113,341 males and 140,332 females [6]. We observed that although BHR in both sexes decreases with age until 20 years old and, thereafter, it increases slightly with advancing age, the average increase in BHR from 25 to 75 years old was only 1.9 bpm in male and 0.7 bpm in female. The clock time to reach BHR appeared between 02 and 05 h on average, and there was no consistent dependency on age or sex. In contrast, the difference between 24-h mean and BHR decreases linearly with age, suggesting that age-dependent decline in the HR increases in HR increment with daily activities can be estimated appropriately by using BHR as the reference point.

Although BHR seems a stable measure on average, the existence of individual differences cannot be denied, and particularly, the robustness of BHR against the pattern of daily activities is unknown. Because BHR usually occurs during sleep, individual difference in the time of sleep during the day may be important. Therefore,

E. Yuda · Y. Yoshida · J. Hayano (✉)
Nagoya City University Graduate School of Medical Sciences, Mizuho-ku, Nagoya, Japan
e-mail: emi21@med.nagoya-cu.ac.jp; yyoshida@med.nagoya-cu.ac.jp;
hayano@med.nagoya-cu.ac.jp

P. Vasant et al. (eds.), *Innovative Computing Trends and Applications*,
EAI/Springer Innovations in Communication and Computing,
https://doi.org/10.1007/978-3-030-03898-4_6

we investigated the effects of time of sleep during the day on the occurrence time and value of BHR. For this purpose, we used 24-h electrocardiogram (ECG) big data constructed by the Allostatic State Mapping by Ambulatory ECG Repository (ALLSTAR) [7–9].

6.2 Methods

The protocol of this study has been approved by the Ethics Review Committee of Nagoya City University Graduate School of Medical Sciences (No. 709).

Database

We studied 24-h ECG and three-axis actigraphic data of the ALLSTAR database [7–9]. ALLSTAR is a big data project accumulating 24-h ambulatory ECG data that has started in 2007. The database consists of 24-h Holter ECG data that were referred for analysis by three ECG analysis centers located at Sapporo, Tokyo, and Nagoya in Japan. The data were anonymized by the center and stored with accompanying information, including age, sex, and recoding date, time, and location (postal code).

Through the homepages of the ALLSTAR research project (http://www.med.nagoya-cu.ac.jp/mededu.dir/allstar/) and also of SUZUKEN CO., LTD. (http://www.suzuken.co.jp/product/holter/detail/), the purposes and information used for the study have been public, in which opportunities for the use of such information are ensured for the research subjects.

In the ALLSTAR data, those eligible for this study were those having both ECG and actigraphic data. In this data, we excluded those of whose ECG showed atrial fibrillation or pacemaker rhythm and included only those in which basic cardiac rhythm was sinus rhythm (defined as >80% of all recorded beats). The data showed that 18,876 males and 23,542 females met all of the criteria and were used in this study.

Data Analyses

The 24-h ECG and actigraphic data were recorded with Holter recorders (Cardy 303 pico+, SUZUKEN CO., LTD., Nagoya, Japan), by which 24-h multichannel ECG and triaxial acceleration data were measured; digitized at 125 Hz and 31.25 Hz, respectively; and stored in memory. The digitized ECG and acceleration data were analyzed using Holter ECG analyzers (Cardy Analyzer 05, SUZUKEN CO., LTD., Nagoya, Japan) by skilled medical technologists.

For ECG data, the temporal positions of all R waves were detected, the rhythm annotations were given to all QRS complexes, and all errors in automated analysis were corrected manually by the technologists. From acceleration data, the actigraphic data were obtained for left-to-right, caudo-cranial, and postero-anterior axes as x, y, and z values, respectively. Subjects were assumed to be in the lying position when the value of Y axis was below a threshold. Also, time series of $x(t)$, $y(t)$, and $z(t)$ were resampled at 10 Hz. After removing direct current component by a high-pass filter, combined into a composite vector value, $A(t)$ as

$$A(t) = \sqrt{x(t)^2 + y(t)^2 + z(t)^2}$$

Definition of the Time of Sleep

The time of sleep during the day was defined as when the body position was assumed to be lying and $A(t)$ was below a threshold defined individually from the distribution of $A(t)$ during the day. Then, subjects were classified into four groups according to the time of sleep: "nighttime sleepers" when >60% of the sleeping time of the day occurred between 00:00 and 06:00, "daytime sleepers" when it occurred between 08:00 and 14:00, "evening sleepers" when it occurred between 16:00 and 22:00, and "undefined" otherwise.

Measurement of BHR

BHR was defined as the minimum median value of sinus rhythm heart rate within 3-min window during the day. Using the beat annotations provided by Holter ECG analyzer, only R–R intervals consisting of consecutive sinus rhythm beats were extracted as normal-to-normal (N–N) intervals. Then, we calculated the median value of N–N intervals moving within 3-min window over the entire 24 h. Then, we took the maximum median interval during the day and calculated BHR as 60,000/bpm (the maximum median interval, ms). We also measured the clock time of BHR in each subject.

Statistical Analysis

Statistical Analysis System program package was used for statistical analysis. The differences between BHR level and timing of BHR with sleep time were evaluated by the general linear model procedure with adjusted for the effects of age and sex. Multiple comparisons were performed using the Bonferroni method. $P < 0.05$ was used as the criteria of statistical significance.

6.3 Results

Data were obtained from 18,875 men (age 66 ± 14 years) and 23,541 women (age 69 ± 15 years). The number and age of subjects classified into four groups according to the time of sleep are shown in Table 6.1.

As shown in Fig. 6.1a, the timing of BHR shifts slightly but significantly with the time of sleep ($P < 0.0001$). BHR occurred at 03:18 for nighttime sleepers on average, while it occurred at 02:35 in evening sleepers and 01:30 in daytime sleepers. The level of BHR, however, did not differ significantly with the time of sleep (52–54 bpm for all; Fig. 6.1b).

Table 6.1 Age and gender of subjects classified according to the time of sleep

	Male		Female	
	N (%)	Age, year	*N* (%)	Age, year
Daytime sleepers	193 (1.0)	61 ± 22	104 (0.4)	70 ± 22
Evening sleepers	491 (2.6)	67 ± 14	325 (1.4)	68 ± 17
Nighttime sleepers	9481 (50.2)	55 ± 21	15,175 (64.5)	60 ± 19
Undefined	8711 (46.2)	64 ± 17	7938 (33.7)	67 ± 17

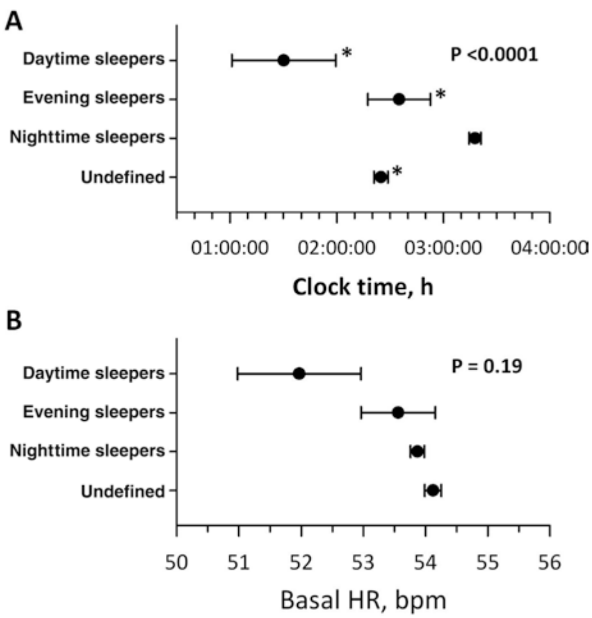

Fig. 6.1 Effects of the time of sleep during the day on the timing (**a**) and level (**b**) of basal heart rate. Data are mean ± SEM adjusted for the effects of age and sex

6.4 Discussion

This study examined the effects of time of sleep during the day on the occurrence time and value of BHR using ALLSTAR big data. We observed that the time of BHR slightly but significantly shifted with the time of sleep in the day, while the level of BHR didn't change significantly with the timing of sleep.

To our knowledge, this is the first study to report the effects of the timing of sleep on BHR using ECG big data. Because the ALLSTAR database covered the entire age range (0 to over 100 years old) for both sexes, our observations are thought to represent averaged features of BHR over all ages and both sexes. Also, the large sample size of the database gave this study a strong statistical power.

Our observations indicated that BHR occurred during night even for daytime and evening sleepers, although the time of BHR shifted to 1–2 h earlier than that for nighttime sleepers. This suggests that the BHR may not the physiological feature accompanying sleep itself but the result of the circadian rhythm of HR [10]. The independence of the level of BHR from timing of sleep may also support this. These results indicate that the BHR may be a physiological feature robust to temporal pattern of activity (time of sleep) and support its usefulness as the reference point of HR.

The limitation of this study is that each datum in ALLSTAR database has been collected for a certain clinical purpose. In this sense, the ALLSTAR database may show the characteristics of patients undergoing Holter ECG monitoring examination in Japan. Although we selected only the subjects whose basic cardiac rhythm was sinus rhythm (defined as >80% of all recorded beats), we need to assume that the data are affected by the underlying diseases and by possible differences in the prevalence of those diseases with age and sex. Nevertheless, we observed the stable features of BHR against the timing of sleep in the ALLSTAR database. This suggests that the BHR may be also robust at least to the diseases that affect the sleep time of the day.

6.5 Conclusions

We found that the time of BHR for daytime and evening sleepers slightly shifted to earlier time than that for nighttime sleepers, while the level of BHR didn't change significantly with the time of sleep during the day. Although BHR is usually observed during sleep, this study indicated that it does not necessarily occur during sleep but occurs at nighttime regardless of whether an individual is sleeping or not. Our observation also indicated that the level of BHR is a robust characteristic against the time of sleep.

Acknowledgments We acknowledge the SUZUKEN CO., LTD. for their support in data collections and anonymized data provisions.

Funding This work was supported by the grant of the Knowledge Hub Aichi, Japan [the Priority Research Project, P3-G1-S1-2b (J. Hayano)], and the Japan Society for the Promotion of Science, Japan [Grant-in-Aid for Scientific Research (C) 23,591,055 (J. Hayano)], [Grant-in-Aid for Scientific Research (C) 25,461,062 to H. Fukuta], [Grant-in-Aid for Scientific Research (B) 15H03095 (T. Nakamura)], and [Grant-in-Aid for Scientific Research (A) 17H00878 (Y. Yamamoto)].

References

1. Sterling, P., Eyer, J.: Allostasis: a new paradigm to explain arousal pathology. In: Fisher, S., Reasin, J. (eds.) Handbook of Life Stress, Cognition and Health, pp. 629–649. Wiley, New York (1988)
2. Ho, J.E., Larson, M.G., Ghorbani, A., Cheng, S., Coglianese, E.E., Vasan, R.S., Wang, T.J.: Long-term cardiovascular risks associated with an elevated heart rate: the Framingham Heart Study. J. Am. Heart Assoc. **3**, e000668 (2014)
3. Khan, H., Kunutsor, S., Kalogeropoulos, A.P., Georgiopoulou, V.V., Newman, A.B., Harris, T.B., Bibbins-Domingo, K., Kauhanen, J., Gheorghiade, M., Fonarow, G.C., Kritchevsky, S.B., Laukkanen, J.A., Butler, J.: Resting heart rate and risk of incident heart failure: three prospective cohort studies and a systematic meta-analysis. J. Am. Heart Assoc. **4**, e001364 (2015)
4. Camm, A.J., Fei, L.: Chronotropic incompetence—part II: clinical implications. Clin. Cardiol. **19**, 503–508 (1996)
5. Camm, A.J., Fei, L.: Chronotropic incompetence—part I: normal regulation of the heart rate. Clin. Cardiol. **19**, 424–428 (1996)
6. Hayano, J., Yoshida, Y., Yuda, E.: Characteristics of basal heart rate during daily life: Relationships with age, gender, and mean heart rate. In: The 11th EAI International Conference on Pervasive Computing Technologies for Healthcare (PervasiveHealth 2017). Barcelona, Spain (2017)
7. Yuda, E., Yoshida, Y., Ogasawara, H., Hayano, J., ALLSTAR Study Group: Ambulatory physical activity monitoring to know healthy life expectancy. In: Yamamoto, Y., Nomura, T., Cerutti, S., Dickhaus, H., Yana, K. (eds.) Proceedings of the 8th International Workshop on Biosignal Interpretation (BSI2016), Osaka, Japan (2016)
8. Yuda, E., Furukawa, Y., Yoshida, Y., Hayano, J., ALLSTAR Research Group: Association between regional difference in heart rate variability and inter-prefecture ranking of healthy life expectancy: ALLSTAR Big Data Project in Japan. In: Jung, J.J., Kim, P. (eds.) Big Data Technologies and Applications: Proceedings of the 7th EAI International Conference, BDTA 2016, pp. 23–28. Springer, Seoul (2017)
9. Hayano, J., Yuda, E., Furukawa, Y., Yoshida, Y.: Association of 24-hour heart rate variability and daytime physical activity: ALLSTAR big data analysis. Int. J. Biosci. Biochem. Bioinforma. **8**, 61–67 (2018)
10. Hayano, J., Jiang, W., Waugh, R., O'Connor, C., Frid, D., Blumenthal, J.A.: Stability over time of circadian rhythm of variability of heart rate in patients with stable coronary artery disease. Am. Heart J. **134**, 411–418 (1997)

Chapter 7
Innovative Instruments for Extraction of Low-Grade Heat from Surface Watercourses for Heating Systems with Heat Pump

V. V. Kharchenko, A. O. Sychov, and G. N. Uzakov

7.1 Introduction

In many countries heat pump installations (HPI) are implemented and actively used in the heating sector for a long time, especially for heating of private houses, where they are a good alternative to gas, oil, or solid fuel boilers as well as devices with direct electrical heating in cases when there is no connection to the main gas pipeline and the electric grid or deliverable fuel can be the only power sources. The main obstacles for a more widespread adoption of such plants are, on the one hand, the high cost and, consequently, long payback period of installations using heat of soil or aquatic environments and, on the other hand, low efficiency at low temperatures of more affordable heat pumps using warmth of outdoor air. The last type is suitable mostly only for regions with relatively mild climates.

A significant share of the total capital expenditure in the construction of heat pumps that use heat soil or aquatic environments is the cost of the circuit arrangement for the selection of low-grade heat. If you use ground or groundwater as a heat source to significantly reduce installation costs, in most cases it is not possible due to the need for a huge excavation. However, in the case of the existence of the open water heat source suitable in parameters—a water body or watercourse—there is an opportunity to reduce installation costs.

Particularly promising in this respect is the use of the heat of the watercourse. Analysis of the situation with the practice of creating such HPI shows that due to the low experience and lack of research in this area, in many cases, this practice is not

V. V. Kharchenko (✉)
FGBNU Federal Scientific Agroengineering Center VIM, Moscow, Russia

A. O. Sychov · G. N. Uzakov
Karshi Engineering Economic Institute, Karshi, Uzbekistan
e-mail: qmii@qmii.uz; kiei_info@edu.uz

P. Vasant et al. (eds.), *Innovative Computing Trends and Applications*,
EAI/Springer Innovations in Communication and Computing,
https://doi.org/10.1007/978-3-030-03898-4_7

the optimal solution since it may lead to increased costs and sometimes to situations where the characteristics of the installation are much worse than expected. In some cases when you try to design HPI with the use of classical methods of selection of heat from the water mass, the results of preliminary calculations make this project unattractive to the customer, and this idea was rejected, although more in-depth approach to the issue and the use of other technical solutions could make such an installation much more cost-effective.

It should also be noted that in addition to natural aquatic environments there are many relatively warm water bodies and watercourses, bearing the bargain anthropogenic or geothermal heat, which are possible to significantly reduce the cost of heating.

7.2 Possible Ways to Improve Indicators

There are several possible methods of selection of heat from a reservoir or watercourse. The most simple, inexpensive, and effective at first glance seems to be open loop without intermediate heat carrier, that is, with the extraction and subsequent discharge of water, but this is not possible in all cases and, in analyzing significant drawbacks, usually not recommended for use. Thus, in practice the applied passive methods for the selection of heat with circuit of an intermediate heat carrier are the most widely used methods for laying the bottom of the so-called mats made of polyethylene pipes that can be called by analogy the horizontal ground collectors at HPI, which use the heat of the soil. However, despite the simplicity of design and low cost of polyethylene pipes, such a scheme of selection of heat from the aquatic environment is not always the most rational.

We reviewed ways of enhancing technical and economic characteristics of heat pump systems using the heat of the water environment, especially the watercourse.

Fig. 7.1 shows a block diagram which describes the rationale for choosing key technical solutions in the case of selection of heat from the environment with low heat output (emission), such as ground [1]. The scheme allows understanding the reasons why the collectors made of polyethylene pipes are the best solution in such conditions.

In the case of selection of heat from the water environment, the picture changes [2]. A fixed water mass in stagnant water, especially in the bottom region, cannot be considered as a source with high heat transfer, but the arising convective flows allow to use schemes with a higher density of the heat flux and less heat transfer surface. Thus, in some situations, large-scale bottom collectors of polyethylene pipe can become more compact, submersible heat exchangers, and in some cases they are already used in practice in creating such heat pump installations. However, today there is a lack of available data and an absence of any comparative studies that would accurately determine the optimal solution in each specific case—the selection of heat from the water.

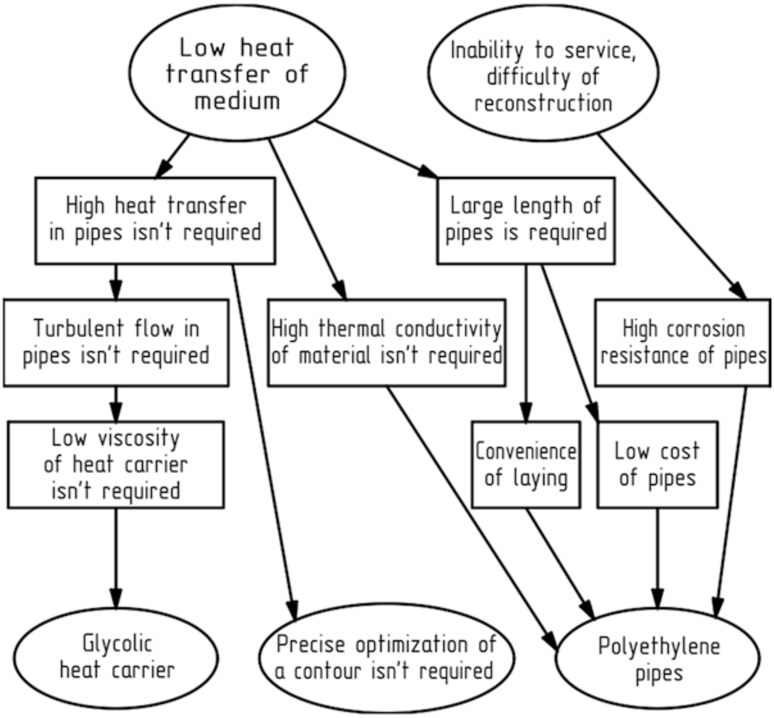

Fig. 7.1 Logic of a choice of optimum technical solutions for warmth selection from medium with a low heat output

In turn, water stream in full can be called a medium with high heat transfer, and to achieve the best technical-economic performance of heat pumps, which use the heat of the watercourse, it is advisable to use this feature. In Fig. 7.2 is a block diagram showing the principal steps to be taken in the design of the heat exchanger and the overall contour of the selection of low-grade heat from the watercourse to achieve the estimated goals.

As can be seen from the diagram, the possible ways require a more careful approach to the calculation and optimization of parameters, but designed according to this manner HPI with metal immersion heat exchangers in many cases should be more profitable than HPI with bottom mats, and in some cases, this is the only acceptable solution.

The important and difficult issue is the choice of the optimal heat carrier meeting all the requirements. In conditions of near-zero temperatures, viscosity starts to play a crucial role. High viscosity at a low temperature of most used solutions, especially based on propylene glycol, significantly affects the performance and makes inefficient metal heat exchangers. Moreover, this factor significantly affects the characteristics of the classic collectors of polyethylene pipes. Thus, the question of choosing the best heat carrier is relevant for any schemes for the selection of low-grade heat.

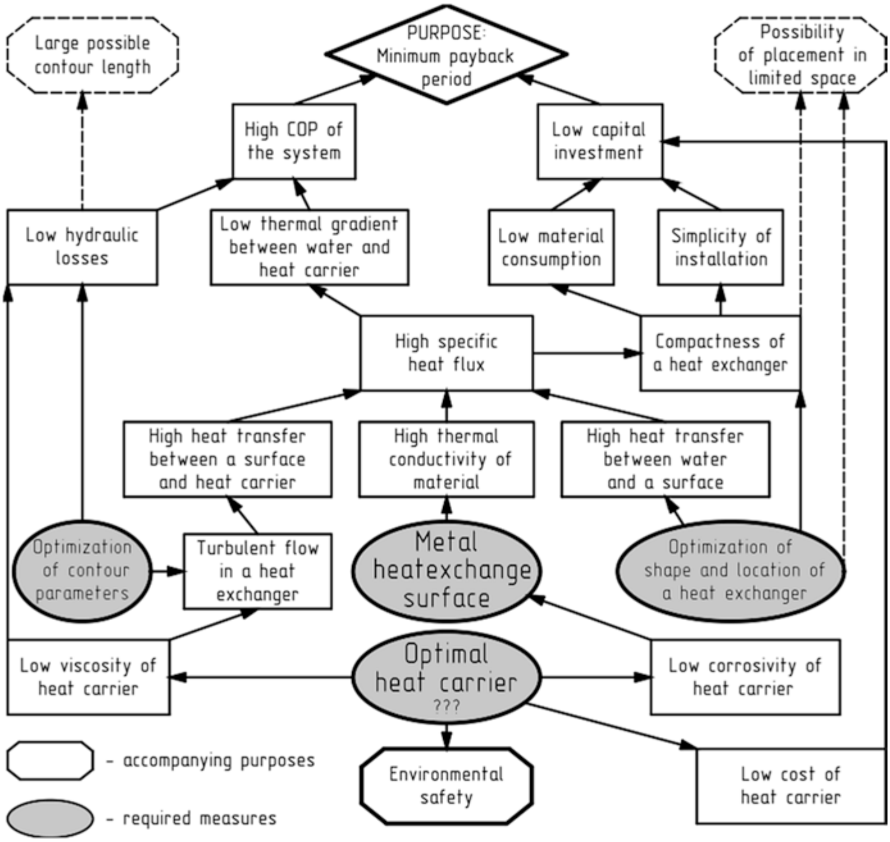

Fig. 7.2 Possible ways to improve technical and economic indicators of heat pump-based systems in case of warmth selection from a watercourse

Analysis of a large number of used in various fields low freezing compounds showed the absence of heat carrier, which would meet all the requirements, but a compromise may be the use of a solution of calcium chloride, despite its corrosiveness, which largely will be mitigated by the use of certain corrosion inhibitors. In addition to low viscosity, the fluid has low cost, which is also a significant factor affecting the overall installation cost, as well as the environmental safety.

7.3 Practical Solutions

One can offer several different designs of water-brine heat exchangers, designed for the selection of heat from the stream corresponding to the above criteria of maximum efficiency. A variant of such heat exchanger based on the use of a flat coil of metal tubing of circular cross-section is shown in Fig. 7.3 [3].

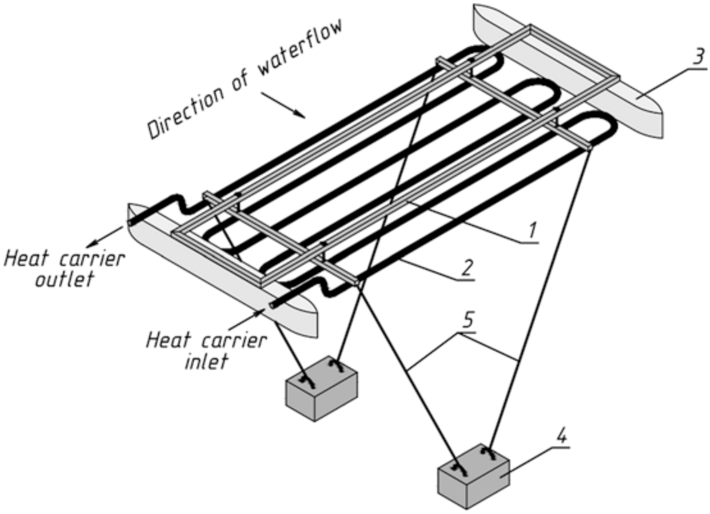

Fig. 7.3 Submersible floating water-brine heat exchanger. *1*—frame, *2*—coil-pipe, *3*—floats, *4*—anchors, *5*—ropes

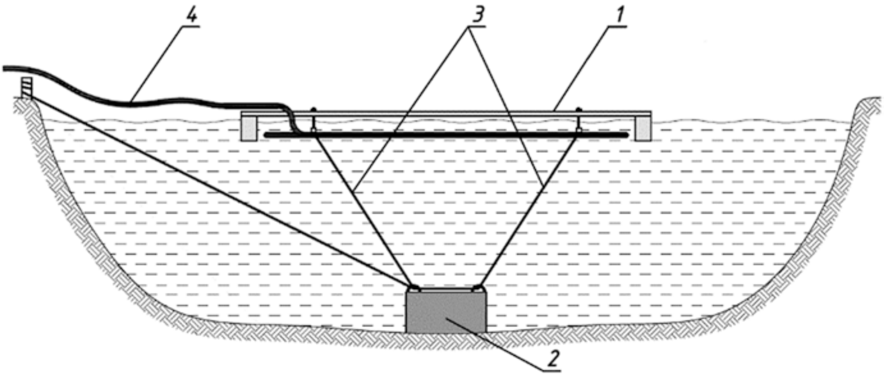

Fig. 7.4 Arrangement of the heat exchanger in a watercourse. *1*—floating heat exchanger, *2*—anchors, *3*—ropes, *4*—flexible hose

In this design, enhancing the heat transfer is primarily achieved through the use of the natural movement of water in the direction of the flow core for heat transfer processes intensification. It is known that the rate of flow of water in an open channel takes the highest values near the surface, and in the case of the ice-cover area of greatest flow velocity is shifted inland, closer to the middle of the stream. For installing the heat exchanger in the zone of greatest velocity, it is equipped with floats, which give it buoyancy, and ropes and anchors so that the heat exchanger can be positioned and retained in the area of best heat transfer (Figs. 7.4 and 7.5).

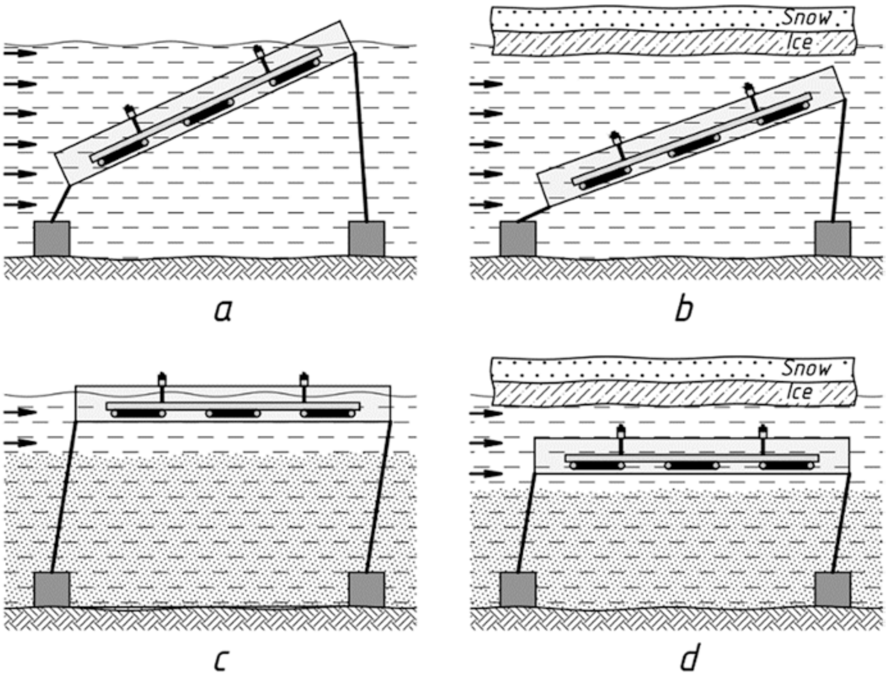

Fig. 7.5 Examples of arrangement of the heat exchanger in a watercourse depending on conditions. (**a**) clear channel; (**b**) existence of an ice cover; (**c**) silted channel; (**d**) the presence of bottom sludge and ice cover

The improving heat transfer characteristics also occur due to the fact that the construction and arrangement of the heat exchanger permit to direct the flow of water in the direction of straight segments of pipe of the coil that intensify the process of heat transfer.

When using the heat exchanger in the freezing conditions of the watercourse for the period the ice cover it is advisable to pull the cables closer to the bottom (Fig. 7.5b, d), and the rest of the time to keep the surface of the watercourse (Fig. 7.5a, b); thus the coil will be in the areas of highest velocity and will not be frozen in the ice. In the same time, even a significant decrease in the level of water in the canal will not result in drying up pipes of the coil, as the heat exchanger will start to drop after the water level.

To test the described method of extraction of heat from the watercourse, as well as for testing other technical solutions aimed at improving technical and economic indicators of HPI, there was collected the experimental setup, which was a heat pump heating and air conditioning system of residential house water-to-air type with capacity up to 7 kW (Fig. 7.6). The system of selection of low-potential heat based on the floating heat exchanger was mounted on a specially selected ice-free watercourse (Fig. 7.7).

In addition to the use of special river heat exchanger, experimental setup is also distinguished by several technical solutions, which are usually not used in classical

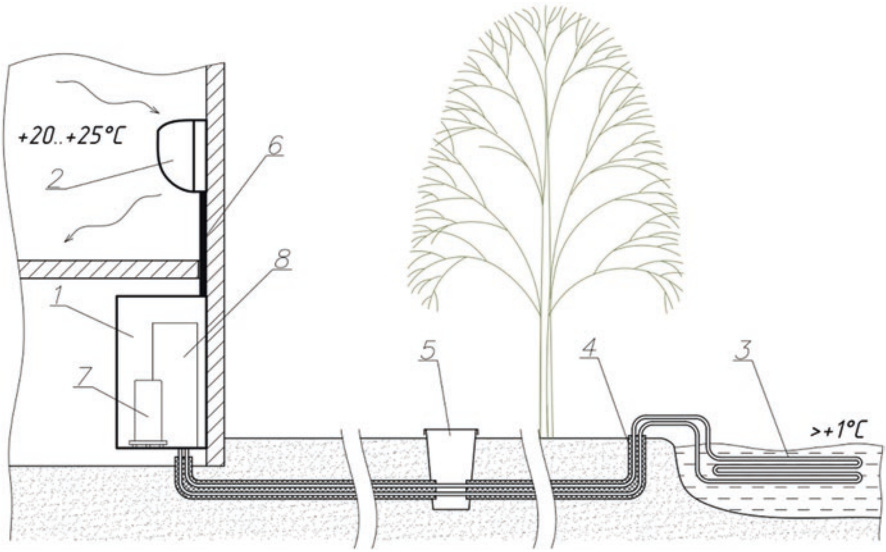

Fig. 7.6 Schematic diagram of the experimental installation. *1*—outdoor unit; *2*—indoor unit; *3*—water-brine heat exchanger; *4*—heat-insulated underground pipeline; *5*—caisson; *6*—freon line; *7*—compressor; *8*—brine-freon heat exchanger

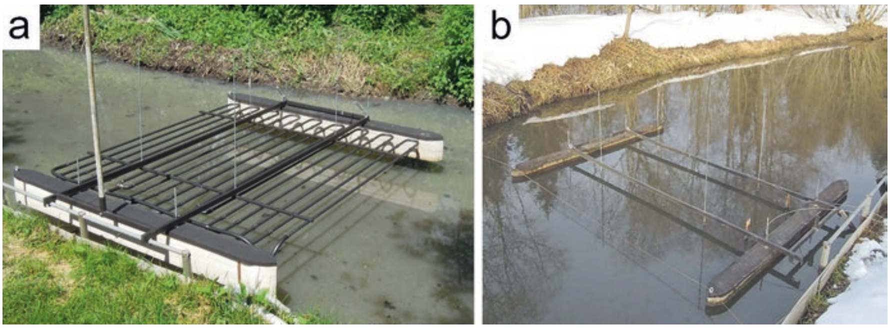

Fig. 7.7 Experimental sample of the floating heat exchanger. (**a**) Lifted over water in the summer; (**b**) in working position in the winter

heat pump systems, but which provide certain advantages and also serve as a subject of research. Such solutions are, for example, as below:

- The use of variable frequency compressor and circulating pump of a low-temperature circuit.
- Direct heating of the internal air in the heat exchanger-condenser of the heat pump without the use of intermediate contours and closed vent system to distribute warm air around the house.
- The ability to connect additional sources of low-grade heat.

For this scheme, the efficiency of the entire system depends on parameters such as the size and configuration of the submersible heat exchanger, the composition and specific consumption of heat carrier, and others. The total coefficient of performance (COP) of the whole installation is also affected by the power required for circulation. To determine the best configuration and optimization of all parameters for the specific initial conditions, previously a special calculation program in MathCAD was compiled [4].

The process of heat carrier heating in a coil-pipe, not covered by ice, is described by the differential equation as below:

$$\frac{dT(x)}{dx} = \frac{\pi \cdot d \cdot K \cdot \left(T_R - T(x)\right)}{G \cdot C}, \tag{7.1}$$

where $T(x)$ is the temperature of heat carrier along the path through the heat exchanger, d is the average pipe diameter, K is the coefficient of heat transfer from water to heat carrier, T_R is the temperature of river water, G is the flow rate of heat carrier, and C is the specific heat of heat carrier.

In cold countries such as Russia, Finland, Sweden, etc., the operation of the designed system can be associated with a possibility of icing, that is, with a formation of ice layer of different thicknesses on walls of the heat exchanger, which is located in water [5].

To design heat exchangers taking into account the possibility of forming an ice layer on the coil-pipe surface, another differential equation was derived:

$$\frac{dT(x)}{dx} = \frac{\pi \cdot \left(d_O + 2 \cdot \Delta_I\left(T(x)\right)\right) \cdot \alpha_I\left(\Delta_I\left(T(x)\right)\right) \cdot \left(T_R - 273.15\right)}{G \cdot C}, \tag{7.2}$$

where $T(x)$ is the temperature of heat carrier depending on the path traveled through the heat exchanger, d_O is the outside pipe diameter, $\Delta_I(T(x))$ is the steady-state thickness of the ice layer on the surface of the pipe depending on the temperature of heat carrier at a given point of the coil-pipe, $\alpha_I(\Delta_I(T(x)))$ is the coefficient of heat transfer from water to the ice-covered pipe depending on the thickness of the ice layer Δ_I at a given point of the coil-pipe, T_R is the temperature of river water, G is the flow rate of heat carrier, and C is the specific heat of heat carrier.

This equation is obtained at the condition that the temperature of the outer surface of the ice layer is 0 ° C (273.15 K), which means a constant temperature gradient between river water and the ice surface at a variable coefficient of heat transfer, which depends on the outer diameter of the ice-covered pipe:

$$\alpha_I\left(\Delta_I\right) = \frac{1}{2} \cdot \lambda_W \cdot \Pr_W^{0.38} \cdot \sqrt{\frac{V_W}{\nu_W \cdot \left(d_O + 2 \cdot \Delta_I\right)}}, \tag{7.3}$$

where λ_W, $\Pr_W$, and ν_W are the thermal conductivity, Prandtl number, and kinematical viscosity of river water, respectively, V_W is the speed of water in the river, and d_O is the outside pipe diameter.

The dependence of ice layer thickness on heat carrier temperature at a given point of the coil-pipe $\Delta_I(T(x))$ is in turn calculated out of the constancy of the linear density of the heat flux through the pipe wall as follows:

$$\left(\frac{d_I + d_O + 2\cdot\Delta_I\left(T(x)\right)}{2}\right)\cdot K\cdot\left(T_R - T(x)\right) = \left(d_O + 2\cdot\Delta_I\left(T(x)\right)\right)\cdot\alpha_I\left(\Delta_I\left(T(x)\right)\right)\cdot\left(T_R - 273.15\right), \tag{7.4}$$

where d_I and d_O are the inside and outside pipe diameter, respectively, K is the coefficient of heat transfer from water to heat carrier, and $\alpha_I(\Delta_I(T(x)))$ is the coefficient of heat transfer from water to ice-covered pipe, depending on the thickness of the ice layer at a given point of the coil-pipe.

The differential Eq. (7.1) has an analytic solution, which simplifies the calculations:

$$T(x) = T_R - \exp\left(\ln\left(T_R - T_0\right) - \frac{\pi\cdot d\cdot K\cdot x}{G\cdot C}\right), \tag{7.5}$$

where T_0 is the temperature of heat carrier at the inlet to the coil-pipe.

The differential Eq. (7.2) does not have a simple analytical solution; therefore, to calculate heat carrier temperature in this case, numerical methods for solving differential equations available in the MathCAD environment, such as the “rkadapt” and “rkfixed” commands, are used.

The algorithm of calculation and optimization of the river heat exchanger include a lot of subroutines, conditional operators, cycles, and iterations, and the performed works, thus, demonstrate the wide possibilities of the MathCAD package, which proved to be indispensable for the solution of the task.

7.4 Conclusion

The use of surface water, especially channels, small rivers, and other watercourses as sources of low-grade heat for heat pump systems, allows reducing the cost of creating such systems. To achieve high technical and economic indicators of HPI, new and most optimal technical solutions are required in each case—as one of these solutions can serve the proposed submersible floating water-brine heat exchanger. Introducing the practice of this and other solutions that can reduce the cost of heat pump installations and payback period would promote wider dissemination of such systems. A particularly promising application of systems such as described above appears to be in the areas where there is widely used irrigation system for watering and irrigation of agricultural structures. Such areas include some territories of southern Russia and southern Kazakhstan, almost all territories of Uzbekistan, and so on.

References

1. Vasil'ev, G.P., Krundyshev, N.S.: Jenergojeffektivnaja sel'skaja shkola v Jaroslavskoj oblasti (Energy Efficient rural school in the Yaroslavl region). AVOK **5** (2002). (Russian language)
2. Kavanaugh, S., Pezent, M.C.: Water-to-air heat pump performance with lake water. In: Proceedings of the sixth symposium on improving building systems in hot and humid climates, Dallas, TX, 3–4 October 1989
3. Sychov, A.O., Kharchenko, V.V.: Heat supply of a rural house using low-potential heat of open water currents. Mechaniz. Electrific. Agric. **1**, 14–17 (2015). (Russian language)
4. Kharchenko, V.V., Sychev, A.O.: Optimization of the low-temperature circuit of a heat pump system based on the heat of surface water. Altern. Energy Ecol. **7**, 31–36 (2013). (Russian language)
5. Kharchenko, V.V., Sychev, A.O.: Calculation of influence of icing on effectiveness of low-potential heat selection from water environment. Energy Autom. **4**, 21–29 (2017). (Russian language)

Chapter 8
Propagation of Microwave Fields in Grain Material of Various Densities

Dmitry Budnikov, Alexey N. Vasilyev, Dmitry Tikhomirov, and Alexey A. Vasilyev

8.1 Introduction

The necessity for grain drying of agricultural materials is determined by the necessity to ensure their quality and the period of safe storage. In order to achieve satisfactory level for the manufacturers' economic performance and maintain reasonable consumer prices, it is necessary to use energy-saving equipment. The development of such technological equipment currently involves the use of computer simulation tools, building scalable models, and prototyping of the required equipment. In the case of development of methods of thermal processing of grain materials by methods of RF and microwave effects, we can use such software products of mathematical and visual modeling, like COMSOL, FEMLAB, QW3D, CST Studio, ANSYS, and some others [1–3]. The processes of postharvest handling of grain, which require thermal effects, can be referred drying, disinfection, micronization, and preparation for feeding. All these processes are highly energy intensive.

The cost of postharvest processing is up to 20% on average of the total production costs of grain production and in some cases even more for countries with unfavorable climate [4]. Thus the development of the energy-saving equipment for after-harvesting processing of grain doesn't lose its relevance. The development of scalable models of equipment of the electromagnetic processing gets the special significance in the field of the fast prototyping and the reducing losses due to errors at various stages of development and implementation.

D. Budnikov (✉) · A. N. Vasilyev · D. Tikhomirov · A. A. Vasilyev
Federal State Budgetary Scientific Institution "Federal Scientific Agroengineering Center VIM" (FSAC VIM), Moscow, Russia

P. Vasant et al. (eds.), *Innovative Computing Trends and Applications*,
EAI/Springer Innovations in Communication and Computing,
https://doi.org/10.1007/978-3-030-03898-4_8

8.2 Main Part

In the case of dielectric materials with a relatively high factor of dielectric losses exposed to RF and microwave field of sufficient intensity, these materials will absorb the energy of the electric fields by converting electric field energy into thermal energy into the material. This phenomenon is known as dielectric or microwave heating; the term depends on the frequency [5]. The heating level depends on the absorbed power and the characteristics of the material.

The power *P*, absorbed in the unit of the volume of the dielectric, depends on the dielectric properties and could be calculated using the following equation:

$$P = 2\pi \cdot f \cdot \varepsilon_0 \cdot \varepsilon'' \cdot E^2, \tag{8.1}$$

where *P* is power, absorbed by the unit of the material; W/m^3; *f*, frequency of the electromagnetic field; Hz; ε_0, permittivity of vacuum (8854 × 10^{-12} F/m); ε'', loss factor; and *E*, intensity of the electric field, V/m.

Dielectric heating in the processing of materials is effective in cases where the loss factor is from 2 to 100 [5]. Lower values of it decrease the heating rate, and higher values decrease the depth of penetration of electromagnetic wave in the material layer.

Research Method

The basis for the mathematical description and modeling by software is the system of Maxwell's equations. Software, like COMSOL Multiphysics, FEMLAB, QW3D, CST Studio, and ANSYS, are designed for the solution of these equations by one method or another.

Electrodynamics simulation in HFSS is based on finite element method (FEM). The solution of the boundary problem is sought in the frequency area. The use of the finite element method provides a high degree of universality of numerical algorithms that are highly effective for a wide range of tasks. In our case the object of study is the active zone filled with a layer of grain. Ultrahigh frequency electromagnetic energy supply is carried out from the side with the horn waveguide from the magnetrons.

The article deals with the possibility of representation not only on dense grain layer but the layer with lower density that is typical for fluidized layer, for example. Such way of modeling is important because heat-moisture transfer in this type of layer is characterized by a greater intensity.

In the modeling process of the electromagnetic effects by numerical simulation software of three-dimensional electromagnetic structures, the material which is exposed to a field is usually presented in the form of solid shapes with given properties describing the product at certain values of density, moisture, and other parameters (Fig. 8.1a). In the first stage of simulation, the modeling was performed,

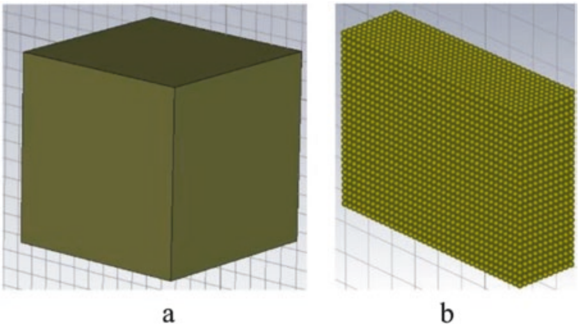

Fig. 8.1 The grain layer representation: (**a**) as a solid structure; (**b**) as a solid layer of substitute forms

and the material was defined with properties that have been reported previously [6–9]. In the case of simulation of field effects on agricultural materials such as grain, feed, and other bulk materials, there is some discrepancy between the properties of the individual grains constituting the layer and the mass of the processed material. It seems very nonrelevant to the description of air gaps and accounting the porosity of layer [6–8]. Thus, it is necessary to consider the option of a presentation layer in the form of volume completely filled with objects that can be represented by the processed material. So, on the second stage of the simulation, the grain in the modeling and mathematical description can be replaced by balls of equivalent diameter. The volume of grain material represented by such method is shown in Fig. 8.1b.

The grain layer after the postharvest handling can be at different densities (dense, loose, fluid, swirl boiling). Measurement of dielectric properties in the cases of the loose layer is almost impossible [6, 9, 10]. For the solving the tasks of modeling and determination of the ε'', the grain layer can be represented with an equivalent volume of grain with a given porosity, which allows to determine the distribution of electromagnetic fields in a layer of predetermined density. Figure 8.2 shows the grain material with different densities.

Each seed can be represented taking into account the inequality distribution of moisture in addition to the submission of the grain layer in the form of a set of seeds. Figure 8.3 shows the seed in form taking into account the equal distribution of moisture and to reflect the changes in humidity from the center of the grains to the surface, which is typical during the drying and disinfection of grain by electrophysical methods of influence.

Properties of grain crops were taken from various sources [6–9] and experimental data [2, 3] for modeling.

Simulations conducted with the grain layer in the form of a set of seeds showed a significant increase in required computer time to obtain results. A representation of the seeds taking into account the unequal humidity, the layers within the grains, led to the need to significantly reduce the number of layers of grains in the simulation.

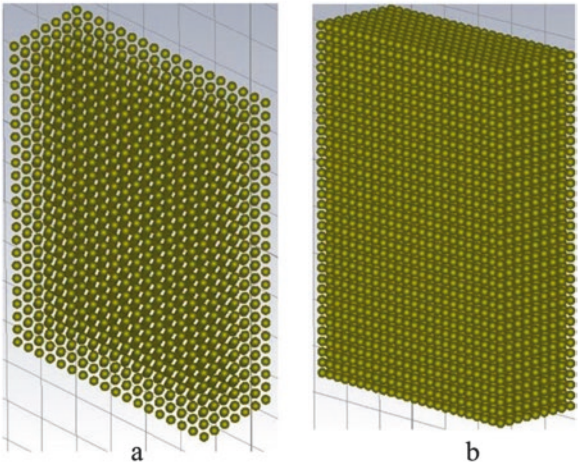

Fig. 8.2 The grain material view: (**a**) soft wheat with humidity 16% and density of the layer 200 kg/m^3; (**b**) soft wheat with humidity 16% and density of the layer 500 kg/m^3

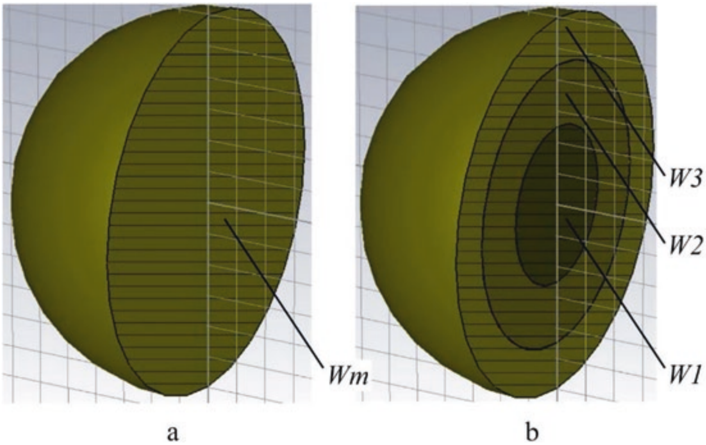

Fig. 8.3 Seed view: (**a**) with equal moisture distribution, *Wm*; (**b**) with variation of the humidity from the center to the surface of the seed, *W*1>*W*2>*W*3

Measurement of Dielectric Properties

It is necessary to have reliable data of dielectric properties of the material at the frequency of acting field for quality modeling of propagation of electromagnetic wave in the material. Methods of measurement are different for different frequency ranges. Principles and measurement techniques of microwave dielectric properties were discussed in several reviews [6, 11].

Microwave dielectric property measurement techniques can be classified as measurements of the reflected and absorbed power using resonant or nonresonant systems with open or closed structures to determine the properties of material samples. Also the construction of a dielectric sample holder for concrete materials is important. Method of short-circuited lines to measure the dielectric properties provides a suitable method for many materials, for example, for solid particles and many agricultural materials [6].

Laboratory Setup

Previously developed laboratory setup [3], along with equipment used by the researchers [5, 6], allows to verify the results of the simulation of microwave field distribution in a dense layer. The need to verify the penetration of the electromagnetic field in a slurry layer of grain emerged at this stage, and the need of the measurement of the coefficient of dielectric losses in this layer led to a revision of the existing installation. A modified version of the laboratory setup is schematically represented in Fig. 8.4.

Thus the implementation of the load of the material could be studied both at full and at partial filling of the volume of the microwave-convective processing area. The state of the fluidized or suspended layer is performed by blowing through a layer air with the required speed from the fan. The air flow rate is controlled by vector frequency converter (VFC). The electromagnetic field strength in the layer of material is measured by a device developed and presented earlier [12], and the determination of the coefficient of dielectric loss by analytical methods (8.2), and the coefficient of dielectric loss is determined analytically by formula (8.2); the temperature control of the seeds is measured by thermocouple built into it.

$$\varepsilon'' = \frac{c_m \cdot \rho_m \cdot \Delta T}{5.56 \times 10^{-11} \cdot E^2 \cdot f \cdot \tau}, \quad (8.2)$$

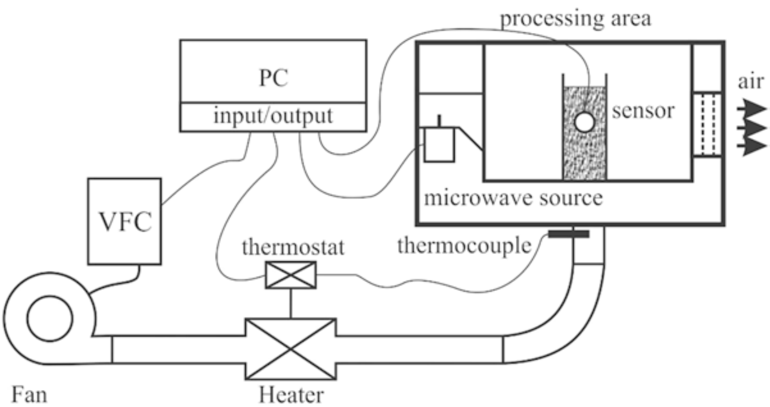

Fig. 8.4 Schematic view of the laboratory setup

where c_m is heat capacity of the material, kJ/kg °C; ρ_m, density of the dry matter of the sample, kg/m^3; ΔT, temperature of the material during process, °C; and τ, time, s.

Measurement Results

Figure 8.5 shows graphs for determining the coefficient of dielectric losses for wheat at a humidity from 11 to 30%.

The obtained results for different densities of the material match the general trend but differ significantly in their level. So, for a dense layer, which corresponds to the density of 660 kg/m^3 in the moisture range 11–30%, the coefficient of dielectric loss changes in the range of 0.18–0.42, for fluidized layer (440 kg/m^3) 0.06–0.15, and for weighted layer (220 kg/m^3) 0.1/0.3. The accuracy of the data for different density levels differs significantly as in the dense layer the error is caused by the used sensors as well as the presence of air gaps in the layer: for fluidized and suspended layers, in addition to the described losses due to the thermal interaction of air with the grain layer and the sensor. The quality of the measurements could be improved using of sensors that are not sensitive to the microwave field, for example, optical, as well as changing in the support method for the desired layer, for example, mechanical.

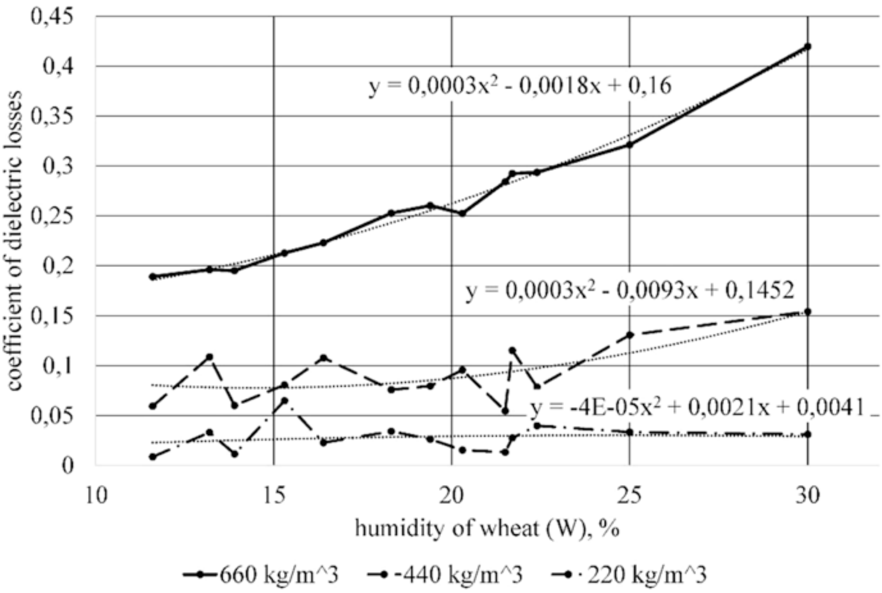

Fig. 8.5 Results of the determination of the coefficient of dielectric losses

Simulation Results

The results of modeling of distribution of electromagnetic field strength in wheat with a moisture content of 16% are presented in Fig. 8.6.

The pattern of distribution of electromagnetic field in the dielectric layer in this case is characterized by the loss (power dissipation) as the wave propagation. The results of modeling show that the distributions of the electromagnetic field of the described variants of implementation of the grain layer are the same, which suggest the possibility of further replacement implementations of the equivalent forms to a solid form. This will significantly reduce the required machine time. Some deviations in the numerical values are due to the lack of considering the influence of reflection waves from the surface of the material and inaccuracy of data on the dielectric properties of materials.

It is also clear from the pattern of distribution of EMF that the selectivity of the heating, that is, typical for areas with higher relative to the rest of the volume of the material humidity (higher dielectric losses), celebrated by many authors [13–17], could be taken into account.

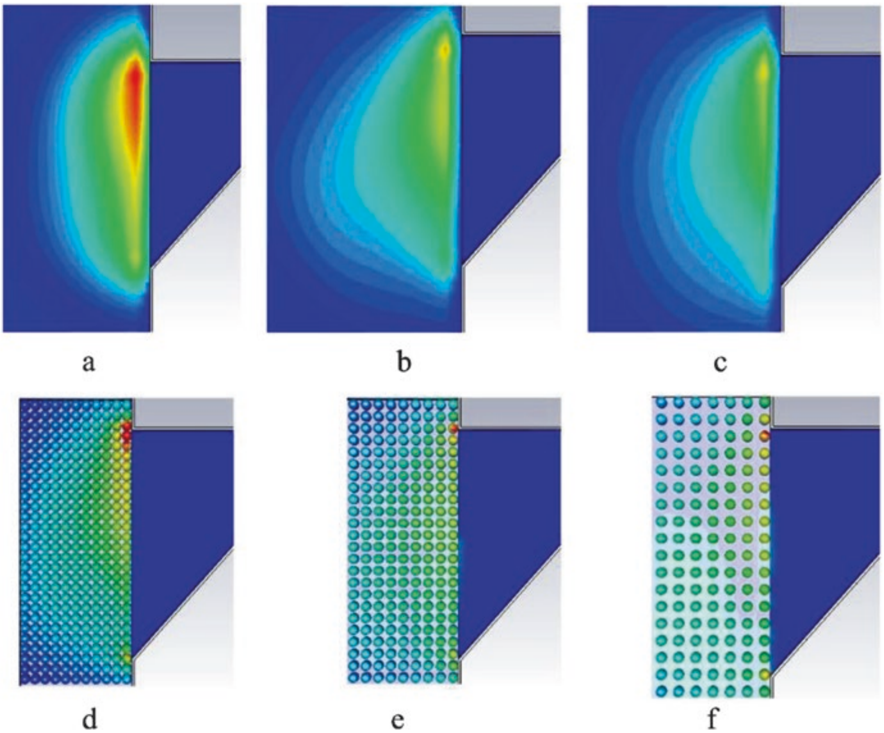

Fig. 8.6 Simulation results for distribution of EMF field strength: (**a**–**c**) in the form of a continuous layer; (**d**–**f**) as a set of spherical grains

8.3 Conclusions

Based on the foregoing, we can conclude the following:

1. Data on the dielectric properties of grains and grain layer should be clarified.
2. It is necessary to conduct experimental studies on the electromagnetic field distribution in the grain layer and compare its results with the results of the numerical experiment.
3. The grain layer in the electrodynamic simulation programs can be implemented as in the solid form and in the form of a set of substitution forms of the source elements (grains).
4. The grain layer should be presented in the continuous form to reduce the intensity of the calculations.
5. Dielectric properties of loose grain layer in the solid form can be obtained through modeling with substitution forms of the appropriate density.

References

1. Ranjbaran, M., Zare, D.: Simulation of energetic- and exergetic performance of microwave-assisted fluidized bed drying of soybeans. Energy. **59**, 484–493 (2013). https://doi.org/10.1016/j.energy.2013.06.057
2. Budnikov, D.A.: Modeling of the effect of structural parameters of the processing zone on the distribution of the microwave field in the electro-technological module for drying and processing of grain. Innov. Agric. **4**(9), 88–91 (2014)
3. Budnikov, D.A.: Measurement of the microwave field strength in the grain layer. Bull. VIESH. **4**(21), 40–44 (2015)
4. Budnikov, D.A.: Representation of the grain layer in the simulation of electromagnetic interference. Bull. VIESH. **4**(25), 50–54 (2016)
5. Wang, Y., Li, Y., Wang, S., Zhang, L., Gao, M.: Juming Tang: Review of dielectric drying of foods and agricultural products. Int. J. Agric. Biol. Eng. **4**, 1 (2011)
6. Nelson, S.: Dielectric Properties of Agricultural Materials and Their Applications, p. 229. Academic, New York (2015)
7. Kraszewski, A., Nelson, S.O.: Composite model of the complex permittivity of cereal grain. J. Agric. Eng Res. **43**, 211–219 (1989)
8. Nelson, S.O.: Dielectric properties of agricultural products and some applications. Res. Agr. Eng. **54**(2), 104–112 (2008)
9. Vankatesh, M.S.: An overview of microwave processing and dielectric properties of agri-food materials. Biosyst. Eng. **88**(1), 1–18 (2004). https://doi.org/10.1016/j.biosystemseng.2004.01.007
10. Antic, A., Hill, J.M.: The double-diffusivity heat transfer model for grain stores incorporating microwave heating. Appl. Math. Model. **27**(8), 629–647 (2003)
11. Budnikov, D.A., Vasilev, A.N., Ospanov, A.B., Karmanov, D.K., Dautkanova, D.R.: Changing parameters of the microwave field in the grain layer. J. Eng. Appl. Sci. **11**(1), 2915–2919 (2016)
12. Budnikov, D.A.: Study of the distribution of the microwave field intensity in the grain layer [Issledovanie raspredelenija naprjazhennosti SVCh polja v zernovom sloe] Inženernyj vestnik Dona (Rus), 2015, No. 3. www.ivdon.ru/ru/magazine/archive/n3y2015/3234

13. Yadav, D.N., Patki, P.E., Sharma, G.K.: Effect of microwave heating of wheat grains on the browning of dough and quality of chapattis. Int. J. Food Sci. Technol. **43**(7), 1217–1225 (2007)
14. Grundas, S., Warchalewski, J.R., Dolińska, R., Gralik, J.: Influence of microwave heating on some physicochemical properties of wheat grain harvest-ed in three consecutive years. AACCI. **85**(2), 224–229 (2008)
15. Pallai-Varsányi, E., Neményi, M., Kovács, A.J., Szijjártó, E.: Selective heating of different grain parts of wheat by microwave energy. In: Advances in Microwave and Radio Frequency Processing, pp. 312–320. Academic, New York (2001)
16. Vasiliev, A.N., Budnikov, D.A., Gracheva, N.N., Smirnov, A.A.: Increasing efficiency of grain drying with the use of electroactivated air and heater control. In: Kharchenko, V., Vasant, P. (eds.) Handbook of Research on Renewable Energy and Electric Resources for Sustainable Rural Development, pp. 255–282. IGI Global, Hershey (2018)
17. Budnikov, D.A., Vasiliev, A.N.: The use of microwave energy at thermal treatment of grain crops. In: Kharchenko, V., Vasant, P. (eds.) Handbook of Research on Renewable Energy and Electric Resources for Sustainable Rural Development, pp. 475–499. IGI Global, Hershey (2018)

Chapter 9
Solar System with Seasonal Thermal Energy Storage

V. M. Pakhaluev, S. Ye. Shcheklein, and A. V. Matveev

Difference in time of arrival and consumption of thermal energy for hot water supply and space heating of residential buildings and industrial premises is a characteristic feature of systems using solar energy. In summer, solar systems produce a significant amount of unclaimed thermal energy, while in winter there is a heat deficit. Therefore, such systems need energy storage devices. A large number of works performed to date confirm this argument [1–3].

The utility of seasonal thermal energy storage (STES) devices is determined by their ability to collect and store the necessary amount of thermal energy for a long time. The time of thermal energy accumulation in summer and its storage to be used in winter is the key indicator of the storage systems [4–6]. A STES with heat insulation along the boundaries of the thermal storage is up to the task.

The design of seasonal thermal energy storage can be of various types [7–9]. One of such types is an underground thermal energy storage represented by a heat-insulated body of soil receiving and giving off heat, where the soil body itself serves as a storage medium. An underground energy storage without thermal insulation exhibits significant energy losses as a thermal storage. The use of modern thermal insulation materials helps maintain the required temperature level in the absence of heating load [10–12].

V. M. Pakhaluev · S. Ye. Shcheklein (✉) · A. V. Matveev
Ural Federal University Named After the First President of Russia B. N. Yeltsin, Yekaterinburg, Russia
e-mail: v.m.pakhaluev@urfu.ru; s.e.shcheklein@urfu.ru

P. Vasant et al. (eds.), *Innovative Computing Trends and Applications*, EAI/Springer Innovations in Communication and Computing,
https://doi.org/10.1007/978-3-030-03898-4_9

9.1 Operation of Seasonal Thermal Energy Storage During the Period of Charging

A mathematical model to study STES performance includes a dual-circuit solar system with a solar collector, water tank to collect the day's worth of heat, and a ground-coupled storage with an insulated body of soil (Fig. 9.1), similar to the one described in [13]. The period of heat accumulation is characterized by an increase in the volume-average temperature of the storage and depends on thermal energy coming from the water heating plant (WHP), with account of thermal losses through the insulation.

$$\left(c_p \rho V_s\right) \cdot \frac{d\Theta}{d\tau} = Q_{\mathrm{WHP}} - Q_{\mathrm{los}} = F_{\mathrm{sc}} \cdot q\left(\tau\right) \cdot \eta_{\mathrm{WHP}} - k \cdot \Theta \cdot S_s, \tag{9.1}$$

$$\eta_{\mathrm{WHP}} = \eta_{\mathrm{sc}}\left(\tau\right) \cdot \eta_{\mathrm{st}} \cdot \eta_{\mathrm{pipe}}, \tag{9.2}$$

where $(c_p \rho V_s)$ is thermal capacity, density, and volume of the ground-coupled storage; $\Theta(\tau)$ is the difference between the volume-average temperature of the storage and that of the surrounding soil; $q(\tau)$ is solar intensity on the solar collector surface; F_{sc} is the surface area of the collector; η_{WHP} is the efficiency of the water-heated plant which is a combination of the efficiencies of the solar collector, storage tank, and connecting pipelines; k is insulation heat transfer coefficient; and S_s is the outer surface area of the storage.

Using the "mean value" theorem to calculate the integral of the product of functions depending on time τ, the change in the storage temperature is given by

$$\theta\left(\tau\right) = BA \int_0^{\tau} Q_{\mathrm{WHP}}\left(\tau\right) d\tau, \tag{9.3}$$

where

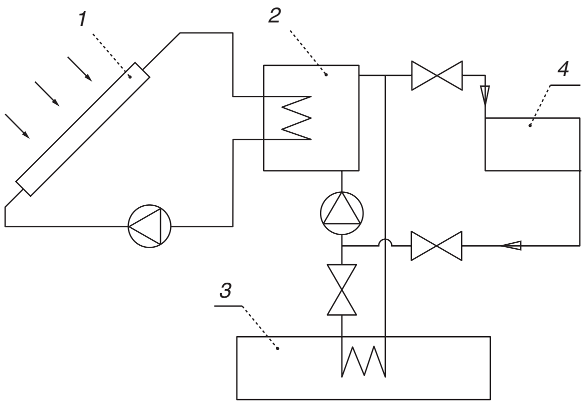

Fig. 9.1 Schematic diagram of the solar system with a seasonal thermal energy storage: *1*–solar collector, *2*—intermediate storage tank, *3*—seasonal thermal energy storage, and *4*–consumer

$$B = F_{sc} \cdot \left(c_p \rho V_s\right), \tag{9.4}$$

$$A = \exp\left[-\frac{0.5 \cdot k \cdot S_s}{\left(c_p \rho V_s\right)} \cdot \tau\right] \tag{9.5}$$

$$Q_{WHP}(\tau) = q(\tau) \cdot \eta_{WHP}(\tau) \tag{9.6}$$

where $Q_{WHP}(\tau)$ is the change in specific thermal output of WHP during the daylight hours.

Storage tank and connecting pipelines are assumed to be well insulated, which allows the heating capacity of a water heating plant in the summer period to be expressed as

$$Q_{WHP}^{N} = \sum_{1}^{N} \left(Q_i \cdot \eta_i\right)^{\text{month}} \tag{9.7}$$

where Q_i and η_i are the monthly values of solar intensity and the corresponding values of collector efficiency for that period, respectively.

The efficiency of solar collector can be determined using the expression

$$\eta_i^{\text{month}} = \eta_0 - 1.33 \frac{\Delta T_i}{I} - 0.007 \frac{\Delta T_i^2}{I} \tag{9.8}$$

where I is solar intensity per square meter of collector surface, η_0 is the optical efficiency of the collector, and ΔT_i is the monthly average difference between the heat carrier temperature in the collector and the ambient temperature.

Figure 9.2 shows the calculated values of heating capacity of a water heating plant with a south-facing vacuum tube collector (η_o = 0.7) arranged at an angle of 56° N to the horizontal. Climatic data used in the calculation were supplied by meteorological station of Yekaterinburg.

To assess the storage heat loss, its shape is assumed to be a rectangular parallelepiped with equal side dimension and height equal to half of it. In this case, the relationship between the surface area S_s and volume V_s is defined by a simple ratio:

$$S_s = 6.35 \cdot V_s^{0.67}. \tag{9.9}$$

Conductive heat losses from the storage to the surrounding soil depend on thermal resistance of insulation itself k_{insul} and that of its boundaries with the soil R_{soil} [14]:

$$k = \left(R_{insul} + 2R_{soil}\right)^{-1} = \left[\frac{\delta_{insul}}{\lambda_{insul}} + 0.75\left(\pi \lambda_{soil} V_s^{0.33}\right)^{-1}\right]^{-1}, \tag{9.10}$$

where δ_{insul} is the thickness of insulation layer and λ_{insul} and λ_{soil} are the heat-conduction coefficients of the insulations and soil, respectively (0.04 W/(m·K) and 0.8 W/(m·K)) [14].

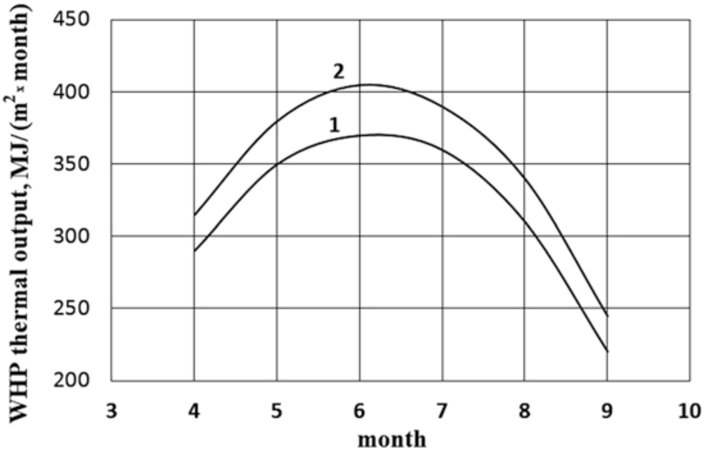

Fig. 9.2 Specific heating capacity of the STES water heating plant equipped with a vacuum collector during the summer months in Yekaterinburg. Lines 1 and 2 at an average temperature of the heat carrier T_{κ} of 75 °C and 50 °C, respectively

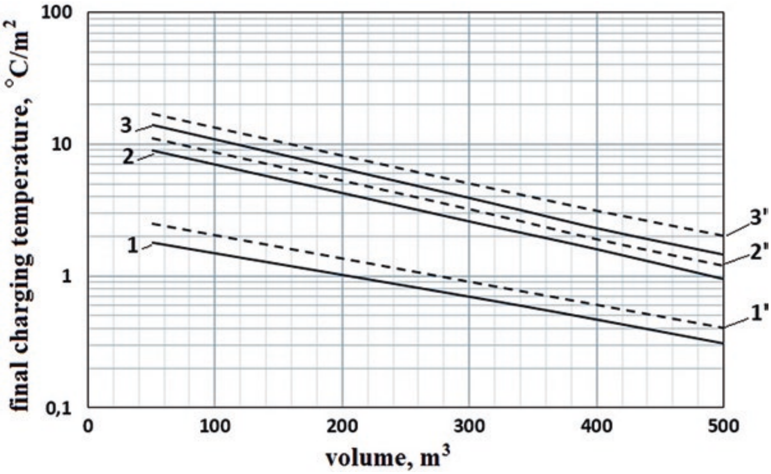

Fig. 9.3 The final temperature of STES charging per square meter of solar collector area (in Yekaterinburg): 1, 2, 3 and 1′, 2′, 3′ are the charging time during 1, 3, and 6 summer months at T_{κ} of 75 °C and 50 °C, respectively

With insulation thickness δ_{insul} of 0.5 m, the k factor equal to 0.08 W/(m^2·K) remains virtually unchanged at V_s of 50–500 m^3.

Using the specific output of water heating plant (Fig. 9.2) and applicable expressions (9.3), (9.7), and (9.10), it was possible to calculate the final heating temperature of STES as a function of its volume and its charging time for 1, 3, and 6 summer months in the climatic conditions of Yekaterinburg (Fig. 9.3).

As follows from Fig. 9.3, with V_s of 300 m^3, storage side dimension of 8.4 m, and height of 4.2 m, the solar collector area needed to heat STES to a temperature Θ of 65 °C in summer (6 months) would be F_{sc} = 32 m^2, while with V_s of 500 m^3, the required area would be 72 m^2.

In calculations, the temperature of the soil surrounding the storage was assumed to be constant and equal to 10 °C.

9.2 Operation of Seasonal Thermal Energy Storage During the Period of Heating

The amount of thermal energy that can be stored in STES and then used for space heating is determined by the final temperature of storage as a result of its charging and by the minimum storage temperature, which is usually assumed equal to the surrounding soil temperature of 8–12 °C. Heat losses during this period are due to conductive heat exchange of the storage through the layer of insulation.

STES operation in the discharge period under the fixed heating load corresponds to

$$\left(c_p \rho V_{\text{STES}}\right) \cdot \frac{d\Theta}{d\tau} + k\Theta S_{\text{STES}} = -Q_{\text{hl}}, \tag{9.11}$$

where $\Theta(\tau)$ is the excess temperature of the storage body as a function of the surrounding soil temperature and Q_{hl} is the value of heating load in winter.

The time of STES operation with the selected heating load in direct heating mode (without a heat pump) is defined by

$$\tau = \left(c_p \rho\right)_{\text{STES}} \cdot k^{-1} \left(\frac{S_{\text{STES}}}{V}\right)^{-1} \cdot \ln \frac{(1+a)}{\left(\frac{\Theta}{\Theta_0} + a\right)} \tag{9.12}$$

$$a = \frac{Q_{\text{hl}}}{\Theta_0} \cdot \left(k \cdot S_{\text{STES}}\right)^{-1} \tag{9.13}$$

where Θ is the final cooling temperature of STES during discharge and Θ_0 is the maximum temperature of the storage during charging period.

For the analysis of Eq. (9.12), the temperature regime of STES operation was selected for the underfloor heating conditions ("warm floor"). A special feature of the system is a reduced temperature of supplied coolant (not more than 45 °C). The required temperature is attained by adding the reverse water into the heating system.

Optionally, a minimum cooling temperature of the storage up to 35 °C was considered for the case when a floor is directly heated by the circulating heat carrier and cooling to the surrounding soil temperature of 10 °C with a backup heat source or a heat pump.

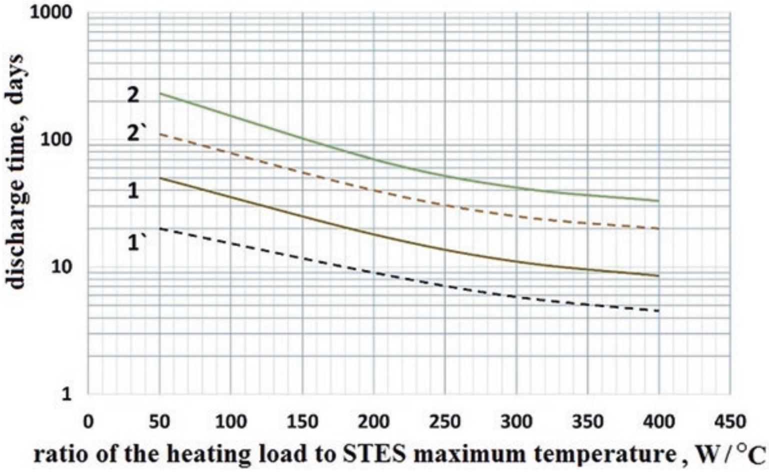

Fig. 9.4 STES discharge time in the modes of complete discharge (1, 2) and discharge to 35 °C (1′, 2′) with the storage capacity of 100 and 500 m^3

In Fig. 9.4, the calculated values of STES operating time depending on the heating load are shown against the maximum charging temperature for the two modes of storage discharge. An example would be an individual house with the underfloor heating, total area of 800 m^2 and a heated area of 70 m^2, requiring a thermal output of 8.4 kW. The maximum operation time would be 120 days for a charging temperature of 90 °C in summer and for the volume of 500 m^3; in the mode of complete discharge to 10 °C, operating time would be 220 days. Operating time is significantly reduced with a rise in heating load when maximum heating temperature of STES is limited to 60–90 °C.

The proposed method for calculating the solar system with seasonal thermal energy storage allows us to estimate the required solar collector area and the STES charging and discharging temperature regimes along with the main geometric parameters of the system.

Acknowledgment This article is prepared with the financial support of the Government of the Russian Federation (contract No.02.A 03.21.0006).

References

1. Kuravi, S., Trahan, J., Goswami, D.Y., Rahman, M.M., Stefanakos, E.K.: Thermal energy storage technologies and systems for concentrating solar power plants. Prog. Energy Combust. Sci. **39**(4), 285–319 (2013)
2. Zhang, H., Baeyens, J., Cáceres, G., Degrève, J., Lv, Y.: Thermal energy storage: Recent developments and practical aspects. Prog. Energy Combust. Sci. **53**, 1–40 (2016)
3. Tian, Y., Zhao, C.Y.: A review of solar collectors and thermal energy storage in solar thermal applications. Appl. Energy. **104**, 538–553 (2013)

4. Liu, L., Zhu, N., Zhao, J.: Thermal equilibrium research of solar seasonal storage system coupling with ground-source heat pump. Energy. **99**, 83–90 (2016)
5. Paiho, S., Hoang, H., Hukkalainen, M.: Energy and emission analyses of solar assisted local energy solutions with seasonal heat storage in a Finnish case district. Renew. Energy. **107**, 147–155 (2017)
6. Wang, X., Zheng, M., Zhang, W., Zhang, S., Yang, T.: Experimental study of a solar-assisted ground-coupled heat pump system with solar seasonal thermal storage in severe cold areas. Energy Build. **42**(11), 2104–2110 (2010)
7. Zalba, B., Marín, J.M., Cabeza, L.F., Mehling, H.: Review on thermal energy storage with phase change: materials, heat transfer analysis and applications. Appl. Therm. Eng. **23**(3), 251–283 (2003)
8. Sharma, A., Tyagi, V.V., Chen, C.R., Buddhi, D.: Review on thermal energy storage with phase change materials and applications. Renew. Sustain. Energy Rev. **13**(2), 318–345 (2009)
9. Anisimov, A.: Energy-saving space heaters from Karelia (thermal storage). Int. J. Altern. Energy Ecol. **5**, 44–46 (2004)
10. Vysochin, V.V.: Mathematical model of a solar system with a seasonal thermal storage. Proc. Odessa Polytech. Univ. **2**(36), 125–129 (2011)
11. Vysochin, V.V.: Effect of size of a seasonal thermal storage on the autonomy of the solar system operation. Proc. Odessa Polytech. Univ. **1**(36), 129–132 (2012)
12. Beckman, B., Gillie, P.: Thermal energy storage/Translated from English. Mir, p. 272 (1987)
13. Kroll, J.A., Ziegler, F.: The use of ground heat storages and evacuated tube solar collectors for meeting the annual heating demand of family-sized houses. Sol. Energy. **85**(11), 2611–2621 (2011)
14. Pekhovich, A.I., Zhidkikh, V.M.: Calculation of the thermal regime of solid substances/ Energia, Leningrad, p. 352 (1976)

Chapter 10
Toward a Capability Maturity Model for Digital Forensic Readiness

Ludwig Englbrecht, Stefan Meier, and Günther Pernul

10.1 Introduction

Following the tremendous increased and advanced fraudulent attacks since 2015, even the most security-aware executive managers, policy-makers, chief executive officers, or other decision-makers were suddenly given a wake-up call. In August 2015, the FBI already warned that losses related to fraudulent email attacks worldwide have been summed up to more than $1.2 billion USD from October 2013 until August 2015 [1].

One of the reasons for such an extensive loss was rooted to attacks on corporate banking accounts caused by the ransomware called *dyre wolf*. This malicious software is a highly effective banking trojan. It is characterized by the fact of being built with feature-rich capabilities and ongoing updates to mitigate its detection. Remarkable is the group behind the malware which enables the unauthorized transaction of large sums of money. A neat combination of knowledge of the banking system, a feasible infrastructure, manpower, social engineering, and technical skills demonstrates a new level of quality in malware-caused fraud. A single target could experience losses of $500,000 to more than $1,000,000 USD [2].

Also attacks related to spy and industrial espionage have led to significant losses during the last years. These cyberattacks threat valuable resources, e.g., intellectual property. The high value of intellectual property and its increased interest by attackers had been underestimated for a long time. Nowadays relevance of such risks and a proper risk management are also increasingly addressed by policy-makers [3].

L. Englbrecht (✉) · G. Pernul
Department of Information Systems, University of Regensburg, Regensburg, Germany
e-mail: ludwig.englbrecht@ur.de; guenther.pernul@ur.de

S. Meier
Meier Computersysteme GmbH, Deining, Germany
e-mail: sm@meier-pc.de

P. Vasant et al. (eds.), *Innovative Computing Trends and Applications*,
EAI/Springer Innovations in Communication and Computing,
https://doi.org/10.1007/978-3-030-03898-4_10

Cyberattacks against IT infrastructures have become more frequent and complex in recent years. The attackers also have become more professional. Cyberattacks are launched from various places. With the interconnection of various systems and enterprises via the Internet, it is also possible to conduct hidden attacks. This could be realized by exploiting various vulnerabilities of connected devices and misusing these devices for other attacks. For example, the *mirai* botnet abused weak devices of the Internet of Things to perform DDoS attacks [4].

Digital forensic (DF) is a good approach to unveil fraud. The perspective in digital forensic investigation needs to change from a reactive view toward a proactive. With the new perspective, various new research questions arise. Given that the forensic analysis task is complex and faces multiple internal and external influences, an interesting question is how an enterprise can evolve digital forensic capabilities in advance to resist vast changes in its demands. Digital forensic readiness (DFR) is an area that aims to solve this particular problem [5].

Being prepared for a digital forensic investigation in the context of DFR has still not been addressed by many companies or governmental institutes [6]. Mouhtaropoulos et al. [7] have analyzed various governmental and academic initiatives for the establishment of forensic readiness. However, due to the broad varying initiatives and an absence of uniformed rules, the authors postulate standardization within the area of DF. They also mention the high amount of accumulated needs in DFR capabilities in organizations. Therefore, implementing DFR within an organization is not a trivial task, and there is a need for further assistance through the whole organization. This work provides a capability maturity model (CMM) to assess the current state of initiatives in DFR and shows a guidance to turn efforts into the right direction.

The paper is structured as follows. In the following section, we present basics in DF, DFR, and CMM. Additionally, an overview of related work in CMM for DFR is presented in Sect. 10.2. The development approach for a digital forensic capability maturity model is presented in Sect. 10.3. In Sect. 10.4 the suggested digital forensic readiness capability maturity model is described. Section 10.5 provides a summary and an outlook on future work.

10.2 Background and Related Work

Digital Forensics and Forensic Sciences

The forensic sciences generally deal with the application of scientific methods for investigations in legal cases [8]. In this context, forensic scientists must adapt questions of a legal case into scientific questions and answer these by using appropriate and scientifically validated methods [9, 10]. This requires a well-defined and well-founded knowledge base and a scientific method as well as an experimental base [11, 12]. Following this argumentation, digital forensics is understood as a forensic science that deals with the application of methods from computer science to questions of the legal system [10]. In detail, this means that digital forensics provides methods to preserve and process digital evidence which guarantee the highest possible objectivity in digital forensic investigations [10].

Nowadays, conducting a digital forensic investigation can be challenging due to the large data sets which need to be stored and analyzed. By facilitating scientifically proven forensic techniques, a digital investigation with any data size can be supported. The scientific methods enable the processing, i.e., preservation, analyzation, interpretation, and presentation of digital evidence in a proper manner. Also the integrity of possible evidence is protected, which enables that the evidence stands up in a court of law [11].

Digital Forensics Readiness

Tan [5] initially mentioned DFR in 2001 and defined it as a mechanism to minimize the costs of digital forensic investigations and to maximize the capability of an organization to collect evidence with a correct legal reliability. Pangalos and Katos [13] extended this definition as "the state of the organization where certain controls are in place in order to facilitate the digital forensic process and to assist in the anticipation of unauthorized actions shown to be disruptive to planned operations." This definition emphasizes the aspect that it is crucial to pursue a proper support of the entire forensic process. The focus is also turned away from just producing credible digital evidence and adds the anticipatory perspective into DFR.

Digital forensics is a relatively young scientific discipline. Also the research in DFR has been conducted from many different views and perspectives. For example, Reyes and Wiles [14] analyze the allocation of adequate resources. The selection and usage of adequate technology have been researched by Carrier and Spafford [15]. Training initiatives are discussed in [15, 16]. Also legal investigation, incident response, and policies have been analyzed according to DFR [5, 17–19].

Most of these publications just discuss a selected aspect of DFR. The need for whole organizations to be forensically ready by regulations has been increased in the past years. This leads toward a comprehensive view on DFR within an organization. Implementing DFR measures is cost intensive, and the desired economical return is lower than in other projects. This puts organizations into the need to balance the costs of being forensically ready and the positive effect of being prepared in case of a digital investigation. The last aspect includes the capability to produce and preserve digital evidences in an efficient way [14, 16].

Carrier and Spafford [15] also distinguish forensic readiness between operational readiness and infrastructural readiness. The operational readiness can be determined by adequate provision of training and equipment present for individuals who are involved in digital forensic activities. Infrastructural readiness can be reached by establishing possibilities to preserve evidences appropriately. Rowlingson [16] covers these elements and proposes a clustering of forensic-related activities in planning, policing, training, and monitoring. These elements support the achievement of DFR massively [16]. Further important aspects of DFR have been stated by Grobler et al. [20]. There DFR is considered a proactive forensic activity. They also mention that the culture and governance of an organization should be considered in DFR implementation. The tight alignment of implementing DFR measures with the management of an organization can assist to fulfill this aspect [20].

By virtue of the high complexity according to forensic readiness initiatives in large-scaled companies, Reddy and Venter [21] propose a forensic readiness management system. This system supports in managing forensic readiness effectively within an organization. Based on the work of Tan [5, 22, 16], the authors define requirements to the forensic readiness management system.

Elyas et al. [23] present an expert perspective on their theoretical framework which is a holistic guidance on how an organization can become forensically ready. The framework consists of a set of forensic factors within various areas of forensic readiness and a set of forensic readiness capabilities.

Capability Maturity Model

Capability maturity models in the area of information technology are generally focused on development processes and phases within organizations and the involved information systems. They build a sound fundamental base for their evaluation according quality assessment. Therefore, the structure of the model is based on a stepwise progress for improvements. Every step acts as an assessment for quantity of processes and methods from enterprises and systems. Based within this assessment approach, corresponding options for improving and options for actions can be derived. Due to the structure of the model, the steps are in a chronological order and are built on each other. This sequence shows how an approach for improvement could be designed [24]. By applying this model, a user can determine the current position of an organization according their capabilities and the quality of various services. A capability maturity model also offers assistance for the development of the enterprise or involved elements of an organization [24].

Based on [24] three main goals of a capability maturity model can be noted: (a) a quality assessment of an organization with its processes and information systems, (b) providing a base for benchmarking with competitors, and (c) showing an approach for (quality) improvements.

A CMM is mainly based on a documentation of the processes and systems within an organization and can involve increased bureaucracy which makes an application of CMM complex and expensive [25]. Nevertheless, a CMM can provide a significant benefit to organizations and responsible employees by providing a systematic schema for determining their current positions for a competitive and future-oriented development.

The most famous and proven capability maturity models in the area of software development are Capability Maturity Model Integration (CMMI) and Software Process Improvement and Capability Determination (SPICE). In this paper, these models are used as a baseline for developing a capability maturity model for digital forensic readiness.

Related Work

Kerrigan [26] performed a study on how prepared companies in Ireland are with reference to digital investigations. He provides a CMM including various measures for the implementation of forensic readiness. The model provides a possibility to assess the forensic capabilities of an enterprise. In this context, the author emphasizes that the highest goal of the model must not be reached compulsively. This level of the capability maturity model involves significant costs and efforts to be reached. The application of the assessment by facilitating the model has been conducted in ten organizations located in Ireland. Additionally, Kerrigan has proposed a capability maturity model for digital investigations named the Digital Investigation Capability Maturity Model (DI-CMM). This model can be applied as a tool for analyzing the investigation capabilities within an organization. The author defined digital investigation capability maturity levels and enriched these with detailed descriptions. Their work also shows with the application of the objective-oriented maturity model in a real-life organization that there is a significant difference to the organizations' subjective assessment according to their digital investigation capabilities. As a conclusion a majority of the organizations overestimated their capabilities according to digital investigations [26].

Chryssanthou and Katos [27] present a framework for assessing forensic readiness. The suggested framework is based on the Systems Security Engineering—Capability Maturity Model (SSE-CMM). The proposed maturity assessment framework has been built up by specifying five different process areas (PA). The authors used generic phases of a digital investigation by mapping them to PAs: *identification*, *acquisition*, *examination*, *analysis*, and *reporting*. The assessment framework for digital forensic has been extended by elements from incident response. The following PAs have been added: *monitoring*, *detection*, *response*, and *restore*.

The forensic readiness levels are used by Chryssanthou and Katos by applying the assessment model in a fictitious scenario with an example company. The assessment is based on linking the PAs to suitable questions. After the fictitious company was questioned, a forensic readiness profile was retrieved. The work shows that the assessment of forensic readiness can be handled with a capability maturity approach. Nevertheless, the development of this capability maturity approach does not follow a comprehensive way, and the model cannot be applied to implement DFR holistically.

In contrast to the approaches described above, we present an approach to develop a DFR-specific CMM with the intention to cover DFR implementing initiatives holistically within an organization. To smoothen the implementation, the approach provides IT-governance-oriented support to reach a desired level in having DFR capabilities present.

10.3 Capability Model Development Approach

In recent years, several different applications and variations of maturity models have been developed. They have been implemented across a multitude of domains. The base model was the CMM from the Software Engineering Institute of the Carnegie Mellon University. The increased development of different capability models in various business areas has also shown downsides. Publications of capability maturity models show that the models or concepts are not scientifically proven according to their development process. A few models seem to be developed as a marketing instrument of a consulting or software development company. The documentation about the development process of a model is also often poorly prepared [28]. To overcome this pitfall, the development of a capability maturity model for DFR in this work underlies a strict and transparent methodology. For this, various concepts for the development of a capability maturity model are described, and a specific approach is selected and adopted.

Baseline Model

Becker et al. [28] provide a scientifically proven principle for developing a capability maturity model. They define and differ five important phases within the developing process: definition of the problem, comparison of existing models, defining a development strategy, iterative development of the model, and concepts for transfer and evaluation. The intended development of a digital forensic readiness maturity model in this work uses a general development framework provided by de Bruin et al. [29]. The framework presents a guideline to develop a theoretically sound, rigorously tested, and widely accepted maturity model. The suggested framework consists of the phases *scope*, *design*, *populate*, *test*, *deploy*, and *maintain*.

Definition of the Maturity Levels for the DFR CMM

The representation of capability profiles is not unrestrictedly applicable for comparing capabilities of an organization with others or companies within the same branch. Due to the fact that the intended capability maturity model is based on the CMMI, essential elements of CMMI can be reused. The CMMI has defined maturity levels to allow an overall assessment of the maturity of an organization. This reorientation of a maturity level aligns to a specific selection of PAs. They should cover the intended assessment holistically. This approach supports the assessment of the whole organization and enables an interorganizational comparison. To provide this holistic assessment of an organization according DFR including all relevant evaluation domains, five maturity levels have been defined. Based on the core concept of the CMMI [24] and the systematic provided by [26], the following maturity levels are defined. Aspects of [21, 26, 27] also influenced the definition of the levels.

Level 1 Level 1 represents non-existing measures according DFR. This is generally characterized by having no formalization, and a digital forensic investigation is performed chaotically and unstructured. There are also no standards or documentations about how a process should be performed. Knowledge about DF and the importance of keeping traces secure and useful for a court of law are not present within the organization.

Level 2 Level 2 defines basic elements in performing DFR-related activities. For example, there is a low or minimal formalization of procedures in the case of a digital investigation. Also a repeatability in various processes is recognizable. Additionally, a basic documentation is present. In this level, minor DFR aspects are fulfilled, and DFR is addressed as a relevant topic inside the organization. It is noticeable that these initiatives are not enough if a real investigation needs to be conducted.

Level 3 Level 3 provides a solid base in performing DFR activities. At this level an organization has standardized forensic procedures, compressively documented processes, and formal trainings. The involved staff has an acceptable understanding of DF and its consequences. This empowers an organization that potential failures in an early stage of a forensic investigation are prevented. According to Tan, the increased usability of evidences is an eminent aspect of DFR [5]. By having measures at this level in place can additionally save costs within a digital investigation.

Level 4 Level 4 describes an advanced state of having DFR initiatives in place. Beyond the previous levels and aspects, this level focuses on a professional implementation of DFR. For example, DFR is an enterprise-wide and strategic issue. At this level the support of an executive manager is committed, and various process improvement measures are in place.

Level 5 The highest level of the model is represented as level 5. The achievement of this level implies a full implementation of DFR including a continuous improvement of DFR-related measures and structures. With the definition of process improvement objectives, implementing formal staff training, and a corresponding accreditation, this level can be reached.

10.4 The Digital Forensic Capability Maturity Model

Based on the development approach, suggested in Sect. 10.3, and the distilled requirement of DFR, presented in section "Digital Forensics Readiness", the following DFR capability maturity model has been developed by conducting and presenting the various maturity levels of the DFR CMM. For each level the main characteristic processes, people, and technology are examined and used in the description. The maturity level of the DFR CMM is described in Table 10.1.

Besides the first level, each maturity level needs every previous maturity level to be completely fulfilled. A specific maturity level can be seen as accomplished if all included PAs satisfy the highest capability level. In our approach each maturity level is aligned to a set of capability levels across the seven enabler of COBIT 5 [30]. These capability levels are defined in Table 10.2 and can be measured by querying an organization-selected DFR-related questions. These questions represent indicators which are present or not. Some measures for implementing DFR need the support by the management or governance of an organization. Due to the fact that

Table 10.1 Description of the defined maturity levels

Level	Description
1—initial	• No documentation is present • No communication structure is defined • No training is in place • No regulations are defined • DF process is performed ad hoc and without structure • No DFR structure is in place
2—managed	• Repeatable processes are in place • Informal training is performed • Minimal formalization is present • A basic documentation is present • Low or informal communication structure is defined • DF-related measures are informally or ad hoc performed
3—defined	• Documented processes are present • Documented usage of tools and methods are present • Standardized procedures are in place • Documentation is reviewed and accepted • Formal trainings are offered and conducted • Formal regulations are in place • Communication is defined and new employees are involved
4—quantitatively Managed	• Minimal requirements for DFR are fulfilled • DFR-related process improvement measurements are in place • Used documents are checked for alignment with goals and objectives • Frequent communication to all staff is implemented • A formal training and accreditation is in place • Principles are accepted and followed • Monitoring and regulation mechanism are established
5—optimized	• Extended requirements for DFR are fulfilled • DFR-related process improvement measurements are in place, and objectives are aligned within the organization government • DFR-related processes are continuously improved and measured • Changes in the documentation structure are incorporated and clearly communicated • Frequently and timely communication to all staff is implemented • A formal training and accreditation is in place • Legislation and laws are reviewed, and DF aspects are integrated into procedures, documents, and/or adopted to organizational structure

Table 10.2 Description of the defined capability levels

Level	Description
0—incomplete	The DF-related objectives are *not* reached
1—performed	The intended goals in DF are reached
2—managed	DF initiatives and activities are managed and not ad hoc performed
3—completely defined	A standardized process for DF activities is in place. The procedures underlie a continuous improvement

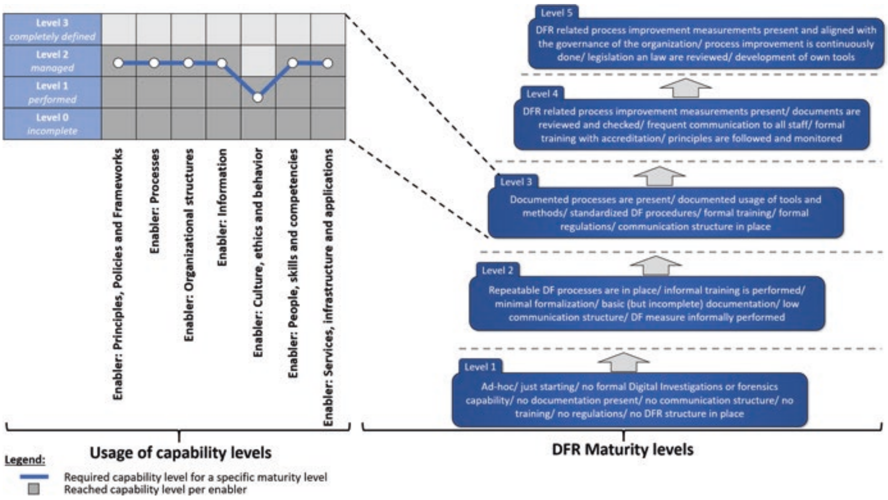

Fig. 10.1 Maturity and capability levels of the DFR CMM

the model is built by facilitating IT-governance principles from COBIT 5, the enabler concept provides a future-orientated guideline for a continuous improvement within the organization. This approach results in an overview of goals the seven enablers need to achieve to successfully implement DFR. With this DFR-specific CMM, a comprehensive and detailed justification of the intended progress can be reached.

The relation between capability and maturity levels and their possible definitions are presented in Fig. 10.1. In this figure also a possible linkage between capability levels and the enabler concept of COBIT 5 is illustrated.

The minimal necessity to have DFR in place is the maturity *level 3*. As a negative side effect, this could mislead managers to think the organization is fully prepared at this level. Even if the minimal level for DFR is reached by an organization, it is necessary to pursue a further development. This guarantees a higher application and faster response to changing circumstances around DFR. The higher levels, *levels 4* and *5*, assist to set up necessary requirements to faster adopt new demands in DFR.

10.5 Conclusion and Future Work

A significant role of digital forensic activities was endorsed due to the increasing amount of threats to the information systems of organizations. If an incident occurs and all information security measures fail, a digital forensic investigation needs to be conducted.

The main goal of this paper is to develop a DFR-specific CMM and to show how its application can assist in implementing DFR capability within an organization. Therefore, significant characteristics of being digital forensic ready have been used.

Due to a study of similar capability maturity models, it was possible to determine the third level as an acceptable state to consider an organization as digital forensic ready. A concrete suggestion of a DFR-specific model has been provided and reflected with the support of IT-governance aspects and instruments. The application of the DFR-specific CMM needs to be evaluated in a real-world scenario with additional expert interviews and is part of future work.

The development and application of a capability maturity model is not a single incentive to assess the maturity level or to improve it. Moreover, the intention of implementing such a model is to establish continuous improvements in specific areas. Assistance is provided by pointing out significant measures, needed to fulfill a desired level. This makes the model useful in practice. Also the continuous assessment and improving by using the capability maturity model can be supported.

Acknowledgment This work is partly performed under the BMBF-DINGfest project which is supported under contract by the German Federal Ministry of Education and Research (16KIS0501K).

References

1. Kitten, T.: FBI alert: business email scam losses exceed 1.2 billion. http://www.bankinfosecurity.com/fbi-alert-business-email-scam-losses-exceed-12-billion-a-8506
2. Kessem, L., Kuhn, J., Mueller, L.: The Dyre Wolf attacks on corporate banking accounts. https://portal.sec.ibm.com/mss/html/en_US/support_resources/pdf/Dyre_Wolf_MSS_Threat_Report.pdf
3. Dowdy, J.: The Cyber security threat to US growth and prosperity. In: Burns, N., Price, J. (eds.) Securing Cyberspace: A New Domain for National Security. Aspen Strategy Group, Washington, DC (2012)
4. Kolias, C., Kambourakis, G., Stavrou, A., Voas, J.: DDoS in the IoT. Mirai and Other Botnets. Computer. **50**, 80–84 (2017)
5. Tan, J.: Forensic readiness (2001)
6. Meier, S., Pernul, G.: Einsatz von digitaler Forensik in Unternehmen und Organisationen. In: Katzenbeisser, S., Lotz, V., Weippl, E. R. (eds.) Sicherheit 2014: Sicherheit, Schutz und Zuverlässigkeit, Beiträge der 7. Jahrestagung des Fachbereichs Sicherheit der Gesellschaft für Informatik e.V. (GI), 19–21. März 2014, Wien, Österreich, pp. 103–114. GI (2014)
7. Mouhtaropoulos, A., Grobler, M., Li, C.-T.: Digital forensic readiness: an insight into governmental and academic initiatives. In: Proceedings of the 2011 European Intelligence and Security Informatics Conference, pp. 191–196. IEEE Computer Society (2011)

8. Kent, K., Chevalier, S., Grance, T., Dang, H.: Guide to Integrating Forensic Techniques into Incident Response: NIST SP 800-86, 2006
9. Inman, K., Rudin, N.: Principles and Practice of Criminalistics: The Profession of Forensic Science. CRC Press, Boca Raton (2000)
10. Dewald, A.: Formalisierung digitaler Spuren und ihre Einbettung in die Forensische Informatik (2012)
11. Gary, P.: A road map for digital forensic research (2001)
12. Cohen, F.: Toward a science of digital forensic evidence examination. Adv. Digital Forensics VI. **337**, 17–35 (2010)
13. Pangalos, G., Katos, V.: Information assurance and forensic readiness. Next Gen. Soc. Technol. Legal Issues. **26**, 181–188 (2010)
14. Reyes, A., Wiles, J.: Developing an enterprise digital investigative/electronic discovery capability. In: The Best Damn Cybercrime and Digital Forensics Book Period, pp. 83–114 (2007)
15. Carrier, B., Spafford, E.H.: Getting physical with the digital investigation process. Int. J. Digital Evidence. **2**, 2003 (2003)
16. Rowlingson, R.: A ten step process for forensic readiness. Int. J. Digital Evidence. **2**, 2004 (2004)
17. Casey, E.: Case study: network intrusion investigation - lessons in forensic preparation. Digit. Investig. **2**, 254–260 (2005)
18. Ahmad, A., Hadgkiss, J., Ruighaver, A.B.: Incident response teams-challenges in supporting the organisational security function. Comput. Secur. **31**, 643–652 (2012)
19. Shedden, P., Ahmad, A., Ruighaver, A.B.: Organisational learning and incident response: promoting effective learning through the incident response process (2010)
20. Grobler, T., Louwrens, C.P., von Solms, S.H.: A framework to guide the implementation of proactive digital forensics in organisations. In: ARES 2010, Fifth International Conference on Availability, Reliability and Security, 15–18 February 2010, Krakow, Poland, pp. 677–682. IEEE Computer Society (2010)
21. Reddy, K., Venter, H.S.: The architecture of a digital forensic readiness management system. Comput. Security. **32**, 73–89 (2013)
22. Yasinsac, A., Manzano, Y.: Policies to enhance computer and network forensics. In: Proceedings of the 2001 IEEE Workshop on Information Assurance and Security, 2001
23. Elyas, M., Ahmad, A., Maynard, S.B., Lonie, A.: Digital forensic readiness. Expert perspectives on a theoretical framework. Comput. Security. **52**, 70–89 (2015)
24. CMMI Product Team: CMMI® for Development, Ver. 1.3, Improving processes for developing better products and services. no. CMU/SEI-2010-TR-033. Software Engineering Institute (2010)
25. Jacobs, S.: Reifegradmodelle, http://www.enzyklopaedie-der-wirtschaftsinformatik.de/lexikon/is-management/Systementwicklung/reifegradmodelle
26. Kerrigan, M.: A capability maturity model for digital investigations. Digital Invest. **10**, 19–33 (2013)
27. Chryssanthou, A., Katos, V.: Assessing forensic readiness. In: Proceedings of the Seventh International Workshop on Digital Forensics & Incident Analysis (WDFIA 2012), 2012
28. Becker, J., Knackstedt, R., Pöppelbuß, J.: Entwicklung von Reifegradmodellen für das IT-management. Wirtsch. Inform. **51**, 249–260 (2009)
29. de Bruin, T., Freeze, R., Kaulkarni, U., Rosemann, M.: Understanding the main phases of developing a maturity assessment model, 2005
30. ISACA: In: ISACA (ed.) COBIT 5. A business framework for the governance and management of enterprise IT, Rolling Meadows (2012)

Chapter 11
Vertical and Horizontal Integration Systems in Industry 4.0

Magdiel Pérez-Lara, Jania Astrid Saucedo-Martínez, Tomás Eloy Salais-Fierro, José Antonio Marmolejo-Saucedo, and Pandian Vasant

11.1 Introduction

Industry 4.0 has been achieving new heights and has high growth expectations, as the current information technology infrastructure enables the industry to adopt it quickly and efficiently. The challenge will be to find human talent with the capacity to develop analytical algorithms that lead to the development of self-learning intelligence, taking advantage of the current infrastructure. In addition, the future of this technology is conditioned to the creation of appropriate scientific areas; without this there would be an obstacle to the adoption and proliferation of this emerging technology.

The technological advances that are currently used in manufacturing are based on Industry 4.0. However, the entire present production process will be transformed in this new technological era. For instance, independent manufacturing cells will be unified as a fully integrated production flow, "intelligent" machines and products shall have the possibility to communicate with each other, and some decisions will

M. Pérez-Lara · J. A. Saucedo-Martínez · T. E. Salais-Fierro
Facultad de Ingeniería Mecánica y Eléctrica, Universidad Autónoma de Nuevo León, Ciudad Universitaria, San Nicolás de los Garza, México
e-mail: magdiel.perezlr@uanl.edu.mx; jania.saucedomrt@uanl.edu.mx; tomas.salaisfr@uanl.edu.mx

J. A. Marmolejo-Saucedo (✉)
Facultad de Ingeniería, Universidad Panamericana, Ciudad de México, México
e-mail: jmarmolejo@up.edu.mx

P. Vasant
Faculty of Science and Information Technology, Universiti Teknologi Petronas, Seri Iskandar, Malaysia

P. Vasant et al. (eds.), *Innovative Computing Trends and Applications*, EAI/Springer Innovations in Communication and Computing,
https://doi.org/10.1007/978-3-030-03898-4_11

be made autonomously. A new man- machine relationship will replace the classic relationships among suppliers, companies, and customers.

In a market that economic opening is a decisive guideline that induces greater demand competitiveness, causing all companies to work in a continuous improvement scheme and high productivity in their processes and in the administration of them, including new management system and business models, it is necessary to apply new techniques that allow the value generation that gives stability in the market. Technological advance in production systems requires corporations to be agile in their operational processes, as well as efficient information management, to create an organizational synergy that provides competitive advantages within the production system and throughout its value chain. This has caused divergences in the management and operations of companies that work under technology criteria in Industry 4.0, of which they don't, this difference reveals the fast transformation and achievements obtained by the corporations that have transformed their processes to the new system.

Systems integration is the first step toward Industry 4.0 vision and achieving its goals [1]. The systems are analyzed as a whole, it considers the productive flow, and in this sense, structural changes are proposed in the organization and management of physical objects, as well as the establishment of connections with information systems [2, 3]; vertical flow refers to how a company develops and executes its activities and includes basic elements such as the organizational structure, its human factor, the relationships of its departments, its technological level, and its administration; in a complementary way, the horizontal flow includes external relations and establishes networks of integration with suppliers, clients, information systems and administration, and technological systems among others [4–6].

This study consists in the creation and structuring of the evaluation tool with the criteria obtained in the first phase and is completed with reliability analysis and validity studies. The evaluation tool will result in the current level of vertical and horizontal integration of the company; this will allow to identify gaps and opportunities to develop the other prominent technologies considered in Industry 4.0 [7].

11.2 Background

The research was carried out through the qualitative content analysis, in which scientific articles, theses, and conference reports were collected and analyzed, obtained from various specialized journals related to the Industry 4.0 technological advances and to the business management. In this first phase, decisive criteria were obtained to propose a systematic evaluation methodology. In addition, knowledge and technological gaps were detected, as well as opportunity areas. The complete study can be consulted in a publication dedicated exclusively to this review [8]. The most important results are presented as follows:

Nine prominent technologies were identified as the backbone of Industry 4.0 [9, 10], including elements of industrial organization and management of information and production processes. These blocks were the focus of the research, so that it obtained the panoramic view of its application in the industrial sector, as well as its importance.

The articles were assigned to the categories. However, the articles revealed interconnections with the other categories, so that the systematic review, in addition to identifying the category with greater weight, revealed the requirements for the successful category application in the industrial sector and its interdependence with the other categories.

Finally, the analysis revealed that the category with the higher growth has been horizontal and vertical integration of systems; this is due to the fact that it represents the industrial base, in terms of administration and establishment of relations with other companies. This review not only shows the nine categories and their applications but also revealed criteria for the value chain management in terms of planning. In addition, the essential characteristics that a company must have to be able to perform in the 4.0 environment include sociotechnical environments as well as physical object virtualization through intelligent systems.

Vertical Integration

The performance of the company lies in the level of synergy it possesses, for it must be considered the crucial elements involved in the creation, development, and product manufacturing as well as its management [11, 12]; the mapping of vertical integration or internal integration is to evaluate the system in order to identify critical areas that must be assisted in a different way, for the vertical integration study have included two components, these are shown separately for the revision purpose, but in the analysis will be merged, because they contain similar elements.

Sociotechnical System

The sociotechnical system is so important, as this system depends on the success of the operations of a company; therefore, this importance is transcendent for its analysis within the vertical structure; the purpose of this system is to provide support to the company so that their activities marked in the plan are executed properly; the sociotechnical system must contain the three elements that are technological system, organizational system, and human operating system [2, 13, 14].

Value Creation Modules

The value creation modules are similar to the sociotechnical system; however, they differ in that the value creation module adds two more elements to complete the activities, causing this module to be analyzed thoroughly and in a particular way in each area. The value creation module's objective is similar to that of the sociotechnical system, which is to provide support to the company operations so that they are executed correctly. Nevertheless, it does not require only the presence of the three elements included in the system described above, and add to the product and processes involved, so that along with the sociotechnical system company operations are executed with high levels of synchronization [14].

Human operating system: it gives due importance to human capital as a critical element of change and is directly involved with the progress of the company [15–20].

Organizational system: in essence, the operations sequence between the hierarchical company levels, responsibility delegation, etc. [21–24].

Technological system: includes all the elements available in technology to carry out the production process activities [4, 25, 26].

Product: can be a product or a service; it is fundamentally the company's reason for being and is included as the result of the three previous systems, without neglecting the particular specifications for each detail and activity within the processes [11, 27].

Processes: these are the activities that give life to the product, so they are considered in the modules of value creation as the means to achieve the objective, in this case would be the product or service; it is a systematic analysis that evaluates the process as functional, to discard activities that do not add value [28–32].

Horizontal Integration

The relationship complexity between strategic goals and the operational part from the different levels of the manufacturing systems inhibits the realization of an intelligent manufacturing system; the Stevens model execution is useful to identify aspects of a manufacturing system that can be targeted for strategic planning, applying standardized techniques and using an agility scenario as an operational goal [12, 33].

Any improvement in the industry is based on the analysis of the current situation and the study of the environment, where they are aimed and which strategies should be considered. For this, it is essential to develop a conceptual model of integration, which describes the control activities in the administration of the manufacturing operations and the level of the company, with a representation of the physical system and an explicit interface for the analysis of the optimal control [34].

Stevens Model

This model is intended for the visualization of the company's performance in the overall scheme of its supply chain operations; with this approach, the level of integration that owns the organization as well as its level of technological absorption is defined; this point is crucial for the opportunity determination that can be found in the company, to be proposed as elements of change.

These change elements will be studied both in the internal organization and throughout company supply chain to place it in one of the four integration levels proposed by Stevens [35] and in this way to visualize schematically the integration that it possesses according to the departments that manage to relate to the operations synergy.

A business model describes the logic of an organization's value chain in terms of how it creates and captures customer value and can be represented concisely by an interrelated set of elements that address the customer, value proposition, organizational architecture, and economic dimensions [3]; the starting point is that all organizations have a business model, which can be explicitly articulated, or not; business models are required for the growth of the organization.

11.3 Methodology

The methodology has been divided into two phases for the instrument construction; one is the design of the instrument, and the second refers to the instrument validity and reliability tests, proposed by Hernández-Sampieri [36].

Instrument Design

To construct the measuring instrument, the process which is divided into 12 phases was followed. Figure 11.1 shows the phases of the construction process of a measuring instrument.

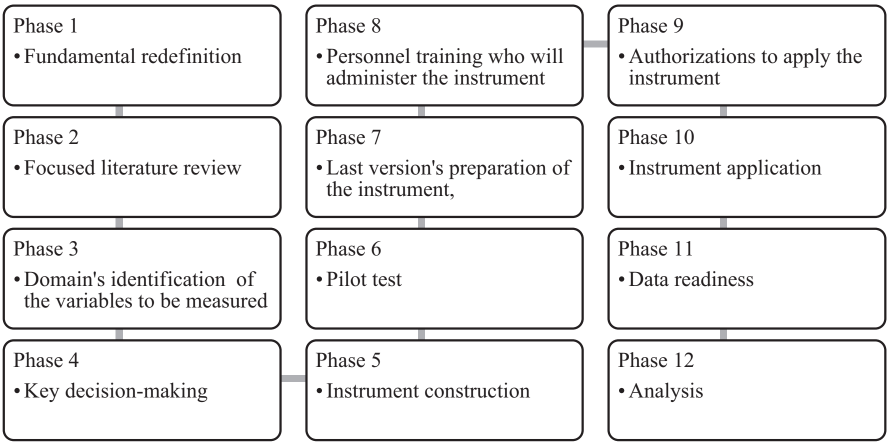

Fig. 11.1 Phases of instrument construction process [36]

Measuring Instrument Requirements

Validity, reliability, and objectivity are elements that should not be treated separately. If any of the three are not met or not analyzed, the instrument is not useful for conducting a study. Table 11.1 shows the measuring instrument requirements, the objectives, and the measuring techniques.

11.4 Information Discussion and Analysis

The analysis of the information obtained consists in the development of the instrument design phases and measuring instrument requirements, as explained below.

Instrument Design

The instrument design was performed exclusively with the monitoring of defined phases.

Phase 1 Fundamental Redefinition The research variables were defined; the proposal will have a goal to be applied in Mexico, on a website, with values on a scale, which reflects the perception of the organization, operations, and clients of the company in the case study.

Phase 2 Focused Literature Review Was performed by reviewing the detailed literature; the findings of this review can be found in Saucedo-Martínez [8].

Phase 3 Domain's Identification of the Variables to Be Measured It precisely identified the components, dimensions, and factors that integrate the variable, based on horizontal and vertical integration systems.

Table 11.1 Measuring instrument requirements [36]

Requirement	Objective	Measuring technique
Validity	It refers to the degree to which an instrument actually measures the variable it intends to measure	Content validity Criterion validity Construct validity Expert validity
Reliability	It refers to the degree to which repeated feedback to the same individual or object produces equal results	Cronbach's alpha
Objectivity	It refers to the degree to which it is permeable or not to the influence of biases and trends of the researcher or researchers who administer, qualify, and interpret	Standardization

Phase 4 Key Decision-Making It was decided to design a new instrument, to be applied in Mexico, applied by a web page, based on a scale questionnaire.

Phase 5 Instrument Construction In this phase the categories and the items were designed.

Phase 6 Pilot Test This test was done with group experts in the academic and research area, such that deficiencies must be detected in the instrument.

Phase 7 Last Version's Preparation of the Instrument Feedback was obtained from the items developed for the instrument, until reaching the final version; Fig. 11.2 shows the survey questionnaire elements.

Phase 8 Personnel Training Who will Administer the Instrument This was done by means of a spreadsheet, to manage the data and to organize them, as well as the codification.

Phase 9 Authorizations to Apply the Instrument The authorization for application was made under confidentiality criteria, and not as a case study, if not to evaluate the requirements of the instrument; this is developed in the second section of the methodology.

Phase 10 Instrument Application Participants to evaluate the instrument are experts in the industrial and service sectors, as well as technology, belonging to important companies in the northern region of Mexico with managerial positions.

Phase 11 Data Readiness The data coding was performed to carry out the analysis of the same.

Phase 12 Analysis The analysis of the information gave rise to the study of the instrument, in which objectivity and reliability can be determined.

Measuring Instrument Requirements Validity

The validity of a measuring instrument is evaluated on the basis of all types of evidence.

The more evidence of content validity, criterion validity, and construct validity has a measuring instrument, the latter will come closer to representing the variables it intends to measure.

$$\text{Total validity} = \text{content validity} + \text{criterion validity} + \text{construct validity}$$

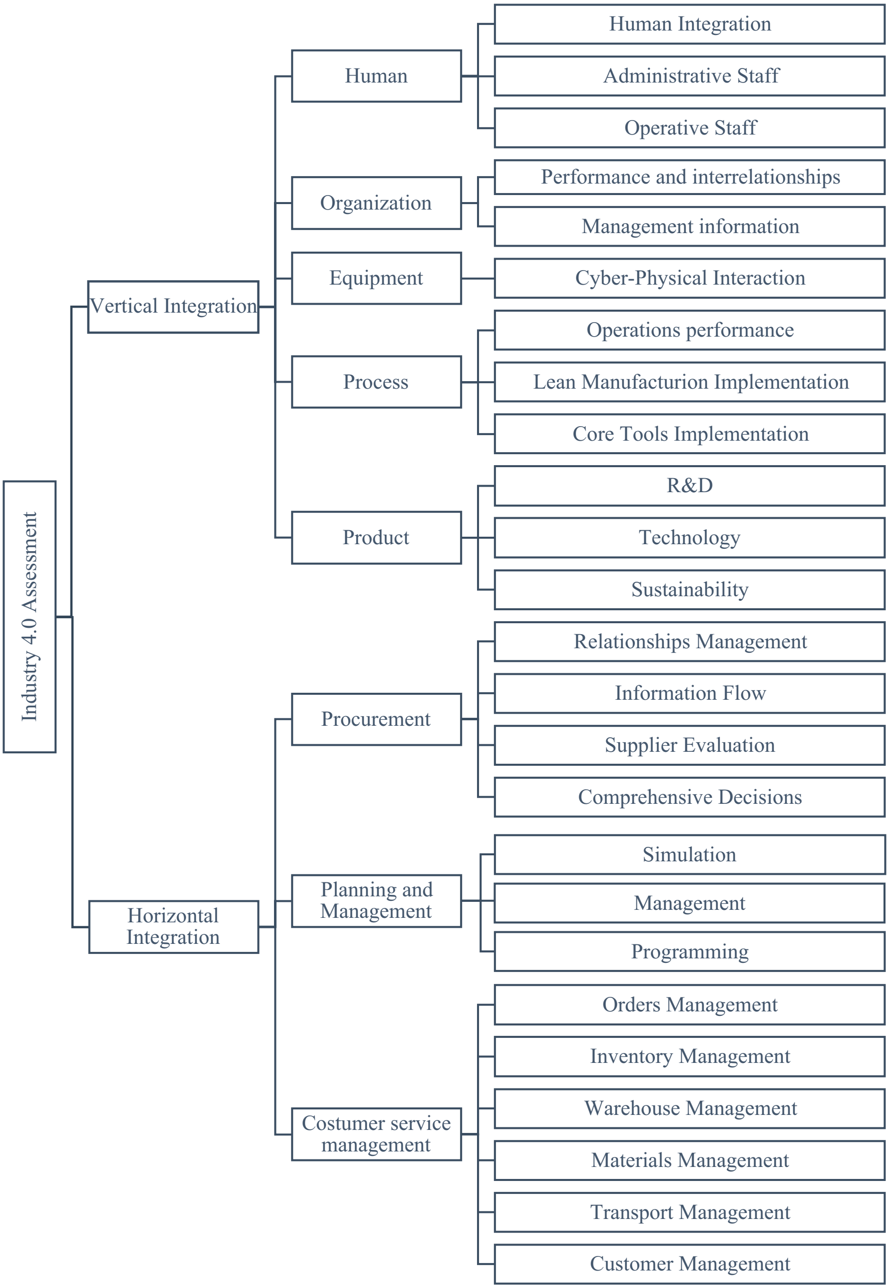

Fig. 11.2 Survey questionnaire elements

Content Validity This validation was carried out in a systematic way, according to the literature review, in which concepts were investigated, until the terms with the highest level of comprehension were defined.

Criterion Validity To perform the criterion validation, tests and comparisons were made with the following tools:

https://www.industrie40-readiness.de from Germany
https://i40-self-assessment.pwc.de from Germany
https://hada.industriaconectada40.gob.es from Spain

Construct Validity This validation can represent the most important and is based on a theoretical basis of correlation of concepts, so that it is expressed as links of the items developed with the rest of the methodology.

Expert Validity This validation was done with experts in the field who reinforced the tool with their points of view, in order to improve the instrument.

Reliability

The instrument reliability was determined by Cronbach's alpha variable. For this purpose, the answers obtained in the application to experts were used; analyzing the data in a spreadsheet was obtained to obtain a value of 99.2%.

Cronbach's alpha used equation

$$\alpha = \frac{k}{k-1}\left|1 - \frac{\sum S_i^2}{S_t^2}\right| \tag{11.1}$$

Objectivity

Standardization Objectivity was obtained through standardization in the instrument application (same instructions and conditions for all participants) and in the evaluation of the results, as well as employing trained and experienced personnel in the instrument.

11.5 Conclusions and Future Work

This revolution is considered holistic from the point of view that includes all the technologies, tools, skills, and knowledge available, to provide systems autonomy and increase level efficiency, customer service, and sustainability.

The inclusion of companies in the new way of operating requires the dissemination of information that allows the understanding and practice of the new modality of carrying out productive activities.

Technologies and the Internet play a preponderant role in the new era; their adoption in companies is imperative.

Companies must have a preparation prior to their application to operate in industry schemes 4.0, to ensure their development in the new system.

The instrument development for evaluating the current system, with validation, reliability, and objectivity tests, contributes to the detection of business gaps and opportunities to improve the industrial environment.

In the future, it is intended to apply to the productive sector, case studies that generate global reports, and analysis that allow investment and growth in technology and process improvement.

Acknowledgments The authors thank the Consejo Nacional de Ciencia y Tecnología (CONACYT) for the support provided to the development of this research, as well as the Universidad Autónoma de Nuevo León for being the study house to knowledge generation and the Facultad de Ingeniería Mecánica y Eléctrica (FIME) for the support granted.

References

1. Schlechtendahl, J., Keinert, M., Kretschmer, F., Lechler, A., Verl, A.: Making existing production systems Industry 4.0-ready: holistic approach to the integration of existing production systems in Industry 4.0 environments. Prod. Eng. **9**(1), 143–148 (2014)
2. Dombrowski, U., Wagner, T.: Mental strain as field of action in the 4th industrial revolution. Proc. CIRP. **17**, 100–105 (2014)
3. Fielt, E.: Conceptualising business models: definitions, frameworks and classifications. J. Bus. Model. **1**(1), 85–105 (2013)
4. Lee, J.: Smart factory systems. Informatik-Spektrum. **38**(3), 230–235 (2015)
5. Vyas, D., Nijholt, A.: From mundane to smart: exploring interactions with 'smart' design objects. Int. J. Mob. Hum. Comput. Interact. **8**(1), 59–82 (2016)
6. Schuh, G., Potente, T., Wesch-potente, C., Weber, A.R., Prote, J.: Collaboration mechanisms to increase productivity in the context of Industrie 4.0. Procedia CIRP. **19**, 51–56 (2014)
7. Schumacher, A., Erol, S., Sihn, W.: A maturity model for assessing industry 4.0 readiness and maturity of manufacturing enterprises. Procedia CIRP. **52**, 161–166 (2016)
8. Saucedo-Martínez, J.A., Pérez-Lara, M., Marmolejo-Saucedo, J.A., Salais-Fierro, T.E., Vasant, P.: Industry 4.0 framework for management and operations: a review. J. Ambient Intell. Humaniz. Comput. **9**(3), 1–13 (2017)
9. A. Gilchrist, 13 Introducing Industry 4.0
10. Toro, C., Barandiaran, I., Posada, J.: A perspective on knowledge based and intelligent systems implementation in industrie 4.0. Procedia Comput. Sci. **60**, 362–370 (2015)
11. Wang, S., Wan, J., Zhang, D., Li, D., Zhang, C.: Towards smart factory for Industry 4.0: a self- organized multi-agent system with big data based feedback and coordination. Comput. Networks. **0**, 1–11 (2015)
12. Joyce, A., Paquin, R.L.: The triple layered business model canvas: a tool to design more sustainable business models. J. Clean. Prod. **135**, 1474–1486 (2016)
13. Wainstein, M.E., Bumpus, A.G.: Business models as drivers of the low carbon power system transition: a multi-level perspective. J. Clean. Prod. **126**, 572–585 (2015)

14. Stock, T., Seliger, G.: Opportunities of sustainable manufacturing in industry 4.0. Procedia CIRP. **40**, 536–541 (2016)
15. Hashemy, S.H., Yousefi, M., Soodi, S., Omidi, B.: Explaining Human resource empowerment pattern and organizational excellence among employees of emergency of Guilan's University hospitals. Procedia Soc. Behav. Sci. **230**, 6–13 (2016)
16. Smits, C.C.A., Justinussen, J.C.S., Bertelsen, R.G.: Human capital development and a social license to operate: examples from arctic energy development in the Faroe Islands, Iceland and Greenland. Energy Res. Soc. Sci. **16**, 122–131 (2016)
17. Pelinescu, E.: The impact of human capital on economic growth. Procedia Econ. Financ. **22**, 184–190 (2015)
18. Felicio, J.A., Couto, E., Caiado, J.: Human capital, social capital and organizational performance. Manag. Decis. **52**(2), 350–364 (2014)
19. Longo, F., Nicoletti, E., Padovano, A.: Smart operators in industry 4.0 : a human-centered approach to enhance operators ' capabilities and competencies within the new smart factory context. Comput. Ind. Eng. **113**, 144–159 (2017)
20. Bauer, W., Hämmerle, M., Schlund, S., Vocke, C.: Transforming to a hyper-connected society and economy – towards an "Industry 4.0". Procedia Manuf. **3**, 417–424 (2015)
21. Ojha, D., Shockley, J., Acharya, C.: Supply chain organizational infrastructure for promoting entrepreneurial emphasis and innovativeness: The role of trust and learning. Int. J. Prod. Econ. **179**, 212–227 (2016)
22. Golmoradi, R., Sattari Ardabili, F.: The effects of social capital and leadership styles on organizational learning. Procedia Soc Behav. Sci. **230**, 372–378 (2016)
23. Ferriols, F.J., Mula, J., Díaz-Madroñero, M.: Supply chain management as the company engine in automotive manufacturing. IFAC Proc. Vol. **46**(9), 682–687 (2013)
24. Bücker, I., Hermann, M., Pentek, T., Otto, B.: Towards a methodology for industrie 4.0 transformation, vol. 1, pp. 209–221. Springer, Cham (2016)
25. Sousa-Zomer, T.T., Cauchick Miguel, P.A.: Sustainable business models as an innovation strategy in the water sector: an empirical investigation of a sustainable product-service system. J. Clean. Prod. **171**, 1–11 (2015)
26. Dachin, A., Burcea, F.-C.: Evaluations of driving effects of the Automotive Industry in the Romanian Economy – a quantitative analysis. Procedia Econ. Financ. **10**(14), 207–216 (2014)
27. Anderl, R.: Advanced engineering of smart products and smart production abstract. Technol. Innov. Product Development, 19th International Seminar on High Technology, pp. 1–14 (2014)
28. Teixeira, A.A.C., Queirós, A.S.S.: Economic growth, human capital and structural change: A dynamic panel data analysis. Res. Policy. **45**(8), 1636–1648 (2016)
29. Erbiyik, H., Saru, M.: Six sigma implementations in supply chain: an application for an Automotive Subsidiary Industry in Bursa in Turkey. Procedia Soc. Behav. Sci. **195**, 2556–2565 (2015)
30. Toro-Jarrín, M.A., Ponce-Jaramillo, I.E., Güemes-Castorena, D.: Methodology for the of building process integration of Business Model Canvas and Technological Roadmap. Technol. Forecast. Soc. Change. **110**, 213–225 (2016)
31. Schöggl, J.P., Baumgartner, R.J., Hofer, D.: Improving sustainability performance in early phases of product design: a checklist for sustainable product development tested in the automotive industry. J. Clean. Prod. **140**, 1602–1617 (2017)
32. Salcito, K., Singer, B.H., Krieger, G.R., Weiss, M.G., Wielga, M., Utzinger, J.: Assessing corporate project impacts in changeable contexts: A human rights perspective. Environ. Impact Assess. Rev. **47**, 36–46 (2014)
33. Jung, K., Morris, K.C., Lyons, K.W., Leong, S., Cho, H.: Mapping strategic goals and operational performance metrics for smart manufacturing systems. Procedia Comput. Sci. **44**, 184–193 (2015)
34. Sprock, T., McGinnis, L.F.: A conceptual model for operational control in smart manufacturing systems. IFAC-PapersOnLine. **28**(3), 1865–1869 (2015)
35. Stevens, G.C.: Integrating the supply chain. (2005)
36. Hernández Sampieri, R., Fernández Collado, C., del Pilar Baptista Lucio, M.: Metodología de la investigación, 6th edn. McGraw-Hill, México (2014)

Index

P. Vasant et al. (eds.), *Innovative Computing Trends and Applications*,
EAI/Springer Innovations in Communication and Computing,
https://doi.org/10.1007/978-3-030-03898-4